**Department of Energy**
Yucca Mountain Project Office
P. O. Box 98608
Las Vegas, NV 89193-8608

WBS 1.2.5
QA: N/A

JUL 06 1990

John J. Linehan, Director
Repository Licensing and
Quality Assurance Directorate
Office of Nuclear Material Safety
and Safeguards
U.S. Nuclear Regulatory Commission
Washington, DC 20555

TRANSMITTAL OF SANDIA NATIONAL LABORATORIES DOCUMENTS REQUESTED BY ON-SITE REPRESENTATIVE

The documents indicated on the enclosure by an asterisk were requested by Paul Prestholt, U.S. Nuclear Regulatory Commission on-site representative. All 17 documents are provided as attachments to the enclosure.

If you have any questions, please contact Ardyth M. Simmons of my staff at (702) 794-7998 or FTS 544-7998.

Carl P. Gertz, Project Manager
Yucca Mountain Project Office

YMP:AMS-3994

Enclosure: See Jacket
Reference List (17 Attachments)

cc w/encl, w/o attachments:
Ralph Stein, HQ (RW-30) FORS
L. J. Desell, HQ (RW-331) FORS
P. T. Prestholt, NRC, Las Vegas, NV
M. A. Glora, SAIC, Las Vegas, NV
C. L. Biddison, SAIC, Las Vegas, NV
A. R. Jennetta, W, Las Vegas, NV



003752724

YMP-5

ENCLOSURE FILED IN JACKET
SAME REC. #

102.2
WM-11
NH03

* = NRC Requests (17 Total)

# REFERENCES


Bauer, S., L. Costin, and J. F. Holland, 1989. Preliminary Analyses in Support of In Situ Thermomechanical Investigations, SAND88-2785, Sandia National Laboratories, Albuquerque, NM.

Bodvarsson, G. S., A. Nemi, A. Spencer, and M. P. Attanayake, 1988. Preliminary Calculations of the Effects of Air and Liquid-Water Drilling on Moisture Conditions in Unsaturated Rocks, LBL-25073, Lawrence Berkeley Laboratory, Berkeley, CA.

Broxton, D., 1989. Petrography of Phenocryst Chemistry of Volcanic Units at Yucca Mountain: A Comparison of Outcrop and Drill Hole Sample, LA-11503-MS, Los Alamos National Laboratory, Los Alamos, NM.

Carlos, B., 1989. Fracture-Coating Minerals in the Topopah Spring Member and Upper Tuff of Calico Hills From Drill Hole J-13, LA-11504-MS, Los Alamos National Laboratory, Los Alamos, NM.

Chipera, S. J., and D. L. Bish, 1989a. The Occurrence and Distribution of Erionite at Yucca Mountain, Nevada, LA-11663-MS, Los Alamos National Laboratory, Los Alamos, NM.

Chipera, S. J., and D. L. Bish, 1989b. Quantitative X-Ray Diffraction Analyses of Samples Used for Sorption Studies by the Isotope and Nuclear Chemistry Division, LA-11669-MS, Los Alamos National Laboratory, Los Alamos, NM.

Costin, L., and S. Bauer, 1989. Preliminary Analysis of the Excavation Investigation Experiments Proposed for the Exploratory Shaft at Yucca Mountain, Nevada Test Site, SAND87-1575, Sandia National Laboratories, Albuquerque, NM.

Crowe, B., C. Harrington, L. McFadden, F. Wells, B. Turrin, and D. Champion, 1988. Preliminary Geologic Map of the Lathrop Wells Volcanic Center, LA-UR-88-4155, Los Alamos National Laboratory, Los Alamos, NM.

Czarnecki, J. B., 1989. "Preliminary Simulations Related to a Large Horizontal Hydraulic Gradient at the North End of Yucca Mountain, Nevada," American Geophysical Union, EOS, vol. 70, No. 15, p. 321.

Deere, D. U., 1989. Letter from D.U. Deere (Chairmen, Nuclear Waste Technical Review Board) to T. Isaacs (DOE), August 11, 1989, concerning configuration and construction of exploratory shafts.

DOE (U.S. Department of Energy), 1986. Final Environmental Assessment: Yucca Mountain Site, Nevada Research and Development Area Nevada, Nevada, DOE/RW-0073, Washington D.C.

DOE (U.S. Department of Energy), 1988a. Environmental Monitoring and Mitigation Plan for Site Characterization: Yucca Mountain Site, Nevada Research and Development Area, Nevada, DOE/RW-0208 (Rev. 2), Washington, D.C.


ENCLOSURE

DOE (U.S. Department of Energy), 1988b. Section 175 Report: Secretary of Energy Report to the Congress Pursuant to Section 175 of the Nuclear Waste Policy Act as Amended, DOE/RW-0205, Washington, D.C.

DOE (U.S. Department of Energy), 1988c. Site Characterization Plan: Yucca Mountain Site, Nevada Research and Development Area, Nevada, 8 Volumes, DOE/RW-0199, Washington, D.C.

DOE (U.S. Department of Energy), 1988d. Yucca Mountain Project Exploratory Shaft Facility Title I Design Summary Report, 4 Volumes, YMP/88-20, Las Vegas, NV.

DOE (U.S. Department of Energy), 1988e. Surface-Based Investigations Plan, 4 Volumes, YMP/88-25, Nevada Operations Office, Las Vegas, NV.

DOE (U.S. Department of Energy), 1988f. Yucca Mountain Project Site Atlas, YMP/88-21, Nevada Operations Office, Las Vegas, NV.

DOE (U.S. Department of Energy), 1989a. Review Record Memorandum, Exploratory Shaft Facility (ESF) Title I Design Acceptability Analysis and Comparative Evaluation of Alternative ESF Locations, YMP/89-3, Las Vegas, NV.

DOE (U.S. Department of Energy), 1989b. Technical Assessment Review Notice: Geologic and Geophysical Evidence Pertaining to Structural Geology in the Vicinity of the Proposed Exploratory Shaft, Yucca Mountain Project Office, Las Vegas, Nevada.

DOE (U.S. Department of Energy), 1989c. Integrated Data System Title I Preliminary Design Technical Assessment Review Record Memorandum, LS9-ESF-JHM-014, Las Vegas, NV.

DOE (U.S. Department of Energy), 1989d. Exploratory Shaft Facility (ESF) Subsystem Design Requirements Document (SDRD) for Title II, YMP/CC-0003 (Rev. 0), Las Vegas, NV.

DOE (U.S. Department of Energy), 1989e. The Yucca Mountain Project Reference Information Base, YMP/CC-0002, Las Vegas, NV.

DOE (U.S. Department of Energy), 1989f. Report to Congress on Reassessment of the Civilian Radioactive Waste Management Program, DOE/RW-0247, Washington, D.C.

Doughty, C., and K. Pruess, 1988. A Similarity Solution for Two-Phase Fluid and Heat Flow Near High-Level Nuclear Waste Packages Placed in Porous Media, SAND88-7071A, Sandia National Laboratories, Albuquerque, NM.

Dudley, A., R. Peters, M. Tierney, and E. Klavetter, 1989. Total System Performance Assessment Code (TOSPAC): Volume 1: Physical and Mathematical Basis, SAND85-0002, Sandia National Laboratories, Albuquerque, NM.

Eaton, R., N. Bixler, and R. Peters, 1988. Computational and Experimental Procedures for Predicting Flow Through Low-Permeability, Partially Saturated, Fractured Rock, SAND88-2626A, Sandia National Laboratories, Albuquerque, NM.

Eaton, R., R. Dykhuizen, and A. Russo, 1989. Analysis of Proposed Laboratory Experiments in Partially Saturated, Small-Pore Fractured Rock, SAND89-0074A, Sandia National Laboratories, Albuquerque, NM.

Easterling, R. C., and I. J. Hall, 1988. Additional Underground Test Data Required for Yucca Mountain Repository Characterization, SAND87-2073, Sandia National Laboratories, Albuquerque, NM.

Einziger, R. E., 1988a. Test Plan for Thermogravimetric Analyses of BWR Spent Fuel Oxidation, PNL-6745/UC/70, Pacific Northwest Laboratory, Richland, WA.

Einziger, R. E., 1988b. Test Plan for Long-Term, Low-Temperature Oxidation of BWR Spent Fuel, PNL-6427/UC/70, Pacific Northwest Laboratory, Richland WA.

Furgerson, R. B., 1989. Remote-Reference Magnetic Survey of the Nevada Test Site and Vicinity, U.S. Geological Survey Open-File Report 82-465, p. 142.

Golder, 1989. Evaluation of Alternative ESF Shaft Construction Methods and Test Sequences for Yucca Mountain Project Office, 833-1017.116, Golder Associates Inc., Redmond, WA.

Hardy, N. P., and C. N. St. John, 1988. Underground Repository Design Methodology for a Repository in Tuff, SAND88-7059A, Sandia National Laboratories, Albuquerque, NM.

Jardine, L. J., and T. Laub, 1988. Use of Performance Assessments to Generate a Repository Q-List, SAND88-0140A, Sandia National Laboratories, Albuquerque, NM.

Kaplan, P., E. Klavetter, and R. Peters, 1989. Approaches to Groundwater Travel Time, SAND88-2868C, Sandia National Laboratories, Albuquerque, NM.

Kaplan, P., and L. Yarrington, 1989. Modeling the Uncertainties in the Parameter Values of a Layered, Variably Saturated Column of Volcanic Tuff Using the Beta Probability Distribution, SAND88-2247C, Sandia National Laboratories, Albuquerque, NM.

Kiciman, O. K., and N. A. Abrahamson, 1988. A Probabilistic Estimation of Seismic Damage at Waste-Handling Facilities of a Repository Located at Yucca Mountain, Nevada, SAND88-7067A, Sandia National Laboratories, Albuquerque, NM.

Kirchoff-Stein, K. S., D. A. Ponce, and B. A. Chochel, 1989. Preliminary Aeromagnetic Map of NTS and Vicinity, Nevada, U.S. Geological Survey Open-File Report 89-446.

Laub, T., 1988. Assessment of Worker and Non-Worker Radiological Safety of a Repository, SAND88-0292A, Sandia National Laboratories, Albuquerque, NM.

Laub, T., L. J. Jardine, C. Ma, R. Sit, S. Zavoisky, and D. Hartsann, 1988. Preliminary Radiological Safety Analysis for Normal Operations of a Prospective Yucca Mountain Repository, SAND87-2070C, Sandia National Laboratories, Albuquerque, NM.

Loux, R. R., 1989a. Letter from R. R. Loux (State of Nevada) to C. Gertz (DOE), May 30, 1989, transmitting State of Nevada's comments on the ESF design acceptability analysis.

Loux, R. R., 1989b. Letter from R. R. Loux (State of Nevada) to S. Rousso (DOE), September 1, 1989, transmitting State of Nevada's comments on the DOE Site Characterization Plan.

* Ma, C. W., and L. J. Jardine, 1988. Offsite Radiation Doses Resulting from Seismic Events at the Yucca Mountain Repository, SAND88-7065A, Sandia National Laboratories, Albuquerque, NM.

Martinez, M., and R. Prindle, 1988. Capillary-Driven Flow in a Fracture Located in a Porous Medium, SAND84-1697, Sandia National Laboratories, Albuquerque, NM.

McCright, R. D., 1988. An Annotated History of Container Candidate Material Selection, UCID-21472, Lawrence Livermore National Laboratory, CA.

McKeegan, K. D., D. Phinney, V. M. Oversby, M. Buchholtz-tenBrink, and D. K. Smith, 1988. Uranium Transport in Topopah Spring Tuff: An Ion-Microscope Study, UCRL-99734, Lawrence Livermore National Laboratory, Livermore, CA.

Moore, L. M., F. M. Byers, and D. E. Broxton, 1989. Statistical Test of Reproducibility and Operator Variance in Thin-Section Modal Analysis of Textures and Phenocrysts in the Topopah Spring Member, Drill Hole USW VH-2, Crater Flat, Nye County, Nevada, LA-11452-MS, Los Alamos National Laboratory, Los Alamos, NM.

* Nimick, F., and R. Peters, 1989. Relevance of Partial Saturation to the Mechanical Behavior of Tuffs, SAND88-2521C, Sandia National Laboratories, Albuquerque, NM.

Nitsche, H., E. M. Standifer, S. C. Lee, R. C. Gatti, and D. B. Tucker, 1989. Solubility and Speciation Studies of Waste Radionuclides Pertinent to Geologic Disposal at Yucca Mountain: Results on Neptunium, Plutonium and Americium in J-13 Groundwater October 1, 1985 - September 30, 1987, LBL-27157, Lawrence Berkeley Laboratory, Berkeley, CA.

NRC (U.S. Nuclear Regulatory Commission), 1988a. Qualification of Existing Data for High-Level Waste Geologic Repositories, NUREG-1298, prepared by W.D. Altman, J.P. Donnelly, and J.E. Kennedy, Washington, D.C.

NRC (U.S. Nuclear Regulatory Commission), 1988b. Technical Position on Items and Activities in the High-Level Waste Geologic Repository Program Subject to Quality Assurance Requirements, NUREG-1318, prepared by A.B. Duncon, S.G. Bilhorn, and J.E. Kennedy, Washington, D.C.

NRC (U.S. Nuclear Regulatory Commission), 1989. NRC Staff Site Characterization Analysis of the Department of Energy's Site Characterization Plan, Yucca Mountain Site, Nevada, NUREG-1347, prepared by the Office of Nuclear Material Safety and Safeguards, Washington D.C.

O'Brien, P., 1989. OGR Repository-Specific Rod Consolidation Study: Effect on Costs, Schedules, and Operations at the Yucca Mountain Repository, SAND86-2357, Sandia National Laboratories, Albuquerque, NM.

Peters, R. R., 1988. Hydrologic Technical Correspondence in Support of the Site Characterization Plan, SAND88-2784, Sandia National Laboratories, Albuquerque, NM.

Peterson, A., 1989. Technical Correspondence in Support of an Evaluation of the Hydrologic Effects of Exploratory Shaft Facility Construction, SAND88-2936, Sandia National Laboratories, Albuquerque, NM.

Reheis, M. C., and J. S. Noller, 1989. New Perspective on Quaternary Faulting in the Southern Walker Lane, Nevada, Nevada Bureau of Mines and Geology Open-File Report 89-1, pp. 57-61.

Reheis, M. C., 1989. "Applications of the Morphology and Genesis of Desert Soils to Quaternary Studies in the Southwestern United States," from the International Geological Congress, Washington, D.C., v. 2, pp. 684.

* Richardson, A., and C. M. St. John, 1988. A Concrete Shaft Liner Design Methodology for Nuclear Waste Repositories, SAND88-7052, Sandia National Laboratories, Albuquerque, NM.

* Richardson, A. M., B. Schmidt, and M. Christopher, 1988. A Proposed Concrete Shaft Liner Design Method for Underground Nuclear Waste Repositories, SAND 88-7120A, Sandia National Laboratories, Albuquerque, NM.

Robison, J. H., D. M. Stephens, R. R. Luckey, and D. A. Baldwin, 1988. Water Levels in Periodically Measured Wells in the Yucca Mountain Area, Nevada, 1981-87, U.S. Geological Survey Open File Report 88-468.

Saltus, R. W., and D. A. Ponce, 1988. Aeromagnetic Map of Nevada-Las Vegas Sheet, Nevada Bureau of Mines and Geology Map 95, scale 1:250,000.

Sanders, M., 1988. Description of Ground Motion Data Processing Codes, SAND 87-1176, Sandia National Laboratories, Albuquerque, NM.

Sass, J. H., A. H. Lachenbrunch, W. W. Dudley Jr., S. S. Priest, and R. J. Munroe, 1988. Temperature, Thermal Conductivity, and Heat Flow near Yucca Mountain Nevada: Some Tectonic and Hydrologic Implications, USGS Open File Report 87-649, 188p.

Schaetz, B. E., and D. M. Roy, 1989. Reactivity of a Tuff-Bearing Concrete: CL-40 CON-14, LA-11532-MS, Los Alamos National Laboratory, Los Alamos, NM.

Scott, R. B., 1989. Isostatic Uplift, Crustal Attenuation, and the Evolution of an Extensional Detachment System in Southwestern Nevada, Nevada Bureau of Mines and Geology Open-File Report 89-1, pp. 19-26.

SNL (Sandia National Laboratories), 1987. Site Characterization Plan Conceptual Design Report, SAND84-2641, 6 Vol., Sandia National Laboratories, Albuquerque, NM.

Stinton, P. O., 1989. "Characterization of the Large Hydraulic Gradient Beneath the North End of Yucca Mountain, Nevada" [abs.], AGU, EOS, vol. 70, No. 15, p. 321.

* Subramanian, C. V., and L. J. Jardine, 1988. Evaluation of Site-Generated Radioactive Waste Treatment and Disposal Methods for the Yucca Mountain Repository, SAND88-1937, Sandia National Laboratories, Albuquerque, NM.

Subramanian, C. V., C. L. Wu, C. D. Degrabrielle, and S. D. Leftwich, 1988. Seismic Design Study of the Waste-Handling Building at the Prospective Yucca Mountain Nuclear Waste Repository, SAND87-1915C, Sandia National Laboratories, Albuquerque, NM.

Subramanian, C. V., A. H. Hadjian, J. King, and R. P. Kennedy, 1989. Preliminary Seismic Design Cost-Benefit Assessment of the Tuff Repository Waste Handling Facilities, SAND88-1600, Sandia National Laboratories, Albuquerque, NM.

Swadley, W. C., and D. L. Hoover, 1989. Geologic Map of the Surficial Deposits of the Topopah Spring Quadrangle, Nye County, Nevada, U.S. Geological Survey Miscellaneous Investigations Series Map I-2018, scale 1:48,000.

Thenhaus, P. C., and T. P. Barnhard, 1989. "Regional Termination and Segmentation of Quaternary Fault Belts in the Great Basin Nevada and Utah," Bulletin of the Seismological Society of America, v. 79, no. 5.

Trisy, I. R., and R. S. Rundberg, 1989a. "Application of Deconvolution to the Analysis of Univalent Ion-Exchange Isotherms in Zeolites X and Y," Zeolites, vol. 9., pp. 217-223.

Trisy, I. R., and R. S. Rundberg 1989b. "Deconvolution of Multivalent Cation Exchange Isotherms," The Journal of Physical Chemistry, vol. 93, No. 14, pp. 5617-5623.

Tsang, Y., and K. Preuss, 1988. Gas Phase Flow Effects on Moisture Migration in the Unsaturated Zone at Yucca Mountain, SAND88-7073A, Sandia National Laboratories, Albuquerque, NM.

Wallace, K., and D. Zorga, 1988. An Analysis of Air Cooling Prior to Reentering a Drift Containing Emplaced Commercial Nuclear Waste, SAND87-7076C, Sandia National Laboratories, Albuquerque, NM.

Wang, J. S. Y., and N. T. Narasimhan, 1988. Hydrologic Modeling of Vertical and Lateral Movement of Partially Saturated Fluid Flow Near a Fault Zone at Yucca Mountain, SAND87-7070, Sandia National Laboratories, Albuquerque, NM.

Weston, 1989. Evaluation of Additional Drifting for Site Characterization of Yucca Mountain, Roy F. Weston, Inc., Washington, D.C.

Yang, I. C., A. K. Turner, T. M. Sayre, and P. Montazer, 1988. Triaxial-Compression Extraction of Pore Water from Unsaturated Tuff, Yucca Mountain, Nevada, U.S. Geological Survey Water-Resources Investigation Report 88-4189.

SAND 88-7071A

# A Similarity Solution for Two-Phase Fluid and Heat Flow Near High-Level Nuclear Waste Packages Emplaced in Porous Media *

C Doughty and K Pruess (Earth Sciences Division, Lawrence Berkeley Laboratory, Berkeley, CA 94720; 415-486-6453)

Fig. 2

The emplacement of a heat source, such as a high-level nuclear waste package, into a geologic medium gives rise to strongly coupled thermal and hydrologic behavior. Under certain conditions a phenomenon known as a heat pipe may develop. In a heat pipe heat transfer is primarily convective. Near the heat source, liquid water vaporizes causing pressurization of the gas phase and gas-phase flow away from the heat source. The water vapor condenses in cooler regions away from the heat source, depositing its latent heat of vaporization there. This sets up a saturation profile, with liquid saturation increasing away from the heat source. The saturation gradient drives the backflow of the liquid phase toward the heat source through capillary forces. The liquid then again vaporizes and repeats the cycle.

Heat transfer in a heat pipe can be much more efficient than conductive heat transfer through geologic media, leading to greatly decreased temperatures at the heat source. The counter-current flow of vapor and liquid water causes a purging of gas-phase components from the near heat-source region, while liquid-phase components are concentrated there as liquid water vaporizes.

In an infinite homogeneous permeable medium with a constant-strength linear heat source, the partial differential equations governing fluid and heat flows in a radial geometry can be converted to ordinary differential equations through the use of a similarity variable, $\eta = r/\sqrt{t}$. These equations are numerically integrated using an iterative "shooting method" to provide a description of temperature, pressure, saturation, heat flow, gas flow, and liquid flow conditions around a heat source such as a nuclear waste package. The similarity solution is verified by numerical simulations. Illustrative solutions are given for a range of hydrologic and thermal parameters.

The figures below show the results obtained for a 200 W/m heat source emplaced in a water-saturated porous medium initially at a temperature of 26 °C and a pressure of 1.013 bars. The heat source is located at $\ln\eta = -\infty$, while the temperature and pressure boundary condition is maintained at $\ln\eta = +\infty$. The heat pipe ($-12 < \ln\eta < -9.5$) is characterized by a large liquid-gas counterflow with zero net fluid flow ($Q_w = Q_g + Q_l$) and constant temperature. Elsewhere the linear temperature profile and small fluid flows indicate that heat flow ($Q_e$) is conduction-dominated.

This work was supported by the NNWSI Performance Assessment Division, Sandia National Laboratories, and the U.S. Department of Energy.

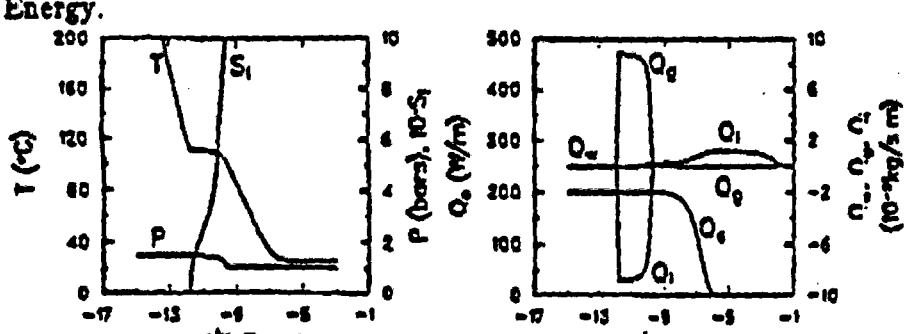


*This work was supported by the U.S. Department of Energy (US DOE) under contract DE-AC04-76DP00789.

9007160158 900706
SAND 88-2626A Received w/Ltr Dated 7/6/90

# Computational and Experimental Procedures for Predicting Flow Through Low-Permeability, Partially Saturated, Highly Fractured Rock**

Roger R. Eaton and Nathan E. Bixler
Fluid and Thermal Sciences Department

Ralph R. Peters
Nevada Nuclear Waste Storage Investigations Project Department
Sandia National Laboratories, Albuquerque, NM 87185

## Abstract

Current interest in storing high-level nuclear waste in underground repositories has resulted in an increased effort to understand the physics of water flow through highly fractured rock with low permeability. The U.S. Department of Energy is investigating a prospective repository site located in volcanic ash (tuff) hundreds of meters above the water table at Yucca Mountain, Nevada, (Figure 1). Consequently, mathematical models and experimental procedures are being developed to provide a better understanding of the hydrology of low-permeability, partially saturated, highly fractured rock. The modeling of the vadose zone of soils and of permeable rocks such as sandstones has received considerable attention for many years; however, the treatment of flow through materials such as Yucca Mountain tuffs has not received this level of attention, primarily because it is outside the realm of interest of agricultural and petroleum technology.

This paper reviews the status of mathematical models and computational and experimental procedures currently being applied to the proposed waste repository site. The computational aspects of these problems are quite challenging because of the highly nonlinear character of Yucca Mountain tuffs. Limited data on the material properties for these tuffs in combination with their highly heterogeneous nature make it advantageous to use both deterministic and stochastic methods.

**The Nevada Nuclear Waste Storage Investigations Project, managed by the Nevada Operations Office of the U.S. Department of Energy (DOE), is examining the feasibility of a repository for high-level nuclear wastes at Yucca Mountain. This work was funded by the DOE under contract number DE-AC04-76DP00789.



102.2

Current computational approaches include finite elements (Bixler [1], and Reeves and Duguid [2]), integrated finite differences (Pruess and Wang [3], and Wang and Narasimhan [4]), and standard finite differences (Travis et al. [5]). All of these approaches include some form of Darcy's law and a mass balance equation. The resulting codes vary in complexity from one-dimensional, single-phase, isothermal flow to multidimensional, multiphase, nonisothermal flows. Most of them use a pressure equilibrium formulation as described by Peters and Klavetter [6]. They all use numerical procedures that maintain computational stability even when the values of the material properties, such as permeability and moisture capacitance, vary by several orders of magnitude.

A limited number of experiments have been carried out on these tuff materials. Difficulties arise because of the extremely low pore pressures that exist in the unsaturated rock (about negative 100 bars for saturation of 0.5) and the long experimental time scales required. Numerous laboratory-scale experiments have been run to determine the pressure-saturation functions for each of the geological strata that exist in the mountain (Peters et al. [7]). Other experiments have been run to determine the nature of water flow through typical rock cores (Reda [8], and Peters et al. [9]). The results of these and other field and laboratory scale studies are discussed. Computational results are compared with experimental results where they are available. These comparisons indicate the need for further experimentation.

## References


1. N. E. Bixler, "NORIA—A Finite Element Computer Program for Analyzing Water, Vapor, Air, and Energy Transport in Porous Media," SAND84-2057, Sandia National Laboratories, Albuquerque, NM, August 1985.

2. M. Reeves and J. O. Duguid, "Water Movement Through Saturated-unsaturated Porous Media: a Finite-Element Galerkin Model," ORNL-4927, Oak Ridge National Laboratory, Oak Ridge, Tennessee, 1975.

3. K. Pruess and J. S. Wang. "Numerical Modeling of Isothermal and Nonisothermal Flow In Unsaturated Fractured Rock," in Flow and Transport Through Unsaturated Fractured Rock. Geophysical Monograph 42. ed. D. D. Evans and T. J. Nicholson. American Geophysical Union, Washington, DC, 1987.

4. J. S. Y. Wang and T. N. Narasimhan, "Hydrologic Mechanisms Governing Fluid Flow in Partially Saturated, Fractured. Porous Tuff at Yucca Mountain," SAND84-7202. Sandia National Laboratories, Albuquerque. NM, April 1985.

5. B. J. Travis, S. W. Hodson, H. E. Nuttal, T. L. Cook, and R. S. Rundberg, "Preliminary Estimates of Water Flow and Radionuclide Transport in Yucca Mountain." Mat. Res. Soc. Symp. Proc. Jol. 26, pp. 1039-1047, 1984.

6. R. R. Peters and E. A. Klavetter, "A Continuum Model for Water Movement in an Unsaturated Fractured Rock Mass." Water Resources Research, Vol. 24. No. 3. pp. 416-430, March 1988.

7. R. R. Peters, and E. A. Klavetter, I. J. Hall, S. C. Blair, P. R. Heller and G. W. Gee. "Fracture and Matrix Hydrologic Characteristics of Tuffaceous Materials from Yucca Mountain, Nye County, Nevada," SAND84-1471, Sandia National Laboratory Albuquerque, NM, December 1984.

8. Daniel C. Reda, "Influence of Traverse Microfractures on the Imbibition of Water Into Initially Dry Tuffaceous Rock," in Flow and Transport Through Unsaturated Fractured Rock, Geophysical Monograph 42, ed. D. D. Evans and T. J. Nicholson. American Geophysical Union, Washington, DC, 1987.

9. R. R. Peters, E. A. Klavetter, J. T. George and J. H. Gauthier, "Measuring and Modeling Water Imbibition Into Tuff," in Flow and Transport Through Unsaturated Fractured Rock, Geophysical Monograph 42, ed. D. D. Evans and T. J. Nicholson, American Geophysical Union, Washington, DC, 1987.

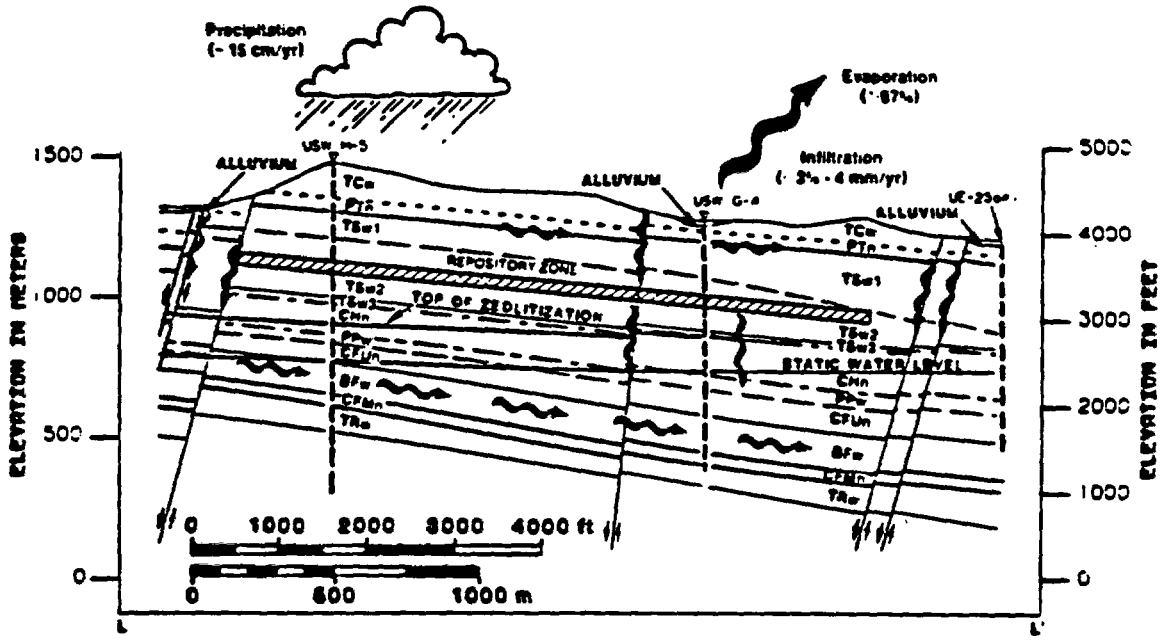


Figure 1: E-W Cross-section of Yucca Mountain Showing Layering of Welded (e.g., TCw) and Non-welded (e.g., PTn) materials. Cross-hatched Area Shows Proposed Repository Position.

<AND 89-0074 A

# Analysis of Proposed Laboratory Experiments in Partially-Saturated Small-Pore Fractured Rock [1]

R. R. EATON R. C. Dykhuizen, and A. J. Russo (Sandia National Laboratories, Albuquerque, NM 87185)

A set of pretest numerical calculations has been made to predict transient saturation profiles through a centimeter-scale small-pore rock with a small discrete fracture. The impetus of this numerical/experimental investigation is to determine the effect of micro fractures on the transport of water through highly-fractured partially-saturated hard rock. In these calculations, the fracture length relative to the contact region existing between the fracture surfaces was numerically varied between the extremes of no fracture to a fracture that completely traversed the two-dimensional test sample. The contact region between the fracture surfaces is considered to have the characteristics of the intact rock mass. The calculated results show that the ratio of the fracture length to the length of the contact region has a significant effect on the rate at which the saturation front traverses the test sample. A set of calculations was also made in which the discrete fracture was modeled using a composite model to simulate the fracture by area weighting the material/fractre properties. Disagreement in the results implies that the composite model is not adquate for these geometries. Experimental test times of a month are predicted for rocks having matrix permeabilities in the range of $10^{-20}$ $m^2$. The results of the discrete fracture calculations are being used to predict appropriate experimental parameter ranges for sample size, fracture size, and matrix material. Gamma-beam densitometry, a nonintrusive diagnostic technique, will be used to measure transient saturation distributions in the planed laboratory experiments.

[1]This work was funded by the the Yucca Mountain Project, managed by the Nevada Operations Office of the U. S. Department of Energy (DOE), which is examining the feasibility of a repository for high-level nuclear wastes at Yucca Mountain. DOE contract number DE-AC04-76DP00789.

SAND88-7059A

ABSTRACT

# UNDERGROUND REPOSITORY DESIGN METHODOLOGY FOR A REPOSITORY IN TUFF*

By

M. P. Hardy and C. M. St. John
J. F. T. Agapito & Associates, Inc.

To be presented at the joint SME/SEF Applied Mechanics Conference, Berkeley - June 20-22, 1988

## ABSTRACT

Excavation stability is required during construction, emplacement, retrieval (if required), and closure of a nuclear waste repository to ensure worker health and safety. Excavation stability is ensured by appropriate excavation procedures and installation of rock support reinforcement systems where required. Based on excavation experience in other tuff, excavation stability is expected to be favorable in the Topopah Spring Member at the Yucca Mountain site, requiring only minimal rock support in the majority of excavations. A priori evaluation of stability is required, however, to evaluate different waste configurations during planning and to support the license application process.

An assessment of stability requires that the potential mechanism of rock deformation and failure be understood. Experience in the Topopah Spring Formation, which includes core hole data and regional geologic mapping, indicate that the host rock at the repository horizon, welded tuff, is strong, chemically stable, and above the water table. The jointing is expected to be predominantly near vertical with variable joint spacings. Deformation is expected to be controlled by jointing. The underground facility will be designed for an operational life of up to 100 years, with temperature changes of over 170°C near the emplaced waste and from 50°C to 100°C around emplacement rooms, depending on the emplacement option.

A methodology for assessing stability based on site conditions, empirical, analytical, and subsequently, observational methods is presented. The emphasis is on analytical methods using numerical excavation experience in tuff at elevated temperatures, and observational methods are only applicable during construction and monitoring. The analytical methodology includes methods for analysis of systematically jointed rock masses (compliant joint methods), randomly jointed and widely spaced discrete joints. Rock loads from in-situ stress, thermal expansion, and seismic events are considered. Ground support requirements are assessed from the extent of the region of joint slip or rock mass failure. The credibility of any analytical methodology depends on the quality of the input parameters and validation of the methodology via comparisons with controlled full-scale demonstrations and back-analysis of appropriate case examples. Such demonstrations and case studies will be provided during the exploratory shaft construction and tests.

*This work was supported by the U. S. Department of Energy (US DOE) under contract DE-AC04-76DP00789.

# USE OF PERFORMANCE ASSESSMENTS TO GENERATE A REPOSITORY Q-LIST

L. J. Jardine
Bechtel National Incorporated
San Francisco, California 94119

and

T. W. Laub
Sandia National Laboratories
Division 6311, Nuclear Waste Engineering Projects
Albuquerque, New Mexico 87185

## SUMMARY

Items identified and classified as important to safety are placed on the repository Q-list. The Q-list identifies structures, systems, and components that are subject to quality assurance requirements beyond standard engineering practices as specified by 10 CFR 60, Part G. These QA requirements correspond to those imposed by 10 CFR 50, Appendix B for safety class systems in nuclear power plants. These QA measures are applied to the repository design, procurement, and construction activities and operations to provide a higher degree of assurance that Q-list items will perform their intended functions. The QA measures are implemented by the direct incorporation of the requirements into appropriate design documents, such as drawings, specifications, and operational procedures.

An assessment to identify items important to safety was completed for the proposed Yucca Mountain repository. The assessment implemented a classification methodology based on general guidance developed by the Department of Energy (DOE) for use by all repository projects (Ref. 1). Although some qualitative judgment techniques were used, the assessment was based on quantitative dose and frequency performance assessments. This paper will discuss the results of applying a performance assessment to generate the initial Yucca Mountain repository Q-list.

Items important to safety are defined by the NRC as "those engineered structures, systems, and components essential to the prevention or mitigation of an accident that could result in a radiation dose to the whole body, or any organ, of 0.5 rem or greater at or beyond the nearest boundary of the unrestricted area" (Ref. 2). This definition provides a single criterion, a dose specification, for identifying items important to safety. For purposes of identifying items important to safety, a second criterion, a minimum frequency of occurrence, has been defined by DOE for applicable or credible accident scenarios (Ref. 1). Therefore, two numerical criteria have been identified that allow quantitative performance assessment methods to be used to identify items important to safety:

This work performed at Sandia National Laboratories was supported by the U.S. Department of Energy under contract number DE-AC04-76DO0789.

(1) The dose criterion--an accident must cause an offsite radiation dose of 0.5 rem or greater to merit consideration in identifying items important to safety

(2) The frequency criterion--an accident must have a frequency of occurrence greater than $1 \times 10^{-5}$ per year to be credible and therefore considered in identifying items important to safety.

If an accident exceeds both of these criteria, then one or more of the systems, structures, or components whose failure results in exceeding these criteria are important to safety. It is important to note that the dose criterion is not a limit for accident consequences; it is a threshold for identifying items important to safety. A dose limit for accidents at a geologic repository has not yet been established in the federal regulations.

A formalized method for classifying items important to safety was developed in accordance with current DOE and NRC guidance (Refs. 1, 3). The method is based on a performance assessment approach as described in Ref. 4 together with the detailed analyses and results from this method. Figure 1 illustrates this method.

To apply the classification methodology, the repository was separated into 13 compartments, each consisting of different zones containing various types of radioactive materials. Assessments were performed within each compartment to determine initiating events and accident conditions that could result in offsite doses. All items in each compartment were then analyzed for their response to a spectrum of initiating events. Twenty-seven event trees were constructed to systematically summarize the initiating events and various accident sequences. Frequencies of occurrence and offsite dose consequences were estimated for each accident sequence.

The 27 event trees contained 149 accident sequences; of these, 45 sequences had zero dose consequences. The other 104 sequences were estimated to have either doses greater than 0.01 mrem or frequencies larger than $10^{-14}$ per year. Of these, only 3 sequences exceeded one of the two important-to-safety screening criteria; three others were close to both criteria, but did not exceed either one. None of the sequences exceeded both criteria.

Scenarios which exceed both criteria are classified as Q-scenarios. Because no sequences exceeded both the dose and frequency criteria, no further analyses were required at this stage in the design to determine which of the structures, systems, or components involved in the Q-scenarios are important to safety. Scenarios which do not exceed the two criteria are classified as either "Non-Q Scenario (NQ)" or "Potential-Q Scenario (PQ)." All NQ scenarios are those well below the screening criteria and thus are eliminated from further consideration in identifying items important to safety.

Any scenarios not classified as Q or NQ scenarios but judged to have a reasonable potential to be upgraded to Q-scenarios, were classified as PQ scenarios. PQ scenarios were subjected to further analysis to determine

which items should be placed on a "potentially" important to safety list. Scenarios were classified as PQ if there were judged to be sufficient uncertainties in these initial performance assessments to warrant further investigation to ensure that the results would not exceed the dose and frequency criteria.

At present, no items are classified as important to safety for the tuff repository; however, there are ten items that are potentially important to safety. The first of these is a crane in the cask receiving and preparation area of the waste-handling building. In this case, a crane drop of a shipping cask is the initiating event of the PQ scenario. The second item potentially important to safety is the shipping cask dropped by the crane. The third, fourth, and fifth items are cranes in hot cells. The sixth item is the packaging hot cell structure. These four items were identified in scenarios initiated by an earthquake. The last four items are the truck and railcar vehicle stops in the cask receiving and preparation area, the waste-handling building fire protection system, the underground waste transporter cask, and the container transfer machine. The assumptions made and the analyses performed to identify and classify these items were extremely conservative, and therefore further refinement of this work is unlikely to identify any items that must be placed on the tuff repository Q-list.

## REFERENCES


1. Department of Energy, "Guidance for Developing the SCP-CDR and SCP Q-lists," Prepared for DOE by Roy F. Weston, Inc., Washington, D.C. (July 1986).

2. Code of Federal Regulations, Title 10, Energy, Chapter 1, Nuclear Regulatory Commission, Part 60, "Disposal of High-Level Radioactive Wastes in Geologic Repositories," Washington D.C. (January 1, 1985).

3. Division of Waste Management, "Draft Generic Technical Position on Items and Activities in the High-Level Waste Geologic Repository Program Subject to 10 CFR Part 60 Quality Assurance Requirements," U.S. Nuclear Regulatory Commission, Washington D.C. (July 1986).

4. H.R. MacDougall, L.W. Scully, and J.R. Tillerson, "Nevada Nuclear Waste Storage Investigations Project Site Characterization Plan Conceptual Design Report," SAND84-2641, Sandia National Laboratories, Albuquerque, New Mexico (September 1987).

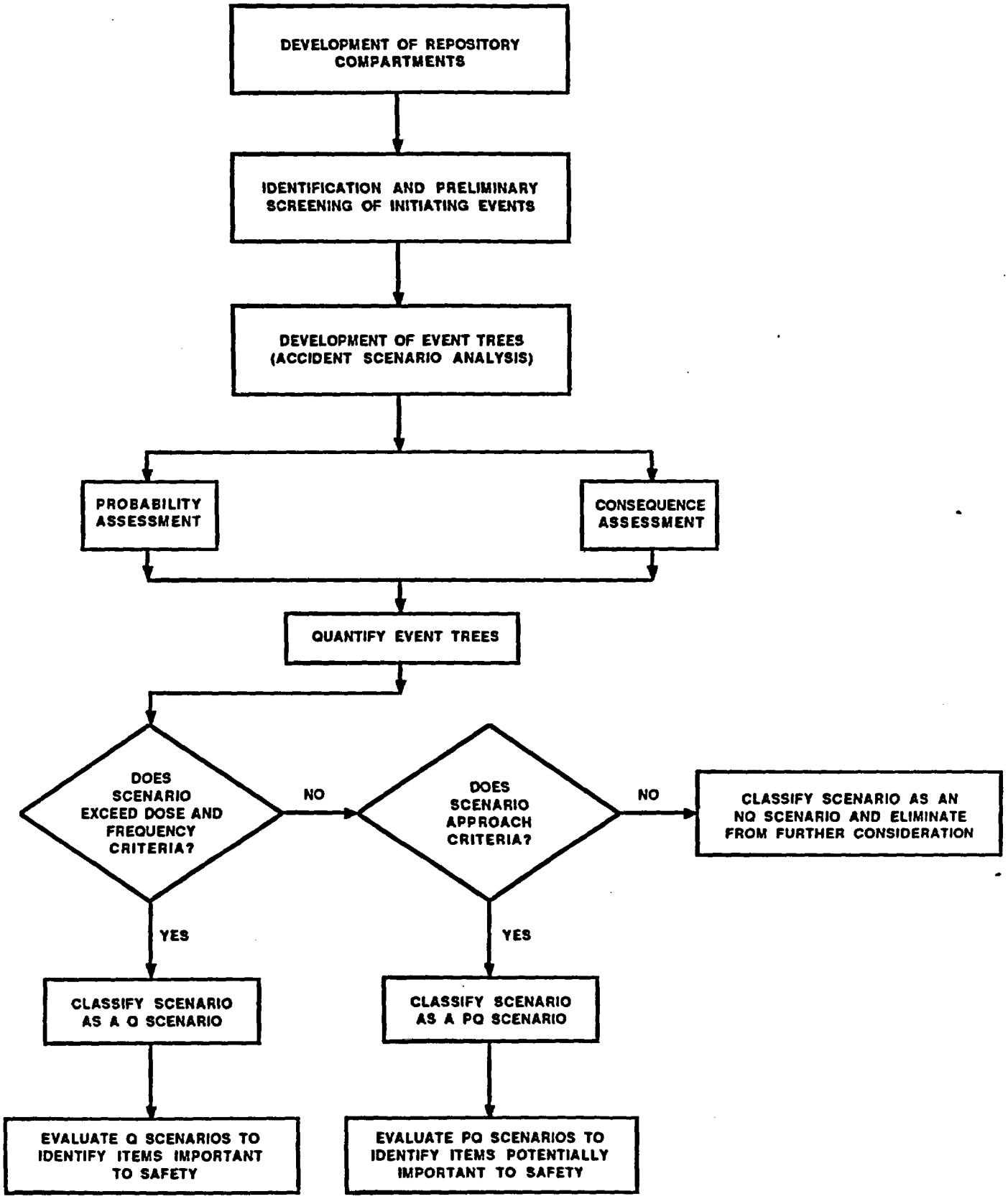


Fig. 1 Performance Assessment Method for Identifying Items Important to Safety

SAND 88-2868C

# APPROACHES TO GROUNDWATER TRAVEL TIME*

SAND88-2868C

Paul Kaplan, Elmer Klavetter, and Ralph Peters
Sandia National Laboratories
Albuquerque, NM 87185

Waste Management '89 Conference Proceedings

## ABSTRACT

One of the objectives of performance assessment for the Yucca Mountain Project is to estimate the groundwater travel time at Yucca Mountain, Nevada, to determine whether the site complies with the criteria specified in the Code of Federal Regulations, Title 10 CFR 60.113 (a)(2). The numerical standard for performance in these criteria is based on the groundwater travel time along the fastest path of likely radionuclide transport from the disturbed zone to the accessible environment. The concept of groundwater travel time, as proposed in the regulations, does not have a unique mathematical statement. The purpose of this paper is to discuss (1) the ambiguities associated with the regulatory specification of groundwater travel time, (2) two different interpretations of groundwater travel time, and (3) the effect of the two interpretations on estimates of the groundwater travel time.

## THE REGULATION

Technical criteria for the disposal of high-level radioactive waste in geologic repositories have been published by the U.S. Nuclear Regulatory Commission (NRC). Included under 10 CFR 60.113, "Performance of particular barriers after permanent closure," is a provision specifying criteria for the geologic setting (1).

> "The geologic repository shall be located so that prewaste-emplacement groundwater travel time along the fastest path of likely radionuclide travel from the disturbed zone to the accessible environment shall be at least 1,000 years or such other travel time as may be approved or specified by the Commission."

The authors have made two assumptions about the intent of the groundwater travel time regulation stated above: (1) the criteria are intended to provide a simple measure of the ability of the natural barriers at the site to restrict the transport of contaminants to the environment, and (2) the calculation of a groundwater travel time is to be performed only along the physical paths by which contaminants are likely to travel.

* This work was supported by the U.S. DOE under contract DE-AC04-76DP00789.

## THE PROBLEM

The regulation defines groundwater travel time in a manner that is ambiguous and allows more than one interpretation. Ambiguities associated with the meaning of groundwater travel time arise, in part, from two simultaneous processes that redistribute mass as fluid flows through a system. The first process is mechanical dispersion (2), which occurs in a moving flow field. The second process is diffusion, which transports mass from one part of a system to another as a result of random molecular motion (3). The combination of both processes in a moving flow field is often called hydrodynamic dispersion (2). As a result of hydrodynamic dispersion, variations in the concentration of mass occur within the flow system. The assumption is also made that the behavior of the particle represents some ensemble property of the quantity of mass injected into the system. This assumption may also result in additional interpretations.

## TWO GROUNDWATER TRAVEL-TIME INTERPRETATIONS

Two different interpretations of groundwater travel time will be used to calculate the cumulative travel time through a hypothetical, one-dimensional, 100 m column of fractured rock. Flow fields have been determined for two different water fluxes through the column. The first flow field has been calculated using a low flux rate. As a consequence, flow through the column is predominantly in the porous matrix with little flow in the fractures. The second flow field has been calculated using a high flux rate. Under this condition, more than 85% of the flow is carried by the fractures. The following two interpretations of the criteria have been used to approximate groundwater travel times at both flux rates.

### Interpretation 1--Particle Track

The travel time of an imaginary particle from the input boundary to the end of the column is calculated as the distance traveled divided by the average velocity. In a system comprising both matrix and fractures, the fastest continuous pathway is used to calculate the groundwater travel time. Neither dispersion nor diffusion is included as a flow mechanism.

### Interpretation 2--Conservative Tracer

The movement of a packet of nonsorbing, nonreacting tracer is calculated. The tracer can move back and forth between the fractures and the matrix as a result of dispersion and diffusion. Travel time is the time required for some fraction of the tracer to move through and exit from the system.

## RESULTS OF THE CALCULATIONS

The results of the groundwater travel-time calculations under low flux conditions are illustrated in Fig. 1, and the results under high flux conditions are illustrated in Fig. 2. The solid curves in both graphs represent the cumulative percent of the injected tracer mass leaving the column versus time in years, and are the consequence of calculating

groundwater travel time using a conservative tracer (Interpretation 2). The range of groundwater travel time over many years is the result of hydrodynamic dispersion. The circle in each figure is the travel time calculated using Interpretation 1. The circles are plotted on the 100% axis for ease of viewing. Table I summarizes the groundwater travel times for both flux rates using the two interpretations of the criteria for each of the two flux conditions.

TABLE I
Calculated Groundwater Travel Times

| Groundwater Travel Time Interpretation | Matrix Flow Low Flux (yr) | Fracture Flow High Flux (yr) |
|---|---|---|
| 1. Particle | 400,000 | 2.6 |
| 2. Tracer | 20,500-1,000,000 | 2.6-1,000,000 |

Low Water Flux

Under low flux conditions, where flow occurs predominately within the porous matrix of the column, the groundwater travel time of the particle is 400,000 yr. This agrees reasonably well with the 50% breakthrough of the tracer as seen in Table II. The tracer first arrives in some quantifiable portion (0.00000000000000000001%) in about 20,000 yr. At the end of a million years, tracer is still leaving the system. The concept of groundwater travel time is meaningless under these circumstances unless some mass fraction of the tracer is specified as illustrated in Table II.

TABLE II
Groundwater Travel Times Using the Cumulative Percent of Tracer Leaving the System

| Tracer (Cumulative %) | Matrix Flow Low Flux (yr) | Fracture Flow High Flux (yr) |
|---|---|---|
| 1 | 140,000 | 4,500 |
| 50 | 360,000 | 10,500 |
| 99 | 1,000,000 | 31,500 |

Fig. 1. Low Water Flux (Predominant Matrix Flow)

Fig. 2. High Water Flux (Predominant Fracture Flow)

## High Water Flux

Under high flux conditions, more than 85% of the water is transmitted through the fractures. The particle traverses the entire column in 2.6 yr (flux has been increased fourfold) (Fig.2). The marked decrease in travel time results from fracture conductivities that are much higher than the matrix conductivity. The fastest path through the column is calculated using Interpretation 1 for groundwater travel time, regardless of the quantity of fluid. The difference between the two interpretations is rather dramatic under high flux conditions as can be seen by the breakthrough curve of the tracer. The particle can be thought of as the first, infinitesimally small amount of tracer that exits the column. It should be pointed out that only 0.000000000000000000000004% of the injected tracer leaves the column when 500 yr have passed.

## DISCUSSION AND CONCLUSION

The calculations illustrate that different interpretations of the GWTT criteria determined can yield vastly different groundwater travel times. The behavior of a single particle may not be representative of the flow field. The use of a tracer, while possibly providing a better perspective of the transfer of mass through the system, requires that the travel time be specified in terms of some fraction of that mass. It is not the purpose of this paper to argue the relative merits of one method over another. The point we wish to make is that to determine a level of compliance with the regulatory criteria the regulation must not be ambiguous.

## REFERENCES

1. U. S. Nuclear Regulatory Commission, "Disposal of High-Level Radioactive Wastes in Geologic Repositories," Code of Federal Regulations, Energy, Title 10, Part 60, Washington, D.C., January 1986.

2. R. A. FREEZE and J. A. CHERRY, "Groundwater," Prentice-Hall, Inc., Englewood Cliffs, New Jersey (1979).

3. J. CRANK, "The Mathematics of Diffusion," Oxford University Press (1979).

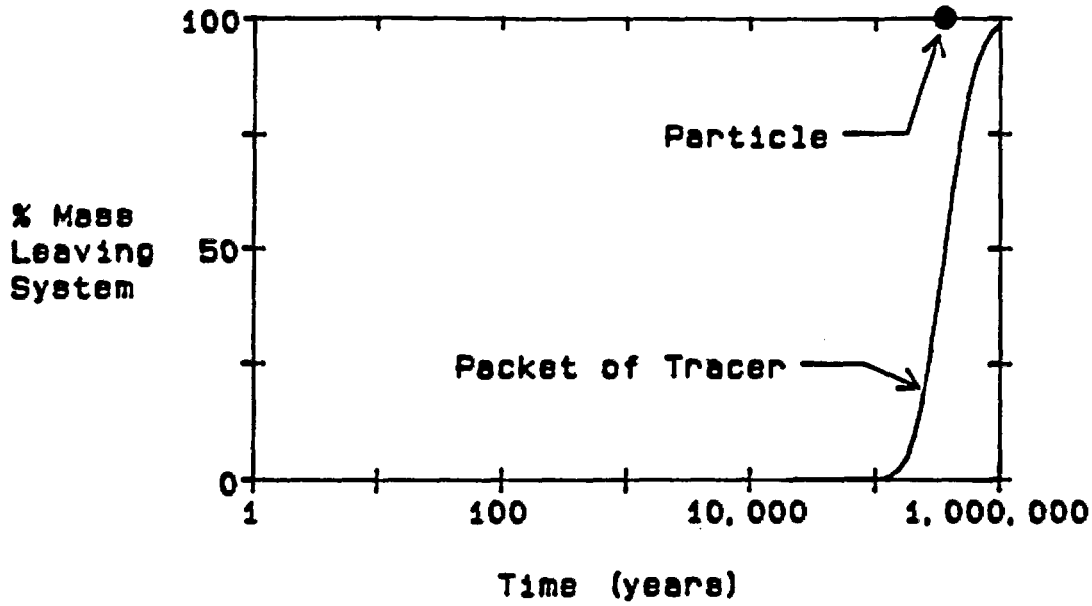
100
50
0
% Mass
Leaving
System
Particle
Packet of Tracer
1
100
10,000
1,000,000
Time (years)

Fig 1

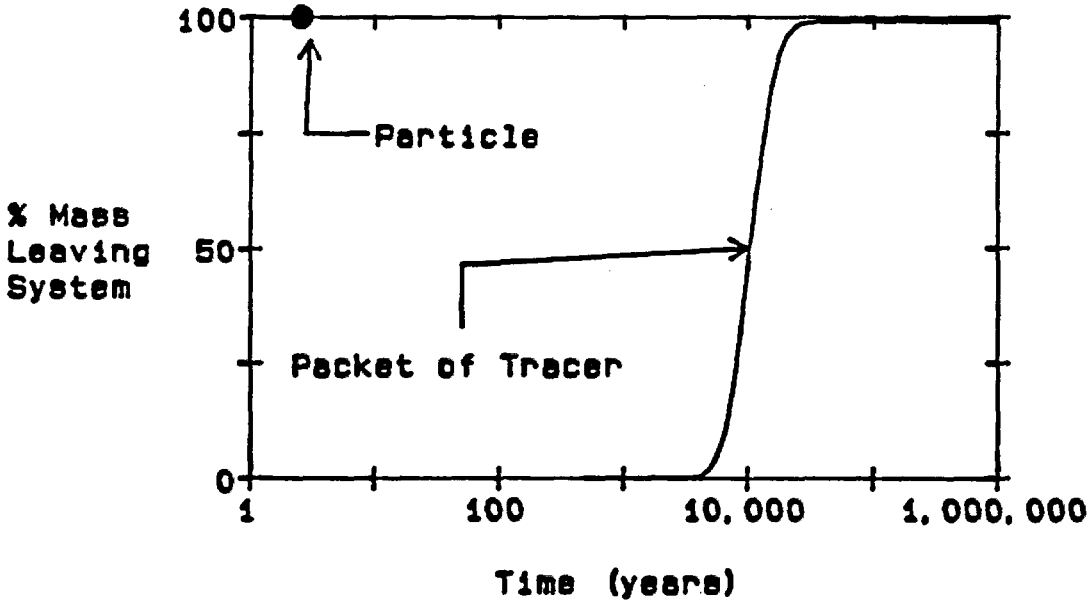
100
50
0
% Mass
Leaving
System
Particle
Packet of Tracer
1
100
10,000
1,000,000
Time (years)

Fig 2

SAND88-2868C

# Approaches to Groundwater Travel Time

Paul Kaplan
Elmer Klavetter
Ralph Peters

Sandia National Laboratories
Albuquerque, New Mexico 87185

This work was supported by the U.S. Department of Energy (US/DOE) under contract #DE-AC04-76DP00789. The analyses for this document were gathered under Quality Assurance Level NQ.

# The Regulation

The geologic repository shall be located so that pre-waste-emplacement *groundwater travel time* along the fastest path of likely radionuclide transport shall be *at least 1,000 years* or such other time as may be specified by the Commission.

10 CFR Part 60.113 (a)(2)

1

# The Problem

How do we interpret the GWTT regulation to remove the ambiguities in assessing the performance of a site for potential licensing of a high-level radioactive waste repository.

# Assumptions

The following assumptions have been made about the intent of the groundwater travel time (GWTT) regulation:

1. The criterion is to provide a simple measure of the ability of the natural barriers to restrict the transport of contaminants to the accessible environment.

2. The calculation of GWTT is to be performed only along the physical paths by which contaminants are likely to travel.

# The Ambiguities

The concept of GWTT as stated in the regulation has no precise meaning and multiple interpretations have been proposed.

Ambiguities associated with the meaning arise, in part, from two simultaneous processes - dispersion and diffusion. Both contribute to the redistribution of mass and a variation in solute concentrations as fluid flows through the system.

To determine a level of compliance with the criteria, the regulation must be unambiguous.

# GWTT Calculations Using Two Different Interpretations

# Hydrologic Flow Fields

Flow fields in a fractured, porous medium were determined for 2 different water fluxes.

Lower Water Flux - flow is predominantly in the porous matrix with sparse flow in the fractures.

Higher Water Flux - water flow is split between the matrix and the fractures. Over 85% of the flow is in the fractures.

# Two GWTT Interpretations

**Particle Track** - The travel time of an imaginary particle from the starting point to the exit is calculated as the distance traveled divided by the average velocity. In a system comprising both matrix and fractures, the fastest continuous pathway is used to calculate the GWTT. Neither dispersion or diffusion are included.

is

**Tracer** - The movement of a packet of nonsorbing, nonreacting tracer is calculated. The tracer can move back and forth between the fractures and the matrix as a result of dispersion and diffusion. Travel time is the time required for some fraction of the tracer to move through the system and exit from it.

**Figure 1**

LOWER WATER FLUX
(Predominant Matrix Flow)

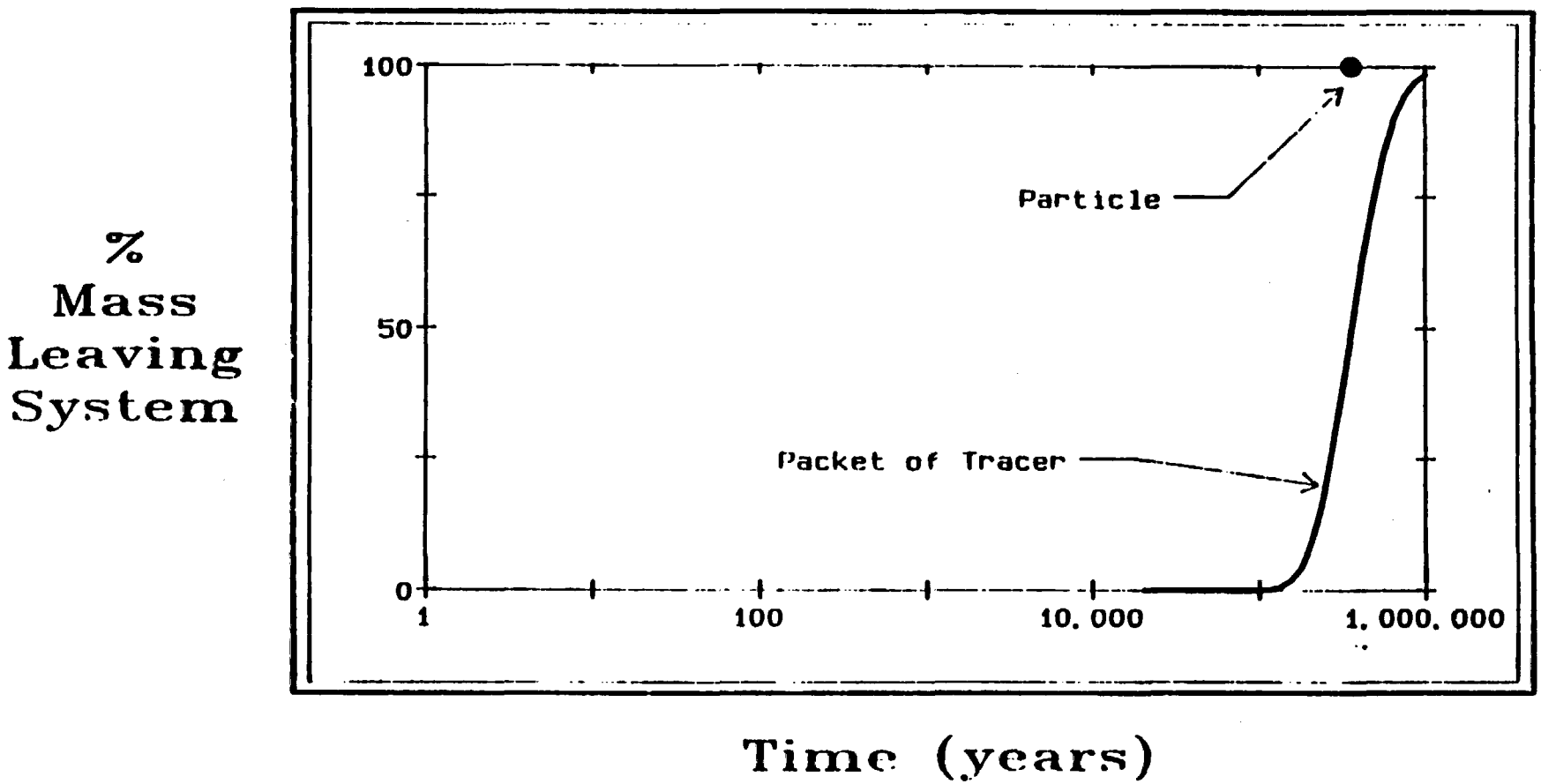

**Figure 2**

## HIGHER WATER FLUX
## (Predominant Fracture Flow)

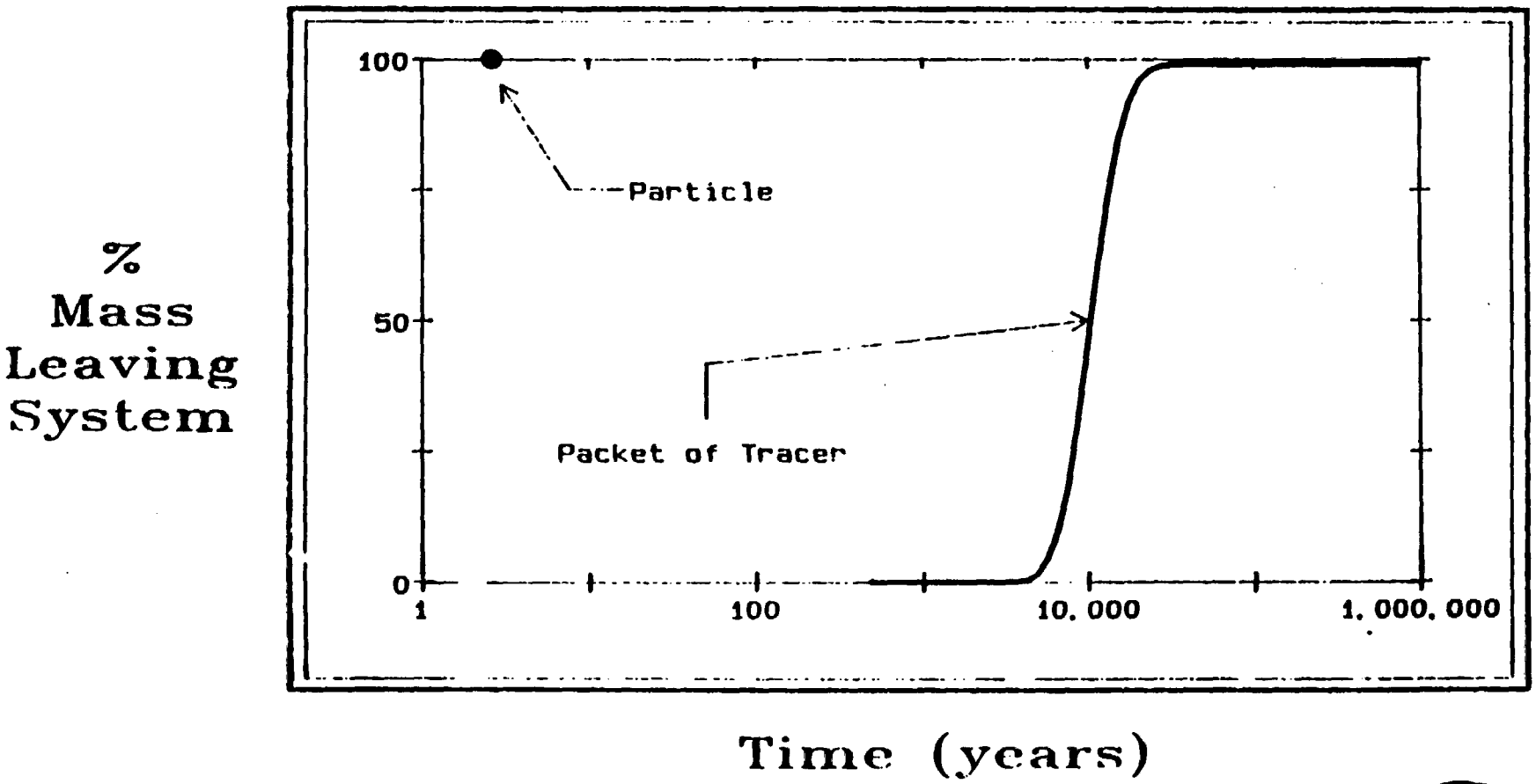

# Calculated GWTT's

| GWTT Interpretation | Low Flux (matrix flow) | High Flux (fracture flow) |
|---|---|---|
| Particle | 400,000 yrs | 2.6 yrs |
| Tracer | 20,500 to 1,000,000 yrs | 2.6 to 1,000,000 yrs |
| 1% tracer | 140,000 yrs | 4,500 yrs |
| 50% tracer | 360,000 yrs | 10,500 yrs |
| 99% tracer | 1,000,000 yrs | 31,500 yrs |

What criteria should be used to pick a groundwater travel time?

On what basis should the criteria be chosen?

# Discussion

Figures 1 and 2 illustrate that different interpretations of the method by which groundwater travel time is calculated can yield vastly different results.

In addition, the tracer interpretation requires a specification of the fraction of mass leaving the system to define a travel time for the regulation.

# Conclusion

Only when a numerical criterion limiting the mass flux at 1,000 years at the compliance boundary is specified can one make an evaluation of whether a site complies with the GWTT regulation.

# APPENDIX

## Information from the Reference Information Base Used in this Report

This report contains no information from the Reference Information Base.

## Candidate Information for the Reference Information Base

This report contains no candidate information for the Reference Information Base.

## Candidate Information for the Site & Engineering Properties Data Base

This report contains no candidate information for the Site and Engineering Properties Data Base.

SAND88 - 2247C

# Modeling the Uncertainties in the Parameter Values of a Layered, Variably Saturated Column of Volcanic Tuff Using the Beta Probability Distribution

Paul G. Kaplan and Lane Yarrington

Sandia National Laboratories
Albuquerque, New Mexico

Abstract

The geologic formations in the unsaturated zone at Yucca Mountain, Nevada, on and adjacent to the Nevada Test Site, are being investigated as the proposed site of a repository for the disposal of high-level radioactive waste. The Department of Energy is conducting studies of this site through the Yucca Mountain Project. The numerical and conceptual tools that will be used to analyze the site are currently under development. This paper reports the status of a probability model that has recently been implemented to address uncertainties in quantitative predictions of parameter values. The model can also be used to quantify the changes in uncertainty that occur as more information is obtained.

Sparse sampling data, unknown errors in measurement, and the inherent variability of natural materials give rise to uncertainties in the choice of appropriate parameter values to represent those materials in models. The beta probability distribution is used to quantify the uncertainties associated with the parameter values and can be used to test the consequences of the analyst's subjective judgment on the density function of the input parameters.

This work performed at Sandia National Laboratories was supported by the U. S. Department of Energy under contract DE-AC04-76D00789. The data used in this paper are NQ.

Ten parameters for each hydrostratigraphic unit are required as input to a numerical model that is now available for preliminary studies of one-dimensional, steady-state flow through variably saturated rock. Natural analog data, site data, theoretical considerations, functional limitations, and subjective judgment are all used to constrain the beta probability density of the input parameters. To obtain a beta distribution requires four quantitative pieces of information: an upper and lower bound, an estimate of the expected value, and an estimate of the coefficient of variation. No prior assumption about the shape of the distribution is required. The shape and the probability density are functionally constrained by the analyst's estimates of the four required values.

The consequences of treating the input parameters as independent, random variables are tested by repeated Monte Carlo sampling of the cumulative density functions of the input parameters. This process generates simulation data that are used to construct histograms of the state variables and the output parameters in a hypothetical groundwater travel time exercise.

## 1. Introduction

The geologic formations in the unsaturated zone at Yucca Mountain, Nevada, on and adjacent to the Nevada Test Site, are being investigated as the proposed site of a repository for the disposal of high-level radioactive waste. The Department of Energy is conducting studies of this site through the Yucca Mountain Project. Sandia National Laboratories is currently one of the organizations developing conceptual and numerical tools that will be used to analyze the behavior of the site. This paper documents the status of a model recently implemented to address uncertainties in the distribution of parameter values that are used in groundwater travel time simulations of a variably saturated environment.

Within the context of this paper both the input and the output parameters will be defined as random variables. A random variable is a numerical variable whose specific value cannot be predicted with certainty before an experiment (Benjamin and Cornell, 1970). To clarify this concept for the application that will follow, consider a random hydrologic variable as a numerical parameter whose specific value cannot be predicted with certainty before measurement. Each individual measurement can be thought of as an experiment. The same value of the variable can occur more than once if measurements are repeated.

If one could take repeated measurements, a histogram describing the frequency with which certain ranges of values occur could be constructed. Eventually the process of repeated measurement would allow the statistical behavior of the variable to be computed. The variable is no longer described as a single-valued entity but as a function of its statistical parameters.

In many geologic and hydrogeologic investigations, the repeated measurements required to compute a statistical description of the behavior of the property of interest are not performed. Therefore, emphasis here shifts from the computation of the statistics of the sampled data to a measure of chance or likelihood based on the sampled data. This is the difference between statistics and probability (Chow, 1964). The concept of the random variable has not been abandoned because a statistical description of the variable cannot be calculated. Instead of a statistical description, a probabilistic description has been constructed based on the extent of information available about the variable.

In this paper, we present a method for generating probabilistic descriptions of uncertain model parameters using the beta probability function (Harr, 1987). To illustrate the method, we have applied it to estimate parameter distributions for a Monte Carlo simulation of groundwater travel time through a layered sequence of variably saturated volcanic tuffs. The exercise is strictly hypothetical.

## 2. Statement of the Problem

The overall objective of the Yucca Mountain Project is to determine whether the natural system in conjunction with a system of engineered barriers does or does not meet a level of safety specified by the regulatory community. On a more limited scope, individual activities within the Project address specific regulatory criteria. The objective of one task is to estimate the liquid groundwater travel time at Yucca Mountain, Nevada, to evaluate compliance with the criteria specified in 10CFR60.113(a)(2)(NRC, 1986). The numerical standard for performance in the regulatory criteria is the groundwater travel time along the fastest path of likely radionuclide transport between two boundaries defined to evaluate compliance, the disturbed zone and the accessible environment. The compliance period is stated as a travel time of at least 1000 years or any other period set by the Nuclear Regulatory Commission. Therefore, the objective of the one task is to determine whether the natural system does or does not meet the groundwater travel time criterion.

Sparse sampling data, errors in measurement, and the inherent variablity of natural materials have given rise to uncertainties in the choice of appropriate parameter values to use in numerical simulations of groundwater flow. This paper discusses one technique currently in use to construct probability density functions of model input parameters. The specific objective of the work of the one task is to quantify the probability that the Yucca Mountain site will fail to meet the groundwater travel time requirement specified in 10CFR60.

## 3. The Beta Distribution

If the input parameters are treated as random variables, a functional description of their probabilistic behavior is required. At a minimum the function has to be constrained by the laws of probability. In addition, it is desirable that the function be unbiased in the sense that the analyst refrains from making any prior assumptions about the shape of the function and, therefore, the probabilistic behavior of the variable. The application and use of the beta probability function described in this paper, which meets the two criteria listed above, is given by Harr (1977, 1987).

The beta probability distribution is defined over the range [a,b] by

$$f(x) = C(x - a)^{\alpha}(b - x)^{\beta} \quad , \tag{1}$$

where $\alpha$ and $\beta$ are > -1 and C, the normalizing constant, is

$$C = (\alpha + \beta + 1)!/[\alpha!\beta!(b - a)^{(\alpha+\beta+1)}] \quad , \tag{2}$$

where $\alpha$ and $\beta$ are integers or as

$$C = \Gamma(\alpha + \beta + 2)/[\Gamma(\alpha + 1)\Gamma(\beta + 1)(b - a)^{(\alpha+\beta+1)}] \tag{3}$$

for noninteger values of $\alpha$ and $\beta$ (Harr, 1977, 1987).

A solution of Equation 1 requires four pieces of information: the minimum and maximum values that define the range of the random variable (a and b, respectively) and the two exponents $\alpha$ and $\beta$. The exponents can be calculated if the expected value E[x] and the coefficient of variation V(x) are known as the following equations illustrate.

$$\sigma[x] = E[x]V(x) \tag{4}$$

$$X = (E[x] - a)/(b - a) \tag{5}$$

$$Y = \sigma[x]/(b - a) \tag{6}$$

$$\alpha = (X^2/Y^2)(1 - X) - (1 + X) \tag{7}$$

$$\beta = [(\alpha + 1)/X] - (\alpha + 2) \tag{8}$$

The exponents $\alpha$ and $\beta$ determine the shape of the function. Table 1 summarizes the conditions on the exponents under which certain shapes occur. Plots of the various shapes are illustrated in Figure 1.

TABLE 1

EFFECT OF $\alpha$ AND $\beta$ ON THE SHAPE OF THE DENSITY FUNCTION

| Shape of the Distribution | $\alpha$ | $\beta$ |
|---|---|---|
| Uniform | 0.0 | 0.0 |
| Left Triangle | 0.0 | 1.0 |
| Right Triangle | 1.0 | 0.0 |
| Symmetrical [about (a + b)/2] | $\alpha = \beta$ | $\beta = \alpha$ |
| Skewed Right | $\alpha < \beta$ | $\beta > \alpha$ |
| Skewed Left | $\alpha > \beta$ | $\beta < \alpha$ |
| U-Shape | $\alpha < 0$ | $\beta < 0$ |
| J-Shape | $\alpha \geq 0$ | $\beta < 0$ |
| Reverse J-Shape | $\alpha \leq 0$ | $\beta > 0$ |

An understanding of the definition and concepts behind two of the parameters used, the expected value E[x] and the coefficient of variation V(x), is necessary. The expected value as used in this paper is not a statistically defined property. The calculation of a mean value $\bar{x}$ of N samples is a basic statistical operation that describes an ensemble average, whereas the concept of expected value emphasizes the point that the ensemble does not exist (Dagan, 1986). In application, the analyst must subjectively decide whether the available data or information reasonably reflect the central tendency of the variable of interest. The coefficient of variation is defined as the ratio of the standard deviation to the expected value. The utility of this parameter in the application here derives from the fact that the coefficient of variation is a description of the inherent variability of a property independent of the sample population and can be used in a probabilistic sense to estimate a standard deviation $\sigma(x)$.

In the application that follows, the values of a, b, E[x], and V(x) are assumptions. The beta probability distribution is a transform that takes those assumptions and generates a function that constrains the outcome of repeated experiments. Each assumption is based on the available data, the physical meaning of the variable, the behavior of analog systems, and the subjective judgment of the analyst. There is nothing absolute about the assumptions. Changing any one of the assumptions used as input is likely to affect the distribution. This is one of the great strengths of the technique. It allows the analyst to test in a quantitative and reproduceable manner the consequences of the assumptions about the probabilistic behavior of the variable. It also provides a ready and simple method for updating the distribution as additional data become available. In the end, Equation 1 is nothing more than a model, one of many used in a simulation. The decision to accept or reject a model is always subjective, and the acceptance criteria frequently change as a deeper understanding of the problem evolves.

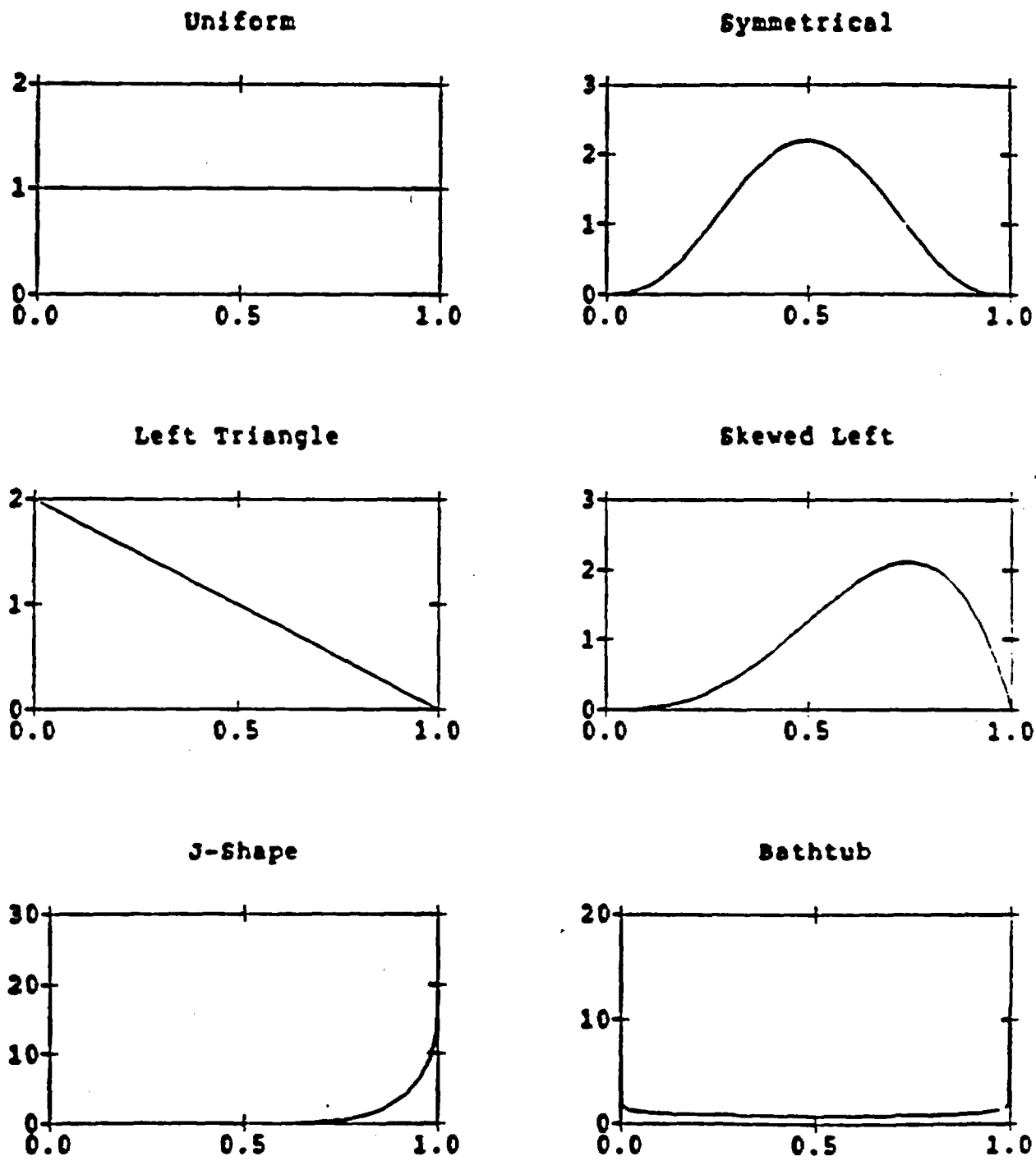


Figure 1. Some Shapes Described By the Beta Distribution

## 4. Using the Beta Distribution in a Groundwater Travel Time Simulation

This section outlines the mathematical models that define the parameters required for a groundwater travel time simulation and the domain through which the flow process will be simulated. A summary of some of the available data is presented. The beta probability distribution will be used to quantify the uncertainties associated with one of the parameters as an example.

### 4.1 Class of Problem

Conceptual models define the parameters that describe the process of variably saturated flow and the physical system being simulated. For the purpose of this exercise, the problem will be treated as a steady-state, one-dimensional flow problem. Only a single fluid phase, the liquid phase, will be considered. The system is assumed to be isothermal, the rock matrix nondeforming, the fluid at constant density. Darcian flow is assumed to occur in response to a matrix and gravitational potential gradient.

These assumptions are simplifications of the real process. The validity of these assumptions as applied to a system comprising layered, pyroclastic rock has yet to be demonstrated.

### 4.2 Mathematical Model

The mathematical model used in this paper to describe unsaturated flow in a fractured, porous medium is the composite model of Klavetter and Peters (1986, 1988). The model's one-dimensional, steady-state form can be expressed as

$$-(K_{m,b} + K_{f,b})\nabla(\psi + z) = q_f + q_m = q_t \quad , \tag{9}$$

where the subscripts m, b, f, and t stand for matrix, bulk, fracture, and total, respectively. The conductivity terms $K_{m,b}$ and $K_{f,b}$ are bulk values for a unit volume of the porous medium and are defined in terms of the total volume $V_t$ and the fracture volume $V_f$ as

$$K_{m,b} = K_m(V_t - V_f)/V_t \tag{10}$$

and

$$K_{f,b} = K_f(V_f/V_t) \quad . \tag{11}$$

The matric potential $\psi$ is a negative pressure potential that results from the capillary and adsorptive forces of the porous medium. The term z is the elevation or gravitational potential and is referenced to an arbitrary datum. The flux terms $q_m$, $q_f$, and $q_t$ are specific discharges representing

the volume of fluid flowing per unit time through a unit area normal to the flow direction (Bear, 1979).

## 4.3 Parameter Models

The hydraulic conductivity and saturation are both defined here as functions of the matric potential $\psi$. The saturation $S(\psi)$ as used here is the "degree of saturation" defined by Campbell (1985) as

$$S(\psi) = V_l/(V_g + V_l) \quad , \tag{12}$$

where the subscripts l and g refer to liquid and gas, respectively. Although $S(\psi)$ appears to be bounded on the range [0,1] by the definition in Equation 12, it is not clear that the bounding values can be achieved under natural conditions (Hillel, 1980).

Equation 13 is the van Genuchten (1978) model describing the desaturation of a porous medium in response to increasing matric potential.

$$S(\psi) = (S_s - S_r)[1/(1 + |\alpha\psi|^n)]^{(1-1/n)} + S_r \quad : \quad \psi \le 0 \quad , \tag{13}$$

where $S_s$ is the maximum saturation the porous material can attain (assumed to be 1.0), $S_r$ is the residual saturation, $\alpha$ is the air entry parameter and is related to the suction force that must be applied to the porous material before fluid will start to drain, and n describes the slope of the desaturation curve. This model describes only the drying curve of what is actually a hysteretic process (Freeze and Cherry, 1979; Nielsen *et al*, 1986).

The equation for $K(\psi)$ uses the parameters $\alpha$ and n as determined by the fit of the van Genuchten model in Equation 13 and the method of Mualem (1976).

$$K(\psi) = K_s [1 - |\alpha\psi|^{(n-1)}(1 + |\alpha\psi|^n)^{-\lambda}]^2/(1 + |\alpha\psi|^n)^{\lambda/2} \quad , \tag{14a}$$

and

$$\lambda = 1 - 1/n \quad . \tag{14b}$$

## 4.4 Velocity Calculations

Average linear flow velocities v through the fractures and matrix are calculated with the following equations from Peters *et al* (1986).

$$v_m = q_m/\phi_m(S_m - S_{m,r}) = -K_{m,b}\nabla(\psi + z)[1/\phi_m(S_m - S_{m,r})] \quad , \tag{15a}$$

and

$$v_f = q_f/\phi_f(S_f - S_{f,r}) = -K_{f,b}\nabla(\psi + z)[1/\phi_f(S_f - S_{f,r})] \quad , \qquad (15b)$$

where $\phi_m$ and $\phi_f$ are the matrix and fracture porosities, respectively, and the subscript r stands for residual.

## 4.5 System Domain

The system that will be simulated in this example extends vertically from the top of the Tuffaceous Beds of the Calico Hills into the Prow Pass Member of the Crater Flat Tuff. The domain is bounded at the base by the water table. The system is modeled after the descriptions of the lithologic log of USW G-4 in Spengler and Chornack (1984) and the lithologic log of USW G-1 in Spengler et al (1981). Alternating units of bedded and nonwelded tuffs of various thicknesses are divided into hydrostratigraphic units in this report on the assumption that a correlation between depositional and diagenetic processes and physical properties may exist. The logs describe the following lithologies: reworked tuffaceous materials, bedded ash-fall tuffs, nonwelded tuffs, and partially welded tuffs.

Unit properties are defined by mathematical and parameter models. Within each unit, each of the properties is assumed to be statistically uniform. The sampled value of the property is assumed to be independent of position within the unit. Variations in the sampled values from experiment to experiment are treated as random, equally probable outcomes of sampling from a unimodal density function of the property.

Labeling the hydrostratigraphic units follows the time stratigraphic units, where CH and PP refer to the Tuffaceous Beds of the Calico Hills and the Prow Pass Member, respectively. Numbering the units designates the paired occurrence of both bedded and nonwelded tuffs, and lower-case n and b refer to nonwelded and bedded, respectively. Table 2 lists the boundary elevations above the water table and thicknesses of the hydrostratigraphy used in this report.

Only one of the hydrostratigraphic units, CH3n, is assigned fracture properties. The corresponding time stratigraphic unit in Drill Hole USW G-1 (Spengler et al, 1981) is described in the lithologic log as partially welded. Although all the units are probably fractured, it is assumed in this exercise that, at high confining stresses, only the partially welded and welded tuffs can sustain fractures having hydrologic properties significantly different from those of the matrix.

TABLE 2

UNIT THICKNESSES AND ELEVATIONS FOR THE HYDROSTRATIGRAPHIC UNITS OF THE CALICO HILLS IN DRILL HOLE USW G-4

| Unit | Top of Unit (m above water table) | Thickness (m) |
|---|---|---|
| CH1n | 111.7 | 4.6 |
| CH1b | 107.1 | 0.5 |
| CH2n | 106.6 | 6.3 |
| CH2b | 100.3 | 2.9 |
| CH3n | 97.4 | 31.8 |
| CH3b | 65.6 | 1.0 |
| CH4n | 64.6 | 30.2 |
| CH4b | 34.4 | 0.1 |
| CH5n | 34.3 | 12.8 |
| CH5b | 21.5 | 17.1 |
| PP1n | 4.4 | 4.4 |

## 4.6 Boundary Conditions

Because of the one-dimensional constraint, only two boundary conditions are required. The upper boundary is a constant infiltration flux boundary. The lower boundary is a water table boundary with a constant matrix potential of $\psi = 0.0$.

## 4.7 Parameters Required

A groundwater travel time simulation that implements the models described previously requires the specification of the 10 parameters listed in Table 3.

TABLE 3

PARAMETERS REQUIRED FOR A SIMULATION OF GROUNDWATER TRAVEL TIME

| Parameter Name | Symbol |
|---|---|
| Matrix Porosity | $\phi_m$ |
| Bulk Matrix Saturated Conductivity | $K_{m,b}$ |
| Matrix Residual Saturation | $S_{m,r}$ |
| Matrix Air Entry | $\alpha_m$ |
| Matrix Desaturation | $n_m$ |
| Fracture Porosity | $\phi_f$ |
| Bulk Fracture Saturated Conductivity | $K_{f,b}$ |
| Fracture Residual Saturation | $S_{f,r}$ |
| Fracture Air Entry | $\alpha_f$ |
| Fracture Desaturation | $n_f$ |

## 4.8 Data in Support of Parameter Estimation

Data derived directly from samples obtained from core holes at Yucca Mountain are compiled in Peters et al (1984, 1986) and Klavetter and Peters (1986, 1987).

In this exercise, natural analog data, in particular soil properties, were used to help bound the statistical behavior of porosity. Data are compiled in Panian (1987). A detailed review of the data is discussed in Wang and Narasimhan (in review).

Samples from Drill Holes USW G-4 and USW G-1 described in Peters et al (1986) were assumed to represent tuffaceous rock and were used as the basis for the model of the hydrostratigraphy presented in this document. Where the sample actually was taken from one of the corresponding hydrostratigraphic units, it was chosen to represent that unit. The only units without corresponding samples were the bedded units of the hydrostratigraphy. Some bedded units have more than one corresponding sample. Where more than one sample existed, the samples were arbitrarily split and assigned to represent bedded units that had no corresponding sample. The fracture properties of hydrostratigraphic unit CH3n are represented by the fracture properties for the thermal/mechanical reference unit CHnz as described in Klavetter and Peters (1986). The values of saturated conductivities and bulk matrix saturated conductivities are assumed to be equal because of the extremely small fracture porosities of the tuffs.

Table 4 illustrates that dividing the samples chosen according to hydrostratigraphic units results in only one sample per unit. Table 5 describes the fracture properties assumed for hydrostratigraphic unit CH3n. A technique for generating probability density functions of the model parameters that define each hydrostratigraphic unit despite the fact that each unit is represented by only one datum is discussed in the next section.

## 4.9 Estimating a Parameter Distribution

As an explicit example of how the process of fitting a beta distribution works, consider the matrix porosity for the unit CH1n. The representative value in Table 4 is given as 0.32. There is no reason to believe that this value does not fairly represent the central tendency of porosity for this unit and these materials, so it is acceptable as an expected value in a probabilistic sense. The next step is to determine a coefficient of variation. Analysis of data for 11 textural classes of soil compiled by Panian (1987) gives coefficients of variation for porosity that range from 0.102 to 0.313. Coefficients of variation of soil properties are also tabulated in Harr (1987), where the value is reported as 0.10. The data in Table 6 suggest that the value of 0.313 may not be representative. For the purpose of this exercise a coefficient of variation of 0.20 will be assumed.

## TABLE 4

MATRIX PROPERTIES OF THE HYDROSTRATIGRAPHIC UNITS OF THE TUFFACEOUS BEDS OF THE CALICO HILLS IN DRILL HOLE USW G-4

| Unit | Sample | Porosity | Bulk Saturated Conductivity (m/s) | Residual Saturation | Air Entry Parameter (1/m) | Desaturation Parameter |
|---|---|---|---|---|---|---|
| CH1n | G1-1500 | 0.32 | 1.5e-11 | 0.0134 | 0.007490 | 1.333 |
| CH1b | G1-1753 | 0.30 | 1.4e-11 | 0.2003 | 0.002000 | 1.954 |
| CH2n | G4-1548 | 0.28 | 1.4e-12 | 0.1095 | 0.003080 | 1.602 |
| CH2b | G1-1780 | 0.25 | 2.1e-12 | 0.0995 | 0.003700 | 1.500 |
| CH3n | G4-1551 | 0.33 | 3.2e-11* | 0.2017 | 0.004150 | 1.894 |
| CH3b | G1-1790 | 0.23 | 5.2e-12 | 0.0135 | 0.001700 | 1.626 |
| CH4n | G1-1637 | 0.31 | 1.3e-11 | 0.0427 | 0.002670 | 1.428 |
| CH4b | G4-1728 | 0.22 | 4.5e-12 | 0.1500 | 0.001580 | 1.685 |
| CH5n | G4-1686 | 0.30 | 4.2e-12 | 0.0600 | 0.006000 | 1.460 |
| CH5b | G4-1737 | 0.24 | 2.6e-12 | 0.1000 | 0.003700 | 1.496 |
| PP1n | G4-1769 | 0.26 | 2.3e-12 | 0.2154 | 0.000605 | 2.487 |

*Arithmetic mean of subsamples G4-4F in Peters *et al*, 1984.

## TABLE 5

FRACTURE PROPERTIES OF HYDROSTRATIGRAPHIC UNIT CH3n OF THE TUFFACEOUS BEDS OF THE CALICO HILLS IN DRILL HOLE USW G-4

| Unit | Sample | Porosity | Bulk Saturated Conductivity (m/s) | Residual Saturation | Air Entry Parameter (1/m) | Desaturation Parameter |
|---|---|---|---|---|---|---|
| CH3n | G4-1551 | 0.000046 | 9.2e-9 | 0.0395 | 1.2851 | 4.23 |

TABLE 6

POROSITY STATISTICS REDUCED FROM PANIAN (1987)

| Soil Class | Number of Samples | Coefficient of Variation |
|---|---|---|
| Sand | 12 | 0.313 |
| Loamy Sand | 27 | 0.164 |
| Sandy Loam | 140 | 0.194 |
| Sandy Clay Loam | 69 | 0.127 |
| Loam | 97 | 0.143 |
| Clay Loam | 127 | 0.117 |
| Silty Loam | 347 | 0.125 |
| Silty Clay Loam | 289 | 0.119 |
| Sandy Clay | 17 | 0.124 |
| Silty Clay | 46 | 0.136 |
| Clay | 141 | 0.102 |

Having chosen an expected value and a coefficient of variation, the minimum and maximum values are assumed to lie at plus and minus three standard deviations from the expected value. Equation 4 is used to calculate the standard deviation $\sigma[x]$, and the two following equations are used to calculate the minimum a and maximum b.

$$a = E[x] - 3\sigma[x] = E[x] - 3(E[x]V(x)) \quad , \tag{16a}$$

and

$$b = E[x] + 3\sigma[x] = E[x] + 3(E[x]V(x)) \quad . \tag{16b}$$

The only qualification is that, should the minimum value calculated using Equation 16a be below 0.0, the arbitrary minimum value will be set at 0.0 as input for calculating the coefficients of the beta distribution. Likewise, should the maximum value calculated using Equation 16b exceed 0.60, a likely maximum, the arbitrary value of 0.60 will be used as the maximum.

The range describes the smallest and largest values of interest and is bounded, in the assumptions above, by the choice of three standard deviations as a constraint. Some insight as to the probability that a value lies outside this range is offered by Chebyshev's inequality (Harr, 1987), which states that for h standard deviations to each side of $\bar{x}$

$$P[(\bar{x} - h\sigma) \le x_i \le (\bar{x} + h\sigma)] \ge 1 - 1/h^2 \quad , \tag{17}$$

where $\sigma$ is the value of $\sigma[x]$, and $x_i$ is a random sample. Substituting 3 for h yields a probability of 0.89. That is, given a random sample of any distribution, 89% of the sampled values will lie within the range bounded by plus and minus three standard deviations. The probability of sampling

within the estimated range is further constrained if more information is available. If the unknown density function is symmetrical about the expected value and unimodal, it can be shown that Gauss' inequality

$$P[(\bar{x} - h\sigma) \leq x_i \leq (\bar{x} + h\sigma)] \geq 1 - 4/9h^2 \qquad (18)$$

is applicable. For plus and minus three standard deviations the probabilities increase to 95%. The expected value E[x]; the coefficient of variation V(x); the minimum a and the maximum b for the hydrostratigraphic unit CHln, which were used to define the beta probability distribution of porosity, were estimated at 0.32, 0.20, 0.128, and 0.512, respectively.

To visualize the density function, an interactive procedure was written and embedded within a commercial software package called RS/Explore. When the procedure is called, the analyst is asked to provide the four pieces of information listed above. A graph of the density and cumulative function appears on the terminal. Figure 2, the probability density of porosity for unit CHln, was generated using this procedure. The objective of the interactive graphics is to allow the analyst to visualize the consequences of the assumptions in the probability model.

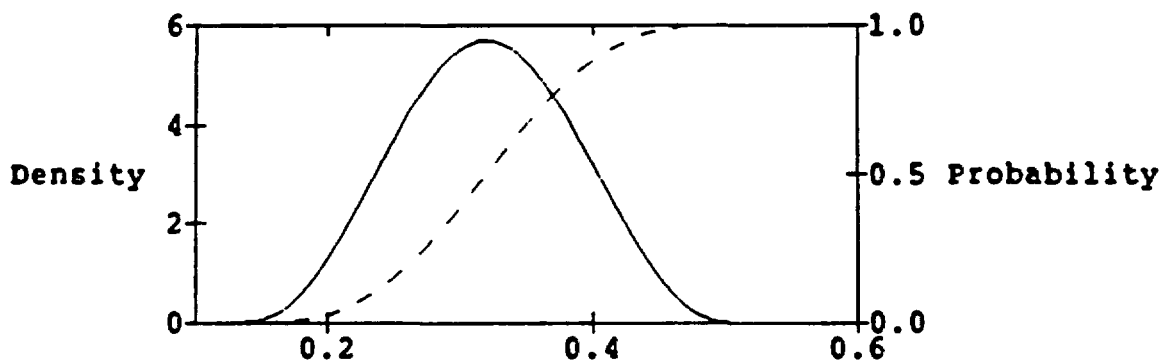


Figure 2. Probability Density and Cumulative Probability of Matrix Porosity for Hydrostratigraphic Unit CHln

## 5. Example of a Groundwater Travel Time Simulation

This section briefly describes the method used to generate a distribution of groundwater travel times from the beta probability distributions of the input parameters.

Implementing a simulation requires input of the parameters that define the beta probability distribution of each of the independent variables in Table 4 to the Latin Hypercube Sampler (LHS) (Iman and Shortencarier, 1984). For the exercise in this paper, the LHS was used to generate 100 random samples from the probability distributions of the 10 input variables for

each of the 11 hydrostratigraphic units. Because only one of the 11 hydrostratigraphic units was assumed to sustain fractures, each of the 100 parameter sets generated by the LHS contains 60 elements (5 matrix parameters for 11 units plus 5 fracture parameters for 1 unit).

Each of the 100 parameters sets from the LHS was used to construct an input file for the flow code LLUVIA (Hopkins and Eaton, 1988). An input flux of 1.0 mm/year was specified for this example. Output from the 100 runs of LLUVIA is loaded into RS/Explore for statistical and graphical analysis.

A histogram of the 100 travel times from the top of the hydrostratigraphic model to the water table generated by this simulation is illustrated in Figure 3. A statistical summary of the travel times is presented in Table 7.

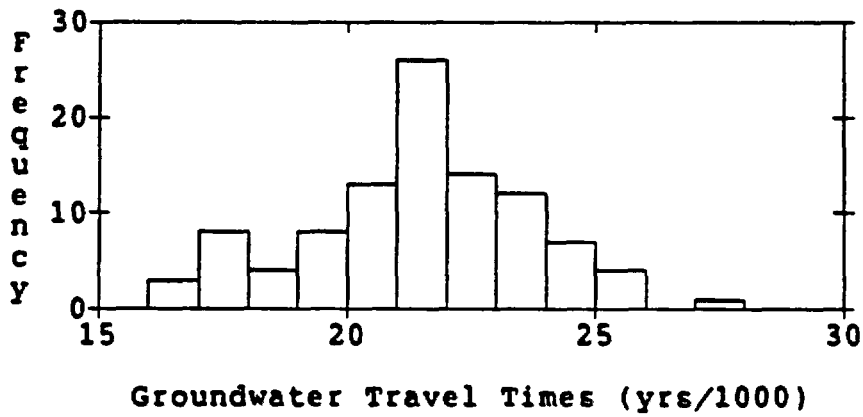


Figure 3. Histogram of 100 Cumulative Groundwater Travel Times

TABLE 7

STATISTICS OF GROUNDWATER TRAVEL TIME SIMULATION

| | |
|---|---|
| Count (N) | 100.00 |
| Mean | 21.44 |
| Median | 21.55 |
| Variance | 4.99 |
| Standard Deviation | 2.23 |
| Maximum | 27.96 |
| Minimum | 16.70 |
| Skewness | -0.10 |
| Kurtosis | -0.01 |
| Coefficient of Variation | 0.10 |

## 6. Summary

The unsaturated zone at Yucca Mountain is composed of complex geologic materials. The parameters used to describe these materials are defined by mathematical models that represent the process of interest. The organization and distribution of these parameters are defined by models of the system domain. Sparse sampling data, uncertainties in the measured values obtained, and the inherent variability of natural materials and system geometry often make it difficult to statistically define the properties of interest.

A method for using the beta probability density function as a technique to generate probabilistic functions that describe the distributions of the material properties of interest is presented in this paper. As an example of how the technique is applied, quantitative and descriptive data from Drill Holes USW G-4 and USW G-1 are used. In addition, natural analog data and the analyst's subjective judgment can be used to constrain the estimates of the four parameters required to construct a beta distribution and are an integral part of the methodology.

The methodology is applied to 10 parameters of interest in a hypothetical 11-layer domain as illustration of the technique. Parameters describing the distributions of the properties in each of the 11 hydrostratigraphic units are generated. The overall purpose of the exercise is to demonstrate how uncertainties in property values can be quantified for numerical simulation. As an example of the utility of the method, the beta distributions are used as input to the LHS. One hundred input decks for the flow code LLUVIA are generated. The output of one hundred travel time simulations is summarized in histogram form and in a table of statistics.

## References


Bear, J., 1979. Hydraulics of Groundwater. McGraw-Hill Book Co., New York.

Benjamin, J. R., and C. A. Cornell, 1970. Probability, Statistics, and Decision for Civil Engineers. McGraw-Hill Book Co., New York.

Campbell, G. S., 1985. Soil Physics with Basic: Transport Models for Soil-Plant Systems. Developments in Soil Science 14. Elsevier, New York.

Chow, V. T., editor, 1964. Handbook of Applied Hydrology-A Compendium of Water-Resources Technology. McGraw-Hill Book Co., New York.

Dagan, G., 1986. Statistical Theory of Groundwater Flow and Transport: Pore to Laboratory, Laboratory to Formation, and Formation to Regional Scale. Water Resources Research 22(9), pp. 120S-134S.

Freeze, R. A., and J. A. Cherry, 1979. Groundwater. Prentice-Hall, Inc., New Jersey.

Harr, M. E., 1977. Mechanics of Particulate Media. McGraw-Hill Book Co., New York.

Harr, M. E., 1987. Reliability Based Design in Civil Engineering. McGraw-Hill Book Co., New York.

Hillel, D., 1980. Fundamentals of Soil Physics. Academic Press, New York.

Hopkins, P., and R. Eaton (in review). LLUVIA - A One-Dimensional, Steady-State Program for Flow Through Partially Saturated Porous Media. SAND88-0558, Sandia National Laboratories, Albuquerque, NM.

Iman, R. L., and M. J. Shortencarier, 1984. A FORTRAN 77 Program and User's Guide for the Generation of Latin Hypercube and Random Samples for Use with Computer Models. SAND83-2365, NUREG/CR-3624, Sandia National Laboratories, Albuquerque, NM.

Klavetter, E. A., and R. R. Peters, 1986. Estimation of Hydraulic Properties of An Unsaturated, Fractured Rock Mass. SAND84-2642, Sandia National Laboratories, Albuquerque, NM.

Klavetter, E. A., and R. R. Peters, 1987. An Evaluation of the Use of Mercury Porosimetry in Calculating Hydrologic Properties of Tuffs from Yucca Mountain, Nevada. SAND86-0286, Sandia National Laboratories, Albuquerque, NM.

Klavetter, E. A., and R. R. Peters, 1988. A Continuum Model for Water Movement in an Unsaturated Fractured Rock Mass. Water Resources Research 24(3), pp. 416-430.

Mualem, Y., 1976. A New Model for Predicting the Hydraulic Conductivity of Unsaturated Porous Media. Water Resources Research 12(3), pp. 513-522.

Nielsen, D. R., M. Th. van Genuchten, and J. W. Biggar, 1986. Water Flow and Solute Transport Processes in the Unsaturated Zone. Water Resources Research 22(9), pp. 89S-108S.

NRC (U.S. Nuclear Regulatory Commission), 1986. Disposal of High-Level Radioactive Wastes in Geologic Repositories. Code of Federal Regulations, Energy, Title 10, Part 60, Washington, D.C..

Panian, T. F., 1987. Unsaturated Flow Properties Data Catalog, Volume II. Publication #45061, Water Resources Center, Desert Research Institute, University of Nevada System.

Peters, R. R., E. A. Klavetter, I. J. Hall, S. C. Blair, P. R. Heller, and G. W. Gee, 1984. Fracture and Matrix Hydrologic Characteristics of Tuffaceous Materials from Yucca Mountain, Nye County, Nevada. SAND84-1471, Sandia National Laboratories, Albuquerque, NM.

Peters, R. R., J. H. Gauthier, and A. L. Dudley, 1986. The Effect of Percolation Rate on Water-Travel Time in Deep, Partially Saturated Zones. SAND85-0854, Sandia National Laboratories, Albuquerque, NM; also in "Proceedings of the Symposium on on Groundwater Flow and Transport Modeling For Performance Assessment of Deep Geologic Disposal of Radioactive Waste - A Critical Evaluation of the State of the Art," Charles R. Cole, ed., Albuquerque, NM, August 1986.

Spengler, R. W., F. M. Byers, and J. B. Warner, 1981. Stratigraphy and Structure of Volcanic Rocks in Drill Hole USW-G1, Yucca Mountain, Nye County, Nevada. USGS-OFR-81-1349, United States Geological Survey, Denver, CO.

Spengler, R. W., and M. P. Chornack, 1984. Stratigraphic and Structural Characteristics of Volcanic Rocks in Core Hole USW G-4, Yucca Mountain, Nye County, Nevada. USGS-OFR-84-789, United States Geological Survey, Denver, CO.

van Genuchten, R., 1978. Calculating the Unsaturated Hydraulic Conductivity with a New Closed Form Analytical Model. Water Resources Bulletin, Princeton University Press, Princeton, NJ.

Wang, J. S. Y., and T. N. Narasimhan, (in review). Processes, Mechanisms, and Modeling Approaches for Partially Saturated Flow in Soil and Rock Media. SAND88-7054, Sandia National Laboratories, Albuquerque, NM.

# APPENDIX

## Information from the Reference Information Base Used in this Report

This report contains no information from the Reference Information Base.

## Candidate Information for the Reference Information Base

This report contains no candidate information for the Reference Information Base.

## Candidate Information for the Site & Engineering Properties Data Base

This report contains no candidate information for the Site and Engineering Properties Data Base.

SAND88-7067A U4411

# A Probabilistic Estimation of Seismic Damage to the Waste Handling Facilities of a Repository Located at Yucca Mountain, Nevada

O.K. Kiciman, N.A. Abrahamson
Bechtel National, Inc., San Francisco, California

## Objective

The study presented in this paper determines the probability of seismically induced damages to the waste handling building (WHB) of the Yucca Mountain, Nevada Repository.

## Methods

The WHB is a reinforced concrete structure with massive shear walls. In general, the shear wall thicknesses are controlled by shielding requirements. This paper presents a probabilistic investigation of the occurrence of seismically induced damage to the WHB. Seismic hazard curves were developed and combined with structural fragility curves to compute damage probabilities.

This seismic hazard analysis considers both ground acceleration at the site and ground rupture under the building. Standard methods are used to estimate the acceleration hazard, assuming that there is no ground rupture under the WHB. However, the vicinity of the site is highly faulted, and an unknown fault may exist under the WHB. This possibility is also considered, and the ground rupture hazard is estimated, using a conservative approach developed in this study.

The rupture hazard methodology developed in this study considers both the probability that there is a fault under the site and the probability that the fault is not detected by trenching. Six different methods are used to estimate the rupture hazard. Three of these methods are site specific and consider the location of nearby faults. The other three methods are regional and consider average properties of the faulting in a 10 x 20 km region surrounding the site. A ground rupture under the building will be accompanied by a ground acceleration. The seismic hazard for this conditional acceleration is also estimated. The results of the study show that the ground rupture hazard is much smaller than the acceleration hazard without a ground rupture under the WHB.

Two analyses were performed on the WHB, (1) a dynamic analysis for ground acceleration, and (2) a static analysis for a vertical fault rupture directly under the building. Shear walls are designed for the acceleration loading. Several design basis earthquakes (DBE) are considered from 0.2 g peak ground acceleration (PGA) to 1.0 g PGA to evaluate the effect of the DBE level on the damage probabilities. The building designed for five different levels of earthquakes varying between 0.2 g and 1.0 g were evaluated but not redesigned for fault displacement effects varying between 0 and 100 cm.

Four damage states are defined for the shear walls of the WHB. These are light, moderate, heavy, and total damage states, and are characterized by interstory drifts defined by the ratio of relative sidesway displacement between floors to the story height. Considering the shear force redistribution among the parallel walls, fragility curves are developed, using the average strength of the walls in the same direction, for each damage state. These fragility curves are convolved with the hazard curves to determine the exceedance probabilities for the damage states. These probabilities are computed for a spectrum of earthquakes with PGAs from 0.2 to 1.0 g.

## Results

The seismic damage probabilities of the WHB are less than 1E-6 for design levels as low as 0.2 g even for the light damage state. The probability of exceeding the heavy damage state is 1.7E-8 and 5E-10 for the 0.2 g and 1.0 g designs, respectively.

## Conclusions

Based on the very low calculated damage probabilities, it is concluded that the seismic hazard to the WHB is low.

# ASSESSMENT OF WORKER AND NON-WORKER RADIOLOGICAL SAFETY OF A REPOSITORY[a]

T. W. Laub
Sandia National Laboratories
NNWSI Repository Engineering Division 6311
Albuquerque, New Mexico 87185

## SUMMARY

Preliminary assessments of worker and non-worker radiological safety for both normal and accident conditions during the preclosure period have been performed for the proposed Yucca Mountain repository. The accident-conditions assessment estimated offsite doses resulting from credible accidents at the repository. Since the purpose of the accident-conditions assessment was to support the development of an initial Q-list, worker doses were not calculated. The normal-conditions assessment estimated offsite public doses as well as onsite worker doses resulting from the various anticipated routine radioactive releases and sources. The purpose of the normal-conditions assessment was to evaluate the preliminary Yucca Mountain repository design and identify those operations and aspects that are most important to radiation safety for the repository (e.g., those operations that are the largest contributors to the occupational doses of individual workers). The general approach and some of the results of these safety assessments are summarized below.

The approach taken for the accident-conditions radiological safety assessment was probabilistic; that is, the frequency of occurrence of an accident was considered in deciding whether or not to calculate offsite dose consequences for that accident, and the end results included estimates of accident frequencies. The procedure used in this assessment consisted of

[a]This work was supported by the U.S. Department of Energy (DOE) under contract DE-AC04-DP00789.

five steps: (1) A repository facility and systems model was developed to use in the development of initiating events. (2) A comprehensive list of internal and external initiating events was developed, and some preliminary screening on the basis of credibility and applicability to the site was performed. (3) An event tree was developed for each of the initiating events that logically and systematically described the various accident sequences resulting from the occurrence of intermediate events. (4) After completion of the event trees, a probability assessment of the accident sequences was performed, and each initiating event was assigned a frequency of occurrence and each intermediate event a probability of occurrence. At this point more screening of accidents was performed on the basis of frequency. (5) The final step of the accident assessment was the calculation of offsite dose consequences for each remaining accident sequence.

There were 149 accident sequences for which offsite dose consequences were calculated. Of these, 45 had essentially zero offsite dose consequences. The remaining 104 accident sequences had offsite dose consequences ranging from 0.01 mrem to about 2 rem. The frequencies of occurrence associated with these accident sequences ranged from an extremely unlikely $10^{-14}$/yr to about $10^{-1}$/yr. Those accidents with offsite dose consequences approaching 2 rem had low frequencies (i.e., below $10^{-5}$/yr).

The approach taken for the normal-conditions assessment is simple and straightforward. To calculate worker doses, the radiation conditions in and around the repository were estimated. These conditions included direct radiation levels, concentrations and composition of gaseous radionuclides, and concentrations and compositions of airborne particulate radionuclides. Direct radiation levels were calculated assuming an average spent fuel age of 10 yrs, a burnup of 27.5 Gwd/MTU for BWR fuel, and a burnup of 33 Gwd/MTU

for PWR fuel. Defense high-level waste was assumed to be 5-year-old sludge and 15-year-old supernate. Airborne radioactivity levels were estimated using analytical techniques developed under some simplifying assumptions such as the importance of resuspension and hot-cell leakage. Offsite public doses were composed entirely of immersion and inhalation doses resulting from atmospheric transport of anticipated releases of radioactive materials.

Whole-body and critical-organ doses from airborne radioactive materials were found to be at least one order of magnitude less than the 1 rem/yr DOE design objective. Worker doses from direct gamma radiation were much more significant than those from airborne radioactivity. As expected, direct radiation doses depended strongly on the mode of operation being used by workers (e.g., contact-handling techniques or remote-handling techniques). Estimated direct doses to repository workers did not exceed the 10 CFR 20 regulatory limit of 5 rem/yr, but did exceed the DOE design objective of 1 rem/yr. Several cask-handling tasks that involved worker contact were identified as major contributors to the direct radiation doses to workers.

Ground-level releases of radioactive materials resulted in a calculated whole-body dose of 0.01 mrem/yr and a maximum critical-organ dose of 0.03 mrem/yr for a maximally exposed offsite individual assumed to be at the site boundary, 5 km from the release point. These doses are well below the limits for normal operations of 25 mrem/yr to the whole body or 75 mrem/yr to any critical organ set forth in 40 CFR 191. The corresponding total population dose (whole-body) for members of the public within an 80-km radius of the site was calculated to be 0.012 person-rem for ground-level releases.

In conclusion, the accident-conditions safety assessment identified several accident sequences that could result in offsite doses approaching 1 rem but

had associated frequencies that were below $10^{-5}$/yr. Nevertheless, the assessment did identify areas of the repository and certain systems and equipment that may require extra attention in design and/or fabrication (e.g., enhanced quality assurance). The normal-conditions assessment indicated that public and worker doses due to airborne sources of radiation will be well below 25 mrem/yr for the public, and well below 1 rem/yr for the worker. The major contributors to worker doses from direct radiation were cask-handling operations that involved worker contact, indicating that, in future design phases, remote-handling techniques for these operations should be investigated for incorporation into the design.

# APPENDIX

This report contains no data from, or for inclusion in, the RIB and/or SEPDB.

SAND87-2070C

# PRELIMINARY PRECLOSURE RADIOLOGICAL SAFETY ANALYSIS FOR NORMAL OPERATIONS OF A PROSPECTIVE YUCCA MOUNTAIN REPOSITORY[a]

L. J. Jardine, C. W. Ma, D. J. Hartman, R. C. Sit, and S. J. Zavoshy,
Bechtel National, Incorporated
San Francisco, California 94119

T. W. Laub
Sandia National Laboratories
Nuclear Waste Engineering Projects Division 6311
Albuquerque, New Mexico 87185

## I. INTRODUCTION

A preliminary radiological safety analysis was performed for the normal operating conditions during the preclosure period at the prospective Yucca Mountain repository. Since the repository is designed to accommodate spent fuel and defense high-level waste (DHLW), an estimate was made of the offsite doses and onsite occupational doses from (1) anticipated routine releases of airborne radioactive materials and from (2) the handling of the spent fuels and DHLW. This paper summarizes the methodology and calculated offsite doses resulting from the postulated routine releases of airborne radioactive materials from the waste-handling building through inhalation and immersion pathways. The calculated onsite occupational doses from the inhalation, immersion, and direct exposure pathways will be reported elsewhere at a later date.

## II. SURFACE WASTE-HANDLING FACILITY AND MAJOR ACTIVITIES

The paper focuses on the waste-handling building of the repository during the preclosure waste-emplacement period. The assumed repository configuration includes a single waste-handling building in which no spent fuel is consolidated. The repository configuration is subject to further study in future design activities. A schematic layout of the waste-handling building is given in Figure 1. Major activities and operations associated with each general area are listed in Table 1.

[a]This work was supported by the U.S. Department of Energy NNWSI Project through a Sandia National Laboratories subcontract.

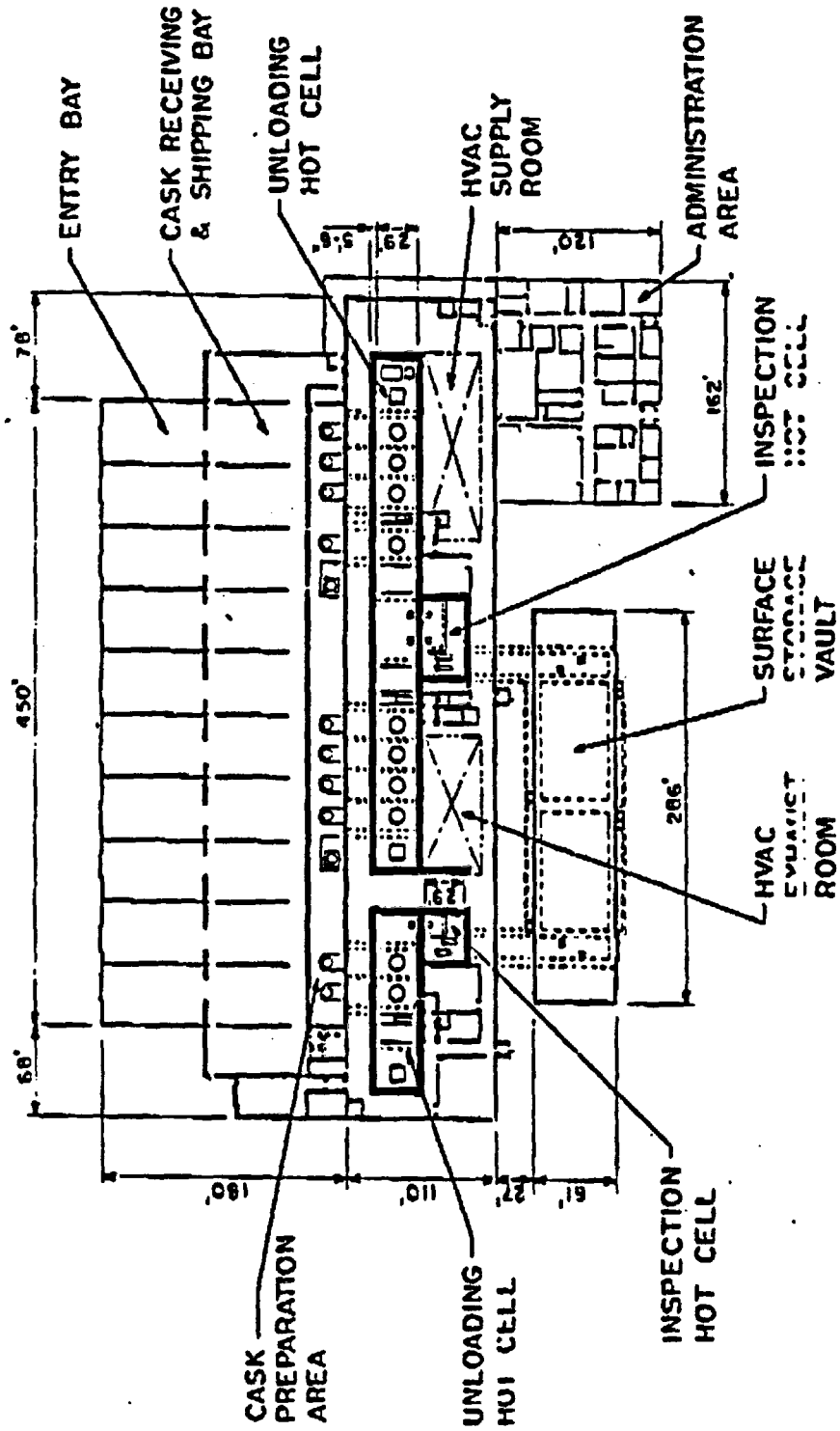


Figure 1

Schematic General Arrangement of the Waste-Handling Building

Table 1

Major Activities and Operations Performed in the Main Surface Waste-Handling Building

| MAJOR AREAS | MAJOR ACTIVITIES AND OPERATIONS |
|---|---|
| 1. Cask receiving and shipping bay | o Transfer shipping casks from offsite trucks or railcars to cask preparation area. |
| 2. Cask preparation area | o Sample cask inner cavity gases. |
| | o Remove cask outer covers and unbolt inner lids. |
| | o Decontaminate cask exteriors and interiors. |
| 3. Unloading hot cells | o Remove cask inner lids and transfer spent fuel assemblies/DHLW canisters from shipping casks into emplacement containers. |
| | o Weld covers to emplacement containers. |
| | o Inspect welds and decontaminate containers. |
| 4. Inspection hot cells | o Move containers to transfer cars and move cars to transfer station. |
| 5. Surface storage vault | o Store emplacement containers in vault temporarily or transfer to underground emplacement area via underground transporters. |

The repository will receive annually up to 3,000 metric tons of uranium (MTU) of spent fuel and up to 800 canisters of DHLW. A total of 60 percent of the spent fuel is assumed to consist of pressurized-water reactor (PWR) fuel with an average burnup of 33 GWD/MTU, and 40 percent boiling-water reactor (BWR) fuel with an average burnup of 27.5 GWD/MTU. This ratio corresponds to an annual throughput of 3,901 PWR fuel assemblies and 6,547 BWR fuel assemblies. These spent fuel assemblies and DHLW canisters will be unloaded from shipping casks in an unloading hot cell and placed in sealed containers, which will be transferred to the underground facility for permanent emplacement.

During normal repository operations, only gaseous and airborne particulate radioactive effluents generated from handling operations for spent fuel may contribute to the offsite radiological exposures. Direct radiations from spent fuels and DHLW canisters cannot contribute significantly to the offsite doses because of the combination of the shielding provided for these sources and because of the distance (5 km) from the waste-handling building to the site boundary. For normal operations, the sealed DHLW canisters will contribute no gaseous or airborne radioactive particulate effluent. Thus, only potential gaseous and airborne radioactive releases associated with spent fuel need to be assessed.

Table 1 indicates that during the waste-handling operations, spent fuel is contained either in shipping casks or in emplacement containers, except during the handling operations in the unloading hot cell It is therefore assumed that airborne radioactive materials from spent fuel will be released only into the unloading hot cell prior to their exhaust to the atmosphere via the HVAC filtration system. During normal waste transfers and handling operations, two mechanisms may result in the release of airborne radioactive materials within the unloading hot cell. The mechanisms are (1) spallation of radioactive crud particles from the exterior surfaces of the fuel assemblies and (2) releases of gaseous and volatile fission products from cracked or failed fuel assemblies. These mechanisms are discussed below.

## III. POTENTIAL AIRBORNE RADIOACTIVE SOURCE TERMS

### A. Crud Particles

Spent fuel assemblies are known to contain radioactive deposits, or crud, on their exterior cladding surfaces. These crud deposits are not always tightly bound; hence, spallation of crud from the surface of the fuel assembly can occur during dry handling operations. Any spallation of crud particles during unloading of the shipping cask and other dry handling operations in the hot cell may generate some airborne radioactive source terms within the unloading hot cell.

Typical crud characteristics have been assessed in literature surveys for both PWR and BWR spent fuel.[1,2] Because a repository handles spent fuel 5 years or older, Co-60, with its relatively long (5.3-year) half-life, is the only major radioactive component of concern in crud. The radioactivity of Co-60 in crud found on fuel rods at the time of reactor shutdown[1] were reported to range from 0.1 to 140 $\mu Ci/cm^2$ (per $cm^2$ of rod exterior surface area) for PWRs and from 97 to 1,250 $\mu Ci/cm^2$ for BWRs. Preliminary estimates of radioactivity were based on assumed average concentrations of Co-60 of 10 $\mu Ci/cm^2$ and 500 $\mu Ci/cm^2$ at the time of reactor shutdown for PWR and BWR fuel assemblies, respectively.

Based on the estimated surface area dimensions of PWR and BWR fuel assemblies,[3] the total available radioactive inventory of Co-60 was calculated as 0.9 Ci and 13 Ci for each 10-year-old PWR and BWR spent fuel assembly, respectively. The total inventory of Co-60 on the surfaces of the PWR and BWR assemblies processed annually by the repository was estimated at $9 \times 10^4$ Ci. There are no data on the fraction of the crud inventory that spalls off from spent fuel assemblies during normal handling operations. To estimate the airborne source term within the unloading hot cell, it was assumed that 1 percent of the crud deposits on the spent fuel assemblies may spall from the surface of assemblies as airborne particulates (particles with a diameter of less than 10 microns) within the unloading hot cell. Table 2 summarizes the radioactivity of the airborne crud particulates.

Table 2

Estimate of Airborne Radioactivity Released within the Unloading Hot Cell Annually from Failed Spent Fuel and Crud

| Isotope | BWR Isotopic Inventory[a] (Ci/assembly) | PWR Isotopic Inventory[a] (Ci/assembly) | Total Airborne Activity Released within the Unloading Hot Cell (Ci/yr) | Total Airborne Activity Released to the Atmosphere (Ci/yr) |
|---|---|---|---|---|
| Crud Particles | | | | |
| Co-60 | 1.3E+01[b] | 9.0E-01 | 9.0E+02 | 9.0E-02 |
| Failed Fuel | | | | |
| H-3 | 7.3E+01 | 2.1E+02 | 2.6E+02[c,d] | 2.6E+02 |
| C-14 | 2.8E-01 | 7.2E-01 | 9.3E-01[c,d] | 9.3E-01 |
| Kr-85 | 7.2E+02 | 2.2E+03 | 8.0E+03[c,d] | 8.0E+03 |
| I-129 | 4.8E-03 | 1.5E-02 | 9.5E-05[c,d] | 9.5E-05 |
| Cs-134 | 6.8E+02 | 2.4E+03 | 7.8E+00[c,d] | 7.8E-04 |
| Cs-135 | 6.6E-02 | 1.6E-01 | 5.9E-04[c,d] | 5.9E-08 |
| Cs-137 | 1.2E+04 | 3.8E+04 | 1.3E+02[c,d] | 1.3E-02 |
| Ba-137m | 1.2E+04 | 3.6E+04 | 1.2E+02[c,d] | 1.2E-02 |
| | | | 8.5E+03 | 8.3E+03 |

Notes:

a. Data based on 10-yr-old spent fuel with burnups of 33 GWD/MTU for PWR fuel and 27.5 GWD/MTU for BWR fuel.[3]

b. 1.3E+01 = $1.3 \times 10^{1}$.

c. Data based on 3,901 PWR fuel assemblies and 6,547 BWR fuel assemblies handled annually.

d. Data based on the assumption that 0.2 percent of rods fail annually.

B. Failed Fuel

Failed fuel is defined in this paper as fuel rods in which the cladding has at some time been breached. If the cladding of a rod has been breached, a fraction of volatile fission products and gases in the gap and plenum areas can escape from the fuel rod as airborne radioactivity. Fuel cladding failures have occurred during normal reactor operations as a consequence of fuel pellet-cladding interactions, cladding hydriding, and cladding corrosion.[4] Although some fuel rods discharged from a reactor may not have been completely breached, the failure mechanisms can contribute to the degradation of the cladding to the extent that stresses, impact forces, or vibrations encountered during normal transportation and handling operations at the repository may cause rod failure at the repository, thereby producing an airborne radioactive source term.

The number of failed fuel rods used to estimate this airborne radioactive source terms is assumed to include those resulting from repository handling operations, reactor operations, and transportation operations. Failed fuel due to reactor operations is conservatively included because of the possibility that a cladding breach may subsequently reseal itself before reactor discharge. Fuel failures that occur during transportation release into the cask cavity a portion of the gap radioactivity, which will be either collected at the repository or released into the unloading hot cell during fuel unloading operations. On the basis of published data,[4,5,6] an average value of 0.1 percent (by number of rods) was assumed for the fuel failure rates during reactor operations. This value is assumed applicable to both PWR and BWR fuel.

Published data on fuel cladding failures during transportation and handling operations in the hot cell could not be identified. It is assumed that the fuel failure rate for the combination of transportation and repository handling operations equals the fuel failure rate for reactor operations (0.1 percent). The total fuel failure rate is, therefore, 0.2 percent of the fuel rods received.

For each failed fuel rod, the released gaseous fission products are assumed to consist of H-3, C-14, and Kr-85. A total of 30 percent of the Kr-85[7] and 10 percent of the H-3 and C-14 inventory in fuel assemblies are assumed to be released when the cladding is breached. Recent experiments[8] indicated that the typical fraction of Kr-85 and H-3 released from the fuel rod gap and plenum is about 1 to 4 percent of the total inventory, even for burnups as high as 56 GWD/MTU. Thus the fractions of 0.3 and 0.1 assumed in this study for releases from failed fuel are believed to be conservative.

On the basis of an empirical model reported by Lorenz et al.,[9,10] the fractions of iodine and cesium released when the cladding is breached at 900°C are $5.3 \times 10^{-4}$ and $2.8 \times 10^{-4}$, respectively. Such a temperature is much greater than any temperature that the spent fuel could ever be expected to experience at the repository during normal operations. Therefore, these source terms are believed to be conservative. For a repository environment, it is assumed that the iodine is released in a gaseous form and cesium in a particulate form.

Using the radionuclide inventories of Roddy et al.,[3] the 0.2 percent fuel failure rates, and the various radionuclide release fractions discussed above, one can calculate the airborne radioactivity released annually from spent fuel into the unloading hot cell. The results are shown in Table 2.

## IV. RADIONUCLIDE RELEASE AND TRANSPORT ANALYSES

### A. Radioactive Releases in Effluents

Airborne radioactive particles released from the spent fuel assemblies into the unloading hot cell are first filtered by the ventilation exhaust system before being released to the atmosphere. Since the proposed filtration system is composed of at least two high-efficiency particulate air (HEPA) filters in series, the combined filtration efficiency is expected to be 99.99 percent. This efficiency results in a filtration decontamination factor (DF) of $10^{-4}$ for any

airborne particles, such as the Co-60 in crud and the Cs-134, Cs-135, Cs-137, and Ba-137m from failed fuel. The gaseous and volatile radionuclides (such as Kr-85, H-3, C-14, and I-129) released in the hot cell are assumed to be released directly to the atmosphere, corresponding to a filtration DF of 1.

When these two DF factors are combined with the postulated airborne radioactivity releases into the hot cell in Table 2, an estimated maximum of $8.3 \times 10^3$ Ci could be released to the atmosphere annually. Essentially 97 percent of the radioactivity released in the waste-handling building effluents comes from Kr-85 and 3 percent from H-3. The other radionuclides contribute less than 0.01 percent to the total estimated curie releases. In addition, any deposition and plateout of airborne radionuclides inside the unloading hot cell or cask cavities were neglected.

B. Atmospheric Dispersion

To evaluate the annual-average atmospheric dispersion factor ($\chi/Q$), a multisector analysis was performed. The annual-average wind data were derived from the meteorological information presented by Church et al.[11,12] Because atmospheric stability data are not yet available for the Yucca Mountain site, these wind data were assumed to be Pasquill Stability Class F which is conservative for a ground level release. Annual-average atmospheric dispersion factors for 16 compass directions (N, NNE, NE, etc.) and four distances (5, 20, 40, and 60 km) from the main waste-handling building for a ground level release were calculated. The site boundary was assumed to be 5 km from the release point.

## V. RADIATION DOSE ASSESSMENTS

Radiation doses were calculated for external exposures caused by immersion in the passing effluent plume and for internal doses caused by inhalation of airborne radionuclides. The methodology described in Regulatory Guide 1.109[13] was followed.

### A. Maximum Individual Dose

For a ground-level release, the maximum $\chi/Q$ value is $1.0 \times 10^{-6}$ sec/m$^3$ from the SSE direction at 5 km from the repository. Table 3 summarizes the calculated annual doses from the inhalation and immersion pathways to a hypothetical maximally exposed individual at this offsite location.

Table 3 indicates that the maximum whole-body dose to an offsite individual from the inhalation pathway is 0.01 mrem/yr. The associated critical organ dose is 0.04 mrem/yr to the lung. The doses due to immersion are 0.35 mrem/yr to the skin and 0.004 mrem/yr to the whole body. Contributions from crud (Co-60) account for approximately 55 percent of the annual lung doses in Table 3; the remaining 45 percent is caused by H-3 (30 percent) and Kr-85 (15 percent) associated with releases from failed fuel. All these doses are well below the 40 CFR 191 Subpart A limits of 25 mrem/yr to the whole body, 75 mrem/yr to the thyroid, and 25 mrem/yr to any other critical organ.[14]

Table 3

Annual Radiation Doses to a Hypothetical, Maximally Exposed, Offsite Individual for Ground-Level Releases

| | Inhalation Dose (rem/yr) | | | | | | | Immersion Dose (rem/y | |
|---|---|---|---|---|---|---|---|---|---|
| Isotope | Thyroid | Lung | Bone | Bone Surface | Red Bone Marrow | Liver | Whole Body | Beta Skin | le |
| **Crud Particles** | | | | | | | | | |
| Co--60 | 1.4E-06 | 1.8E-05 | 1.2E-06 | 1.2E-06 | 1.5E-06 | 2.8E-06 | 4.4E-08 | 8.6E-10 | 5.6E-0 |
| **Failed Fuel** | | | | | | | | | |
| H----3 | 1.0E-05 | 1.0E-05 | 3.7E-06 | 6.6E-06 | 8.3E-06 | 8.3E-06 | 1.0E-05 | 0.0E+00 | 0.0E+0 |
| C---14 | 1.0E-07 | 1.0E-07 | 5.3E-07 | 1.2E-08 | 0.0E+00 | 0.0E+00 | 1.0E-07 | 7.5E-10 | 0.0E+0 |
| Kr--85 | 0.0E+00 | 4.9E-06 | 0.0E+00 | 0.0E+00 | 0.0E+00 | 0.0E+00 | 0.0E+00 | 3.4E-04 | 4.1E-06 |
| I--129 | 1.3E-07 | 2.1E-09 | 5.9E-11 | 1.3E-11 | 1.4E-11 | 1.1E-11 | 1.6E-10 | 3.5E-14 | 2.8E-1 |
| Cs-134 | 1.0E-08 | 2.4E-09 | 9.2E-09 | 1.1E-08 | 1.2E-08 | 1.3E-08 | 1.8E-08 | 1.8E-11 | 2.8E-10 |
| Cs-135 | 1.1E-13 | 2.3E-14 | 2.2E-13 | 1.3E-13 | 1.1E-13 | 1.1E-13 | 9.0E-14 | 1.6E-15 | 0.0E+00 |
| Cs-137 | 1.4E-07 | 3.0E-08 | 1.9E-07 | 1.7E-07 | 1.6E-07 | 1.7E-07 | 1.7E-07 | 5.5E-10 | 0.0E+00 |
| Ba-137M | 0.0E+00 | 0.0E+00 | 0.0E+00 | 0.0E+00 | 0.0E+00 | 0.0E+00 | 0.0E-00 | 1.2E-10 | 1.7E-09 |
| | 1.1E-05 | 1.6E-05 | 4.5E-06 | 6.8E-06 | 8.5E-06 | 8.5E-06 | 1.1E-05 | 3.5E-04 | 4.2E-06 |
| Total Dose | 1.3E-05 | 3.4E-05 | 5.7E-06 | 8.1E-06 | 1.0E-05 | 1.1E-05 | 1.1E-05 | 3.5E-04 | 4.2E-06 |

B. Population Doses

To determine the population dose, the population within 80 km of the repository (totaling about 11,000) was considered. This is consistent with the methods established by the Nuclear Regulatory Commission for nuclear power plants.[15]

The population dose was evaluated for a ground-level release, and the results are summarized in Table 4. Table 4 indicates that the annual total population dose (whole body) is 0.004 man-rem/yr.

## VI. CONCLUSIONS

Offsite doses from the inhalation and immersion pathways were calculated for the public using a set of estimated airborne source terms and parameters for the effluent treatment system of the waste-handling building under normal repository operations. Although no operating experience or data for the source terms exist for a nuclear waste repository, these estimated source terms were judged to be more severe than those likely to be encountered. Consequently, the releases of radioactive materials and the associated calculated offsite doses are believed to represent upper bounds.

For ground-level releases, these source terms resulted in a calculated whole-body dose of 0.01 mrem/yr and a critical organ lung dose of 0.04 mrem/yr for a maximally exposed, offsite individual. The hypothetical individual was assumed to be at the site boundary, 5 km from the release point. These calculated doses are well below the EPA limits for normal operations of 25 mrem/yr to the whole body or 75 mrem/yr to the thyroid and 25 mrem/yr to any other critical organ, as set forth in 40 CFR 191.

Table 4

Annual Total Population Doses for a 80 km Radius from the Yucca Mountain Repository for Ground-Level Releases

| | Inhalation Dose (man-rem/yr) | | | | | | | Immersion Dose (man-rem/yr) | |
|---|---|---|---|---|---|---|---|---|---|
| Source Term | Thyroid | Lung | Bone | Bone Surface | Red Bone Marrow | Liver | Whole Body | Beta Skin | Whole Bo |
| Crud Particles | 5.2E-04 | 6.4E-03 | 4.4E-04 | 4.4E-04 | 5.6E-04 | 1.0E-03 | 1.6E-05 | 3.1E-07 | 2.0E-05 |
| Failed Fuel | 3.9E-03 | 5.6E-03 | 1.6E-03 | 2.4E-03 | 3.0E-03 | 3.1E-03 | 3.9E-03 | 1.3E-01 | 1.5E-03 |
| Total Dose | 4.5E-03 | 1.2E-02 | 2.1E-03 | 2.9E-03 | 3.6E-03 | 4.1E-03 | 4.0E-03 | 1.3E-01 | 1.5E-03 |

The corresponding total population dose (whole-body) for members of the public within a 80 km radius from the site was calculated to be 0.004 man-rem for ground-level releases. Such doses are not significant compared with the background radiation doses received by the total population of approximately 11,000 within the 80 km radius from the prospective repository site near Yucca Mountain. Therefore, this preliminary study concludes that, during normal preclosure repository operations, public exposures from airborne radioactive releases will be well below the EPA limits.

REFERENCES

1. R. E. EINZINGER and J. A. COOK, "Pre-Test Visual Examination and Crud Characterization of LWR Rods Used in the Long-Term, Low-Temperature Whole Rod Test," NUREG/CR-3285, HEDL-TME 83-9, U.S. Nuclear Regulatory Commission (1984).

2. L. J. JARDINE, "Preliminary Characterization of Radioactive Crud for Design of Dry Spent-Fuel Handling Facilities," Transactions of the American Nuclear Society, 1986 Winter Meeting, November 16-20, 53, 120, Washington, DC (1986).

3. J. W. RODDY, H. C. CLAIBORNE, R. C. ASHLINE, P. J. JOHNSON, B. T. RHYNE, "Physical and Decay Characteristics of Commercial LWR Spent Fuel," ORNL/TM-9591/V1&R1, Oak Ridge National Laboratory (1986).

4. C. W. FUNK and L. D. JACOBSON, "Inventory and Characterization of Spent LWR Fuel," HEDL-TME 77-82, Hanford Engineering Development Laboratory, Westinghouse Hanford Company, (1979).

5. R. E. WOODY, "The Characteristics of Spent LWR Fuel Relevant to its Storage in Geologic Repositories," HEDL-TME 83-28, Hanford Engineering Development Laboratory, Westinghouse Hanford Company, Richland, WA (1983).

6. J. M. VIEBROCK and D. H. MALIN, "Domestic Light Water Reactor Fuel Design Evolution," DOE/ET/47912-3, NAC-C-8129, Volume III, Nuclear Assurance Corporation, Atlanta, GA (1981).

7. NRC (U.S. Nuclear Regulatory Commission), "Assumptions Used for Evaluating the Potential Radiological Consequences of a Fuel Handling Accident in the Fuel Handling and Storage Facility for Boiling and Pressurized Water Reactors," Safety Guide 25, U.S. Nuclear Regulatory Commission (1972).

8. M. PEEHS, R. BOKELMANN, and J. FLEISCH "Spent Fuel Dry Storage Performance in Inert Atmosphere," Third International Spent Fuel Storage Technology Symposium/Workshop, April 8-10, Seattle, WA (1986).

9. R. A. LORENZ, J. L. COLLINS, A. P. MALINAUSKAS, O. L. KIRLAND, and R. L. TOWNS, "Fission Product Release from Highly Irradiated LWR Fuel," NUREG/CR-0722, ORNL/NUREG/TM-287/R2, Oak Ridge National Laboratory (1980).

10. R. A. LORENZ, J. L. COLLINS, and A. P. MALINAUSKAS," Fission Product Source Terms for the LWR Loss-of-Coolant Accident," NUREG/CR-1188, ORNL/NUREG/TM-321, Oak Ridge National Laboratory (1980).

11. H. W. CHURCH, D. L. FREEMAN, K. BORO, R. T. EGAMI, "Meteorological Tower Data for the Nevada Nuclear Waste Storage Investigations (NNWSI)," Quarterly Report, July 1982 - September 1982, Yucca Alluvial (YA) Site, SAND83-1912, Sandia National Laboratories (1984).

12. H. W. CHURCH, D. L. FREEMAN, K. BORO, R. T. EGAMI, "Meteorological Tower Data for the Nevada Nuclear Waste Storage Investigations (NNWSI)," Tri-Quarterly Report, October 1982 - June 1983, Yucca Alluvial (YA) Site, SAND84-1327, Sandia National Laboratories (1984).

13. NRC (U.S. Nuclear Regulatory Commission), "Calculation of Annual Doses to Man from Routine Releases of Reactor Effluents for the Purpose of Evaluating Compliance with 10 CFR Part 50, Appendix I," Regulatory Guide 1.109, Revision 1, U.S. Nuclear Regulatory Commission (1977).

14. EPA (U.S. Environmental Protection Agency), "Environmental Radiation Protection Standards for Management and Disposal of Spent Fuel, High-Level and Transuranic Radioactive Wastes," Code of Federal Regulations, Protection of the Environment, Title 40, Part 191 (1986).

15. NRC (U.S. Nuclear Regulatory Commission), "Domestic Licensing of Production and Utilization Facilities," Code of Federal Regulations, Energy, Title 10, Part 50, Appendix I (1986).

"BEST AVAILABLE COPY"

**RIB Data Used in this Study:**

| RIB Section No. | Description |
|---|---|
| 2.6.2 | Waste receipt rates:<br>3,000 MTU/yr spent fuel<br>400 MTU/yr HLW |
| 2.1.1.2.1-2 | Average spent fuel burnup:<br>33 GWD/MTU (PWR)<br>27.5 GWD/MTU (BWR) |

**Data that may be Added to RIB:**

Because of the preliminary nature of this study, the results are not recommended for inclusion in the RIB.

**SEPDB Information**

There is no information in this study for inclusion in the SEPDB.

SAND 88-7066A

# Offsite Radiation Doses Resulting From Seismic Events at the Yucca Mountain Repository

C. W. Ma and L. J. Jardine
Bechtel National, Inc.

## Objective

This paper describes a study to evaluate the offsite radiological consequences from seismic events that are postulated to occur during the preclosure period at the proposed Yucca Mountain repository. In this study, the radiation doses to a maximally exposed member of the public at the site boundary are described. The work reported here is part of a larger preliminary study of the costs and benefits of designing the waste-handling building (WHB) at the repository for seismic events of varying severity.

## Methods

Four structural damage states have been specified for the WHB These damage states are defined and quantified in terms of structural deformations, crack sizes, and spalling concrete pieces of the WHB's reinforced concrete walls. The damage is caused by seismic events, of increasing severity, that exceed the seismic design bases. During an earthquake, spalling concrete pieces may hit and damage spent fuel assemblies that are being processed or that are temporarily stored in the hot cells. This damage may result in the release of (1) Kr-85 from breached fuel rods and (2) airborne particulates from the fractured spent fuel pellets. For each of the four damage states, impact energy, source terms, radionuclide release fractions, airborne particulate deposition, and atmospheric dispersion were estimated. Radiation doses were then determined for a maximally exposed individual at the site boundary, 5 km from the release point. For a given seismic design, each damage state has a specific probability of occurrence. These probabilities were calculated for five seismic design bases (0.2 to 1.0 g) by integrating the site-specific seismic hazard and the structural fragility of the WHB.

## Results

The study showed that the source term of the airborne spent fuel particulates is the dominant factor in the radiation dose to an individual offsite. The individual doses ranged from 0 to a maximum of 9 rem for the worst case. However, all of the calculated probabilities of damage states resulting in significant offsite doses are less than about $10^{-8}$/yr for the various seismic design bases. These extremely small probabilities suggest that the occurrence of such damage states and the corresponding offsite doses resulting from any postulated seismic event are not credible. These results are summarized in Figure 1.

## Conclusions

Significant offsite doses occurring as a consequence of seismic events exceeding the seismic design bases studied are incredible. Thus, it is concluded that seismic events exceeding the WHB seismic design bases will not result in any offsite doses that are both credible and significant during the preclosure period.

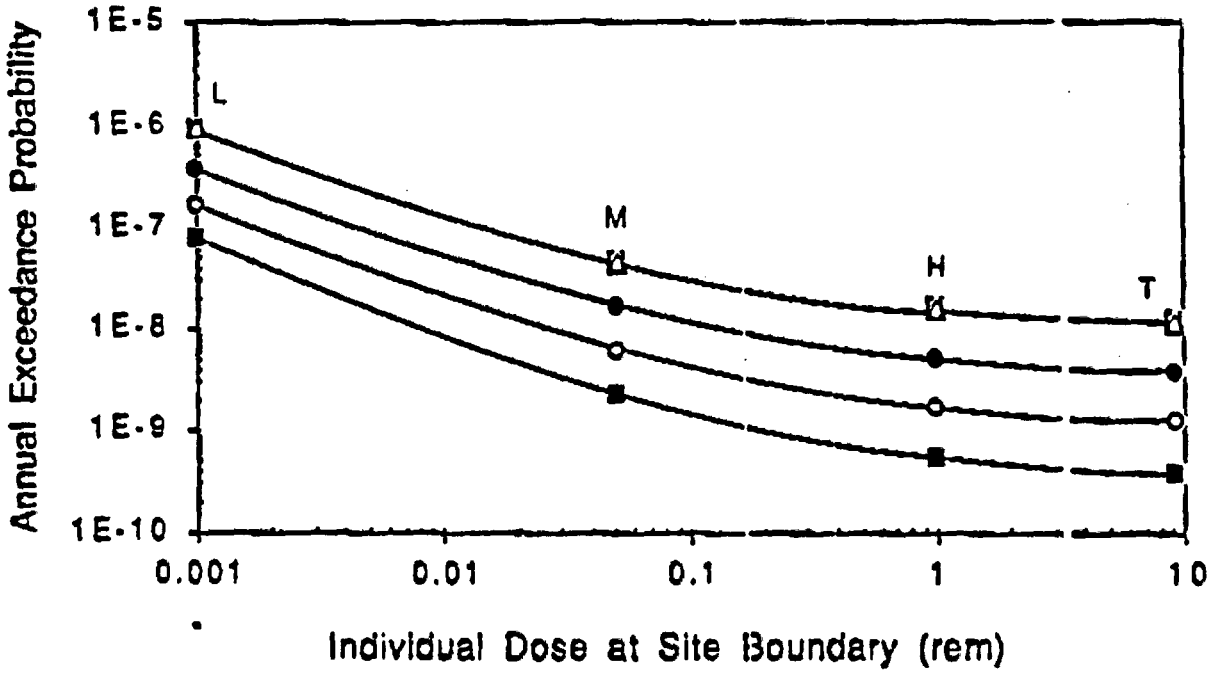


□ 0.2g Design Δ 0.4g Design ● 0.6g Design ○ 0.8g Design ■ 1.0g Design

L - Light M - Moderate H - Heavy T - Total

**Figure 1**

**Probability of Radiation Doses for Various Seismic Designs**

SAND 88-2521C

# Relevance of Partial Saturation to the Mechanical Behavior of Tuffs*

Francis B. Nimick and Ralph R. Peters
Nuclear Waste Repository Technology Department
Sandia National Laboratories
Albuquerque, NM 87185

ABSTRACT: In this paper, equivalent confining pressures are estimated for samples of tuff using an expression that relates capillary pressure and effective confining pressure to the saturation state of the pores. These confining pressures are compared to the pressures calculated from strain measurements during drying; the calculations use elasticity theory.

It is found that stresses and strains are caused by capillary forces in certain partially saturated rocks. This phenomenon has a direct impact on experiments that rely on strain measurements to calculate a rock property. Specific problem areas are the performance of unconfined mechanical tests, calculation of elastic parameters from laboratory data on unjacketed samples, and determination of in situ stress by any method involving stress relaxation.

## 1 INTRODUCTION

For many years, the rock mechanics community has been aware of the potential effects of water on the compressive strength of rock. Qualitatively, wet rocks are weaker than dry rocks. Paterson (1978) provides a summary of the literature pertaining to the topic; some of the more detailed papers include Colback and Wiid (1965), Chenevert (1969), and Michalopoulous and Triandafilidis (1976).

The explanations for the relative values of compressive strength include (1) a decrease in the surface free energy of the solid framework in the presence of water (Colback and Wiid, 1965; Swolfs, 1972); (2) enhanced mobility of dislocations in minerals (Griggs and Blacic, 1965; Griggs, 1967); and (3) an increase in the effective confining pressure caused by the capillary forces in the pores of a partially saturated (i.e., air-dried) rock (Chenevert, 1969; Rao et al., 1987).

---

*This work was supported by the U.S. Department of Energy (U.S. DOE) under contract DE-AC04-76DP00789. The data used in the study were obtained on samples taken from Yucca Mountain, Nevada, as part of the Yucca Mountain Project, which is administered by the Nevada Operations Office of the U.S. Department of Energy.

Data are available from a number of tuffaceous samples which support the last of the possible explanations mentioned above. In the following sections, these data are described; the description includes both the experimental observations and some associated hypotheses concerning the physics of the process. More importantly, two separate lines of experimental evidence lead to similar, quantitative estimates of the capillary forces in the pores of partially saturated samples.

Although the data to be discussed in subsequent sections are interesting, similar observations have been made in other rock types in the past. The goal of this paper is to use the quantitative estimates of pore pressures as a spur to outline the implications for routine measurements of mechanical properties in the laboratory and in the field.

## 2 DESCRIPTION OF DATA

During the more than eight years that samples from Yucca Mountain have been tested, several sets of data were collected by different investigators to determine different rock properties. First, the length changes of a number of saturated samples were examined using a dilatometer while they were equilibrating with ambient laboratory conditions. The combination of this first data set with a second data set of elastic properties (e.g., Young's moduli, Poisson's ratios) obtained on a different set of samples during uniaxial compression tests allowed the calculation of equivalent pressures which would have caused the same strains if the dilatometer samples had been subjected to hydrostatic compression. Finally, hydrologic properties were measured on a third set of samples; these properties have been used in several equations from the hydrologic literature to estimate pore pressures as a function of the saturation of the pores.

### 2.1 Dilatometric Data

The first set of data (see Table 1) is a collection of strain measurements that were made on eleven small (2.54 x 0.32 x 0.32 cm) samples of four types of tuff (two welded devitrified, one welded vitric, two nonwelded vitric, and six nonwelded zeolitic). Each sample was saturated and then placed in a dual-pushrod dilatometer and allowed to equilibrate with the laboratory environment (i.e., ambient temperature and relative humidity). The measure of equilibration was achievement of stable length within the resolution of the dilatometer (approximately 4 x $10^{-5}$ in.). Without exception, the samples contracted and reached stable lengths in 5 to 40 hr. The strains experienced by the samples ranged from 0.0001 to 0.0023.

### 2.2 Elastic Properties

The contraction of the samples must be caused by forces exerted on the samples. In order to relate the sample contractions to the causative forces, the relationship between applied stresses and the resulting strains must be known. It has been determined from many compression experiments that, in general, the tuffs at Yucca Mountain are linearly elastic materials for most of the range of stresses below the failure stress. Consequently, elastic theory is used to relate the sample

contractions to the causative forces. The second data set, consisting of values for Young's moduli (E) and Poisson's ratios ($\nu$) for the tuffs of interest, is given in Table 1, together with the data from the dilatometer measurements.

Table 1. Observed Strains, Elastic Properties, and Calculated Equivalent Confining Pressures for Dilatometric Properties

| Sample ID[a] | Tuff Type[b] | Time to Stable Length (hr) | Observed Strain[c] | Young's Modulus[d] (GPa) | Poisson's Ratio[d] | Equivalent Confining Pressure[d] (MPa) |
|---|---|---|---|---|---|---|
| G1-504.1 | wd | 35 | 0.00010 | 19.9 ± 3.0 | 0.17 ± 0.04 | 3.0 ± 1.6 |
| G1-1151.1 | wd | 12 | 0.00016 | 32.7 ± 4.6 | 0.22 ± 0.03 | 9.3 ± 3.3 |
| G1-1288.9 | wv | 15 | 0.00010 | 23.7 ± 2.5[e] | 0.15 ± 0.05[e] | 3.4 ± 1.7 |
| G1-1342 | wv | 30 | 0.00020 | 15.8 ± 2.0[e] | 0.17 ± 0.05[e] | 4.8 ± 1.5 |
| G1-1362.4 | nwv | 5 | 0.00016 | 15.8 ± 2.0[e] | 0.17 ± 0.05[e] | 3.8 ± 1.4 |
| G1-1395.8 | nwz | >20[f] | 0.00228[f] | 6.0 ± 1.8 | 0.23 ± 0.05 | >25.3[f] ± 8.9 |
| G1-1470.2 | nwz | 30 | 0.00168 | 6.0 ± 1.8 | 0.23 ± 0.05 | 18.7 ± 6.6 |
| G1-1470.7 | nwz | 15 | 0.00174 | 6.0 ± 1.8 | 0.23 ± 0.05 | 19.3 ± 6.8 |
| G1-1744 | nwz | 40 | 0.00144 | 11.5 ± 4.0 | 0.16 ± 0.05[e] | 24.4 ± 9.2 |
| G1-1763.7 | nwz | >7[f] | 0.00104[f] | 11.5 ± 4.0 | 0.16 ± 0.05[e] | >17.6[f] ± 6.7 |
| G1-1799.8 | nwz | 30 | 0.00182 | 11.5 ± 4.0 | 0.16 ± 0.05[e] | 30.8 ±11.7 |

a. All samples are from Corehole USW G-1; the number in the sample ID is the sampling depth in feet.
b. wd = welded devitrified; wv = welded vitric; nwv = nonwelded vitric; nwz = nonwelded zeolitized.
c. Standard deviations are not available for strain. An equivalent, in the form of experiment uncertainty, is estimated to be approximately $4.8 \times 10^{-5}$.
d. Numbers given are the mean value and one standard deviation [(n-1) degrees of freedom] for samples from this tuff type.
e. Data available for one experiment only; value for standard deviation assumed based on expert judgement.
f. No upper limit is available because temperature was increased before a stable length was achieved.

## 2.3 Estimated Stresses

It is assumed that length changes in the contracting samples occur by elastic deformation of an isotropic homogeneous material. Thus, the two elastic properties (E and $\nu$) and the observed axial strains ($\epsilon_a$) are used to estimate the equivalent confining pressure ($P_c$) to which each dilatometric sample would need to be subjected to obtain the observed axial strain:

$$P_c = \epsilon_a \left( \frac{E}{1-2\nu} \right) \quad . \tag{1}$$

In addition, the uncertainty (U) in the calculated value of $P_c$ can be estimated using the following equation (derived from Equation 1 using the approach of Abernethy et al., 1985):

$$U_{P_c} = \left(\frac{1}{1 - 2\nu}\right)\left[\left(EU_{\varepsilon_a}\right)^2 + \left(\varepsilon_a U_E\right)^2 + \left(\frac{2\varepsilon_a EU_\nu}{1 - 2\nu}\right)^2\right]^{1/2} \quad . \tag{2}$$

The calculated values of $P_c$ and $U_{P_c}$ also are given in Table 1.

The uncertainties in $P_c$ that are shown in Table 1 as standard deviations are relatively large, ranging from 31 to 53% of the calculated values. The size of these uncertainties is attributable to the variability of the materials, as reflected in the standard deviations for the two elastic parameters, and to the large relative uncertainty in the strain data.

## 2.4 Hydrologic Theory

In partially saturated rock, the pressure of water in the pores is negative and exerts a stress on the pore walls that is assumed to be equivalent to a hydrostatic confining pressure applied to the exterior of the rock. Capillary-bundle theory (e.g., Hillel, 1971) can be used to estimate the capillary pressure as a function of the pore-size distribution of the rock sample. In general, if two rock samples have the same saturation, the capillary pressure and the confining pressure resulting from capillary forces will be larger for the sample with smaller pores. One can relate the capillary pressure to the resulting confining pressure if the functional relationship between sample saturation and capillary pressure is known (e.g., McTigue et al., 1984).

The third set of data available for rock samples from Yucca Mountain consists of data relating sample saturation and capillary forces. These data were obtained by drying the sample and measuring the relative humidity of air in thermodynamic equilibrium with the sample. The capillary pressure in the sample may be determined using the relative-humidity value and the psychrometric equation (see Campbell, 1977)

$$\psi = -(R/M)T \ln (RH/100) \quad , \tag{3}$$

where $\psi$ is the capillary pressure, R is the universal gas constant, M is the molecular weight of the water, T is the absolute temperature, and RH is the relative humidity (expressed in percent) of the air in equilibrium with the sample. The data were taken as the sample was being dried; data for a sample being saturated would show a general shift of the curve to capillary-force values closer to zero. These sample-drying data are appropriate for comparisons with the dilatometer data because the samples in the dilatometer also were being dried. The curve used to fit the saturation versus capillary-pressure data is based on a function suggested by van Genuchten (1980).

The relationship between capillary pressure and an equivalent confining pressure has been discussed by a variety of authors [see Narasimhan (1982) and Rao et al. (1987)]. In the paper by McTigue et al. (1984) the relationship between a change in capillary pressure and the resulting change in stress is given by the following equation:

$$d\sigma = (s - s_r)\, d\psi \qquad (4)$$

where s is the saturation and $s_r$ is the residual saturation.

Thus, in order to find the change in effective confining pressure between some initial saturation (e.g., full saturation) and a given final state (e.g., the saturation associated with a sample in equilibrium with room air of a known relative humidity) the function relating saturation and capillary pressure is substituted into Equation 4, which is then integrated between the initial and final capillary pressures.

Calculation of the effective confining pressure resulting from the capillary pressure in a specific sample of unsaturated tuff requires knowledge of the relative humidity of the air during the time the samples were tested in the dilatometer as well as the water saturation curve of the dilatometer sample. Unfortunately, neither piece of information is available for the dilatometric samples discussed earlier.

The approach that has been taken for this work is to obtain saturation curves from data published for tuff which will maximize and minimize the confining pressure that is calculated in the manner described above. The values of capillary pressure that were selected as final states for the integration in Equation 4 correspond to relative humidities of 20, 40, 60, and 80%. The range of relative humidities is used because the laboratory humidity at the time of the dilatometer measurements is unknown, but is estimated to lie in this range with the most probable value(s) being less than 50%. Data for saturation curves were taken from Peters et al. (1984).

## 3 RESULTS

Figures 1a-1c compare equivalent confining pressures that were estimated using the two different techniques. The points plotted as a function of relative humidity are obtained from hydrologic data: the vertical brackets indicate the range of pressures calculated for each of the dilatometer samples using measured strains from the first data set and estimates of the elastic properties from the second data set (see Table 1).

The following concepts are important to one's understanding of Figure 1. The relative humidity of the laboratory during dilatometer measurements is unknown. Thus, only qualitative statements can be made about environmental conditions. Also, the values calculated from hydrologic theory using data from a number of rock samples should provide upper and lower bounds on pressures which are estimated by this technique.

Figures 1a and 1b show estimated confining pressures for welded devitrified and nonwelded zeolitized tuff, respectively. In both cases, pressures estimated from dilatometer and mechanical property data fall within the bounds obtained from hydrologic theory. Also, estimated confining pressures for these two rock types can be quite large, especially for the zeolitized tuff.

Figure 1c presents data for samples of vitric tuff. Qualitatively, because densely welded tuff has lower porosity, smaller average pore diameters, and lower permeability, welded tuff should experience larger equivalent confining pressures than would nonwelded vitric tuff under the same conditions. Nonwelded vitric tuff is expected to experience equiva-

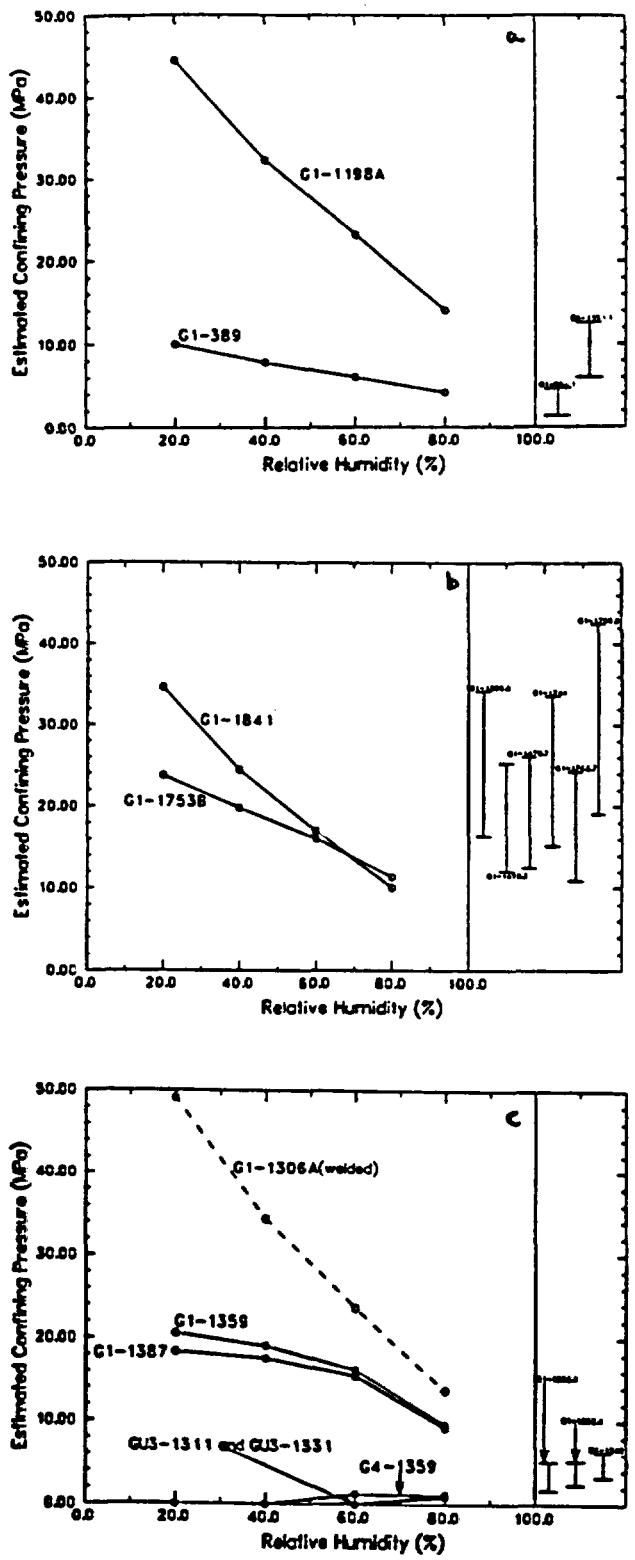


Figure 1. Estimated Confining Pressures in Tuff as Estimated by Two Independent Techniques. Hydrologic Estimates are in the Left Portion of Each Plot. Dilatometer-Mechanical Estimates are in the Right Portion. 1a - Welded, Devitrified Tuff. 1b - Nonwelded, Zeolitized Tuff. 1c - Vitric Tuff.

lent confining pressures similar to those shown for the two lower sets of points shown as a function of relative humidity in Figure 1c. It is inferred that the three vitric dilatometer samples all represent non-welded or partially welded material, and that the two middle curves in Figure 1c were obtained for moderately welded vitric tuff.

## 4 DISCUSSION

The preceding section presented calculations of equivalent confining pressures estimated by two independent methods. The good agreement of equivalent confining pressure values (Figure 1) determined by these two methods implies that significant capillary forces may exist for conditions of low relative humidity. Implications of the potential effects of capillary forces on standard rock mechanics tests are discussed briefly in the following sections.

### 4.1 Mechanical Property Testing

The relative effects of partial saturation on the compressive strength of rocks have been previously observed. However, what apparently has not been considered is the number of pitfalls awaiting one who is unaware of the potential effects of reequilibration of samples during testing. For example, performing a valid unconfined compression test using an unjacketed saturated sample may be impossible for materials with hydrologic properties similar to those of the zeolitized tuffs discussed earlier. If the laboratory air is sufficiently dry that the sample loses a substantial portion of its water, such tests actually may be equivalent to tests performed under confining pressures of 30 MPa or more because of capillary forces resulting from sample drying. For the zeolitized samples, such confining pressures would increase the compressive strength of the sample by more than 15% of the unconfined value and would change the deformation behavior from linear-elastic toward nonlinear or ductile behavior. In addition, samples would be subjected to a continually increasing confining pressure from test initiation through sample failure or sample moisture equilibration, whichever came first. The rate of this pressure increase would not be steady, but would probably be exponentially decreasing during a test. Thus, interpretation of the resulting stress-strain data would be quite difficult.

The scenario discussed in the preceding paragraph would be more likely at lower strain rates (or stress rates). Tests conducted at strain rates of $10^{-6}$ $s^{-1}$ or less will experience stresses resulting from capillary effects unless a laboratory has relative humidities greater than 70 to 80%. In creep tests, strains caused by capillary forces could obscure the transitions in creep behavior.

Finally, because of strain induced by capillary forces, erroneous estimates of elastic parameters (e.g., Young's modulus and Poisson's ratio) could be made. The stress-strain behavior during a $10^{-7}$ $s^{-1}$ test has been calculated in two ways for each of two materials. First, the strictly linear response was calculated using an average value for Young's modulus. Second, the effect of capillary-force-induced strain was added using the measured strains (as a function of time) for two of the dilatometer samples. The apparent Young's moduli calculated for the second case were lower than the average measured values by 8% for the

welded devitrified material and by 24% for the nonwelded zeolitized material.

So far, the discussion has focused on rocks that began a test in an initially saturated state. Similar problems will occur for rocks that begin a test dry, especially for rocks that have been dried in an oven or in a vacuum. Such rocks also will tend to equilibrate with the laboratory air, although evidence suggests that the rate of equilibration is slower. Nevertheless, the reequilibration process will lead to equivalent confining pressures in these samples as well.

The magnitude of the effects of capillary forces will vary depending on the hydrologic properties of the rock, the relative humidity and temperature of the testing laboratory, the duration of an individual test, and the geometry (especially the surface area) of the sample. The first three of these factors have already been discussed. The fourth factor addresses whether the sample is jacketed during testing. National and international testing procedures (e.g., ASTM or ISRM) suggest that samples be jacketed for all triaxial tests and for uniaxial creep tests on soft rock. Procedures for uniaxial compression and tensile strength tests do not address the need to jacket test samples.

If a sample is jacketed, the exposure to the laboratory environment usually is, at most, through an open vent where pore pressure normally would be monitored. This opening is a trivial amount of surface area relative to the total area of a sample; therefore, jacketed samples should undergo little if any reequilibration with the relative humidity of a laboratory.

## 4.2 In Situ Stress Determination

Many techniques for the determination of in situ stress are based on the measurement of sample strains resulting from stress relaxation and the calculation of relevant stresses using a number of methods. These techniques are subject to the same potential problems as are the laboratory tests. Samples collected from in situ states will change dimensions if the air to which they are exposed has a relative humidity different from the humidity value in equilibrium with the in situ saturation state of the sample. The amount of dimension change will depend on the hydrologic properties and the length of time over which the strain measurements are made. For comparison, the dilatometer samples contracted 0.1-2.3 millistrain when equilibrating with laboratory air. During strain measurements for determining in situ stress, strains are of the same magnitude (e.g., Teufel, 1981). Thus, the potential exists for strains induced by capillary forces to complicate or completely obscure the strains expected from stress relaxation.

Conversely, if the in situ stress can be measured accurately, the interpretation of the data may require modification from the usual approach. Normally, three components of in situ stress are considered: gravitational, tectonic, and residual. If a rock is partially saturated in situ, then the capillary forces should be considered as a fourth component. The capillary forces would be an effective hydrostatic stress which contribute to all three principal stresses equally. According to the calculations earlier in the paper, this effective hydrostatic stress could comprise a significant portion of the overall in situ stresses.

## 5 SUMMARY AND CONCLUSIONS

Equivalent confining pressures caused by capillary forces in tuff have been calculated using two methods--analysis of strains induced by capillary forces and estimation using hydrologic theory. The equivalent pressures calculated by the two methods are in substantial agreement. All rock samples will experience equivalent confining pressures if they are allowed to equilibrate with air of less than 100% relative humidity. The magnitude of the equivalent confining pressures will be greater for lower relative humidities, samples with smaller pores and lower porosity, longer test times, and larger ratios of surface area to volume.

In the laboratory, unconfined tests (both tensile and compressive) are subject to the potential problems associated with reequilibration. These problems include the effects of an equivalent confining pressure on the boundary conditions assumed for a test (i.e., that a test is being conducted under a uniaxial state of stress) and potential errors in the interpretation of strain data obtained during the test. Elastic parameters may be in error because of additional strains caused by the capillary forces. Creep behavior may be complicated or obscured by the capillary-force-induced strains. If the equivalent confining pressure is of sufficient magnitude, the deformation mode may change from elastic-brittle to a more ductile response.

A similar understanding is important when strains are used to determine the in situ stress state. The strains induced by capillary forces could be as large as those that result from stress relaxation. Such relative magnitudes may invalidate in situ stresses calculated from the strain data.

The major conclusion of this paper takes the form of a recommendation. In order to ensure that samples do not undergo strains as a result of equilibration with the testing environment, two options exist. It is strongly recommended that any sample on which strains are to be measured should be

- isolated from the ambient relative humidity by means of a jacket or other coating material, or

- tested in a known environment with which the sample is already in equilibrium.

The latter option usually will be impractical for fully saturated or oven-dried samples in a laboratory or for field measurements of in situ stress. Thus, jacketing of samples immediately after achievement of the desired saturation state of the sample would be the preferred option. This approach should be added to those widely accepted testing procedures which do not currently include such a provision.

## REFERENCES

Abernethy, R. B., R. P. Benedict, and R. B. Dowdell, 1985. ASME measurement uncertainty; Jour. Fluid Eng., Vol. 107, pp. 161-164.

Campbell, G. S., 1977. An Introduction to Environmental Biophysics; Springer-Verlag, New York, NY.

Chenevert, M. E., 1969. Adsorptive pore pressures of argillaceous rocks; Proc. 11th Symp. on Rock Mechanics, pp. 599-627.

Colback, P. S. B., and B. L. Wiid, 1965. The Influence of moisture content on the compressive strength of rocks; Proc. Rock Mechanics Symp. held at Univ. of Toronto, January 1965. Ottawa: Dept. Mines Tech. Surv., pp. 65-83.

Griggs, D. T., 1967. Hydrolytic Weakening of quartz and other silicates; Geophysics Journal Roy. Astron. Soc., Vol. 4, pp. 19-31.

Griggs, D. T., and J. D. Blacic, 1965. Quartz: Anomalous weakness of synthetic crystals; Science, Vol. 147, pp. 292-295.

Hillel, D., 1971. Soil and Water; Academic Press, New York, NY.

McTigue, D. F., R. K. Wilson, and J. W. Nunziato, 1984. An effective stress principle for partially saturated media; SAND82-1977, Sandia National Laboratories, Albuquerque, NM.

Michalopoulos, A. P., and G. E. Triandifilidis, 1976. Influence of water on hardness, strength and compressibility of rock; Bull. Assoc. Eng. Geol., Vol XIII, No. 1, pp. 1-22.

Narasimhan, T. N., 1982. Physics of saturated-unsaturated subsurface flow: in T. N. Narasimhan (ed.). Recent Trends in Hydrogeology; Geol. Soc. Amer. Spec. Paper 189, pp. 3-23.

Paterson, M. S., 1978. Experimental Rock Deformation - The Brittle Field; Springer-Verlag, New York, NY.

Peters, R. R., E. A. Klavetter, I. J. Hall, S. C. Blair, P. R. Heller, and G. W. Gee, 1984. Fracture and matrix hydrologic characteristics of tuffaceous materials from Yucca Mountain, Nye County, Nevada; SAND84-1471, Sandia National Laboratories, Albuquerque, NM.

Rao, K. S., G. V. Rao, and T. Ramamurthy, 1987. Discussion of paper by K. L. Gunsallus and F. H. Kulhawy, "A comparative evaluation of rock strength measures;" Int. J. Rock Mech. Min. Sci. & Geomech. Abstr., Vol. 21, pp. 233-248.

Swolfs, H. S., 1972. Chemical effects of pore fluids on rock properties; in T. D. Cook (ed.), Underground Waste Management and Environmental Implications; Amer. Assoc. Petrol. Geol. Mem. 18, pp. 224-234.

Teufel, L. W., 1981. Strain relaxation method for predicting hydraulic fracture azimuth from oriented core; SPE/DOE Low Permeability Symposium, Denver, CO, May 27-29, 1981, pp. 81-86.

van Genuchten, M. Th., 1980. A closed-form equation for predicting the hydraulic conductivity of unsaturated soils; Soil Sci. Am. J., Vol. 44, pp. 892-898.

SAND 88-7052C FINAL

# A Concrete Shaft Liner Design Methodology for Nuclear Waste Repositories

Archie M. Richardson, Mining Engineer
Parsons Brinckerhoff Quade & Douglas Inc., San Francisco, California, USA

Christopher M. St. John, Director of Engineering
Principia Mechanica, London, England

ABSTRACT: Considerations important to design of cast-in-place concrete liners for repository shafts are discussed. Requirements for repository shaft liners and design criteria appropriate to those requirements are presented. Types of loads acting on a liner and modes of deformation are discussed. Methods are proposed for calculating load magnitudes and liner stresses and for evaluating liner performance.

## 1 INTRODUCTION

Vertical shafts are integral to the underground nuclear waste repository program in the U.S., both for the site characterization and operations phases. Following standard mining industry practice, cast-in-place concrete liners are planned for some of these shafts. Even planned composite liners for sites where groundwater inflow is a potential problem will typically include an outer concrete liner cast directly against the excavated rock (Poppen et al., 1987). Important advantages of simple concrete liners include excellent security from rockfall, convenient attachment of shaft equipment, low resistance to airflow, contractor familiarity, and protection of the wall rock from weathering.

Shaft (and tunnel) liner design has historically been an important part of underground engineering and has received extensive theoretical investigation. Circular geometries, including cylindrical inclusions, are mathematically tractable if simple idealizations for wall rock behavior can be justified. However, a complete understanding of the true nature of ground-liner interaction that occurs after initial installation has been and continues to be elusive. Various design approaches have arisen in response to the wide range of conditions that have been encountered at different installations. Before liners for deep repository shafts are selected, a consistent design methodology must be established that considers ground pressure, induced thermal and seismic effects. This paper outlines such a methodology for design of cast-in place concrete shaft liners. Its major steps are illustrated by the flowchart in Figure 1. For initial design of shafts, a collection of relatively simple analyses emphasizing closed-form solutions can be used to calculate liner loads, determine critical stresses in the liner, and evaluate the performance of the liner. Final verification of that design for future licensing of the shafts as part of the repository is an additional step that may include sensitivity studies, and detailed stress analysis accounting for material nonlinearity and dynamic effects. The

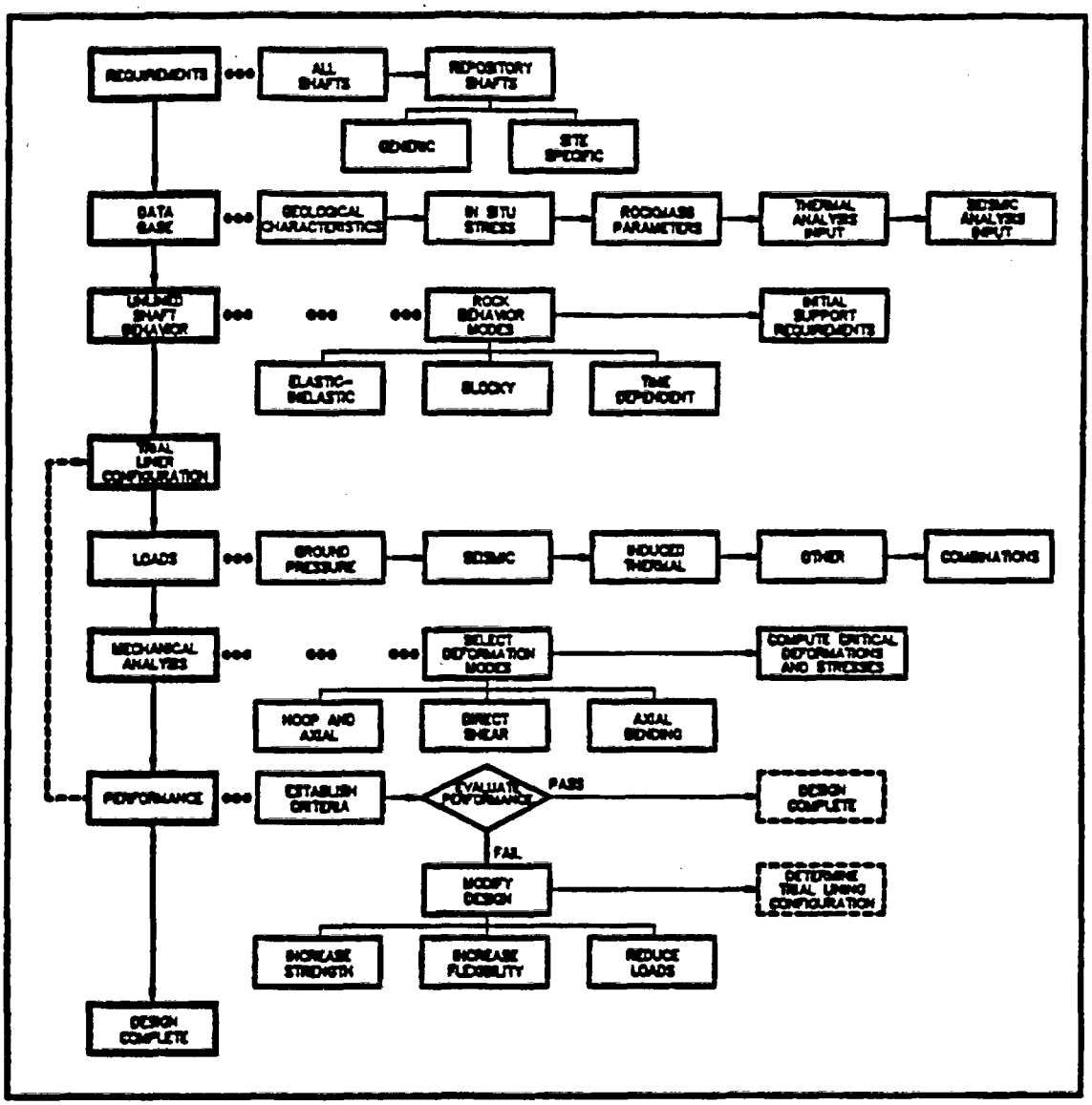


Figure 1. Flow chart of proposed liner design methodology.

overall methodology serves as a framework that remains valid for any level of analysis considered appropriate.

## 2 REQUIREMENTS

The general requirements for repository shafts are defined in the hierarchy of requirement documents established for the national high-level waste program by various U.S. government agencies. At the top level of this hierarchy is 10 CFR Part 60.133 (NRC, 1986), which sets performance objectives for repository openings that provide operational

safety and retrievability requirements under expected repository conditions, specifically including thermal loading.

The Generic Requirements Document for a Mined Geologic Disposal System (DOE, 1986), at the second level of the hierarchy, interprets and expands these into more specific functional requirements for all repository shafts. Appendix E of this document specifically applies to the exploratory shafts and requires their liners to; 1) provide structural integrity to the shaft opening, 2) provide a means for anchoring shaft fittings, 3) provide water control, and 4) complement operational seals. Appendix E also requires the exploratory shaft liners to be designed and constructed with the same criteria, standards, and quality assurance levels required for the repository (to the extent known at the time of their design).

Further U.S. Government requirements will be site specific but have not been fully developed as of this writing. Shafts excavated through water-bearing strata, however, will require strict water control. If dissolution of the host rock by water is a potential issue, watertight liners will be required. Water control will not be as crucial where essentially dry conditions may be confidently predicted for the preclosure life of the facility and where the host rock has a low solubility. Similarly, requirements for resistance to seismic loads will reflect shaft functions and the anticipated natural and manmade seismic environment.

It is crucial that the requirements and performance criteria adopted realistically reflect the importance of specific shafts to public health and safety and the consequences of liner failure.

## 3 DATA BASE

The repository shaft design will benefit from a detailed data base obtained from exploratory shaft facility testing programs, but the exploratory shafts themselves must be designed with only preliminary site data obtained by drilling from the surface. When more detailed site data has been collected through testing and monitoring at the underground test facility, it is possible these shafts may need to be retrofitted to meet repository performance requirements, especially regarding thermal loading. This possibility can be minimized with a suitably conservative initial design. Retrofitting, if required, could be performed by several methods that will not present major construction difficulties with this type of liner.

## 4 UNLINED SHAFT BEHAVIOR

Although shafts may be sunk and lined by several methods, standard U.S. mining practice is to cast a concrete liner concurrent with sinking. The liner installation lags the sinking by some distance determined by operational efficiency and support requirements. Geologic and geotechnical mapping requirements may dictate the length of the unlined section for exploration shafts. Some form of temporary support may be required to assure a safe working environment and to minimize disturbance of the rock mass before the liner is emplaced. The mode of rock behavior in the unlined shaft section must be established, both for an initial estimate of temporary support requirements and for selection of material models for subsequent determination of liner loads. An analytical approach is appropriate when the formation is generally massive. Such an

approach might include using relatively simple closed form solutions to check for inelastic behavior. Initial support requirements for an elastoplastic material can be investigated using methods described by Detournay and Fairhurst (1987), which enable determination of the relaxed zone under nonuniform in situ stress conditions, as well as the internal pressure required to limit its extent. A number of methods exist for determining support requirements for blocks, providing the orientation of joint sets (and preferably the specific location of major block-forming joints) are known in advance of excavation. If inelastic or blocky behavior is shown to be limited in extent under predicted conditions, or can be reliably controlled with initial support, subsequent analysis of liner loads may be simplified by using linear elastic methods. Empirical methods, such as rock mass classifications, are useful for estimating initial support requirements in tunnels but have not yet been fully adapted and verified for vertical shaft use. Development of site-specific rock mass classifications for future design would be a useful output from the exploratory shaft program.

Initial support requirements can only be approximated prior to excavation. The actual support installed will likely be determined during construction, by the consensus of parties responsible for worker safety.

# 5 LINER LOADS

## 5.1 General

Loads for liner design can be established after the mode of rock behavior in an unlined shaft has been evaluated. The outer surface of a liner is acted upon by radial and shear tractions that develop as the liner offers passive resistance to distortions of the surrounding rock mass. Tractions resulting from this "interaction" behavior are often used as "loads" in liner calculations. However, they differ from classic engineering loads in that their magnitude depends on the stiffness ratio between the liner and the rock. In this methodology, "free-field" stresses, strains and displacements (those that would occur at the shaft location if the shaft did not exist) will be referred to as "loads". Defining loads in this manner makes them independent of the liner, and also facilitates calculations by requiring interaction to be considered only once during liner stress computations, rather than separately in each load calculation. This is especially useful where different types of loads are combined, which commonly occurs in repository shaft design calculations.

## 5.2 Water Pressure

If a waterproof liner is required, then hydrostatic pressure will generally dominate the liner design and is readily calculated.

## 5.3 Ground Pressure

In this discussion, the term "ground pressure" will be used for all loads imposed on the shaft liner by the surrounding rock mass that arise from the process of excavating the shaft.

If the unlined shaft analysis of Section 4 shows that the rock remains elastic after excavation, then no support from the liner is required although it must still fulfill other functional requirements. Ground

pressure will st develop on the liner as a resu of elastic expansion of the newly unconfined rock as the shaft is deepened. The magnitude of this load will be a function of the distance from the face to the point of liner installation, and may be expressed as a percentage of the free-field in situ stresses. Several studies of this phenomenon (e.g., Ranken and Ghaboussi, 1975; Pariseau, 1977) have indicated little load will develop in this manner if the liner is installed further than one shaft diameter from the advancing face. Mapping and other requirements in repository shafts make it likely that this liner installation gap will be greater than one diameter. For initial design, a gap must be postulated and the percentage determined. This percentage may be calculated by numerical simulation of the excavation process. The value for the ground pressure is generally less than 25% of the free-field in situ stress for typical liner/rock stiffness ratios and practical construction sequences. Ranken and Ghaboussi's work suggests that a 10 to 15% ratio is appropriate if the liner is not installed closer than one shaft diameter from the shaft bottom.

If the analysis shows that inelastic behavior will occur, then the liner will have a structural ground-support function. One approach to estimating the liner support requirements is to use a classic elastic-plastic method in which it is assumed that the maximum pressure the liner is likely to experience is the uniform internal pressure required to eliminate inelastic rock behavior. This calculation is readily performed, whether the initial rock stresses are isotropic or anisotropic. However, the analysis is an oversimplification because it is likely that the liner will neither apply a uniform pressure, nor be installed sufficiently early to prevent inelastic behavior. A detailed discussion of this approach is presented by Hustrulid (1984), who applied it to a preliminary analysis of Nevada Nuclear Waste Storage Investigation (NNWSI) project exploratory shafts. Although not inherently conservative, the method tends to be conservative in practice.

An alternative is to perform a ground-liner interaction analysis (e.g. Brady and Brown, 1985). This approach is simple if uniform in-situ stresses can be assumed, because the relaxed zone around the shaft is circular and the pressure exerted on the liner is uniform. If this assumption is not valid, closed form calculations of ground pressures are more difficult, although the solution discussed by Detournay and Fairhurst (1977) may be applied. A better alternative is to use a more general numerical model, such as a finite element model, which also allows the interaction with the liner to be included in the analysis.

For initial design purposes it is recommended that the ground be considered to behave elastically if nonlinear behavior is shown to be limited in extent and stabilized by initial support. If substantial inelastic behavior is predicted, then recourse must be made to a numerical model in which the timing of liner installation is simulated. Initial support may be designed to carry part of the ground pressure. Concerns about the service life of initial support suggest the conservative assumption that the initial support does not reduce liner loads.

If long-term creep is expected, then the load on the liner will eventually approach the in-situ stresses unless the shaft is overexcavated and frangible backpacking is installed to compensate for closure. The amount of overexcavation necessary to isolate the shaft may be predicted from site-specific creep equations and the design life of the shaft.

Final ground pressure loads are composed of free-field normal stresses perpendicular to the vertical shaft axis. If the liner is cast directly

against, and supported by, the rock, then vertical loads need not be considered. Also significant shear strains and curvatures are unlikely to develop purely as a result of the excavation of the shaft.

## 5.4 Induced Thermal Loads

Thermal loads, resulting from expansion of the rock near emplacement areas as it is heated by decaying waste, must be considered in designing those shafts that will remain functional during the period of waste emplacement. This "induced" thermal loading takes the form of stresses and strains imposed on the liner from far-field thermal expansion, rather than stresses resulting from "direct" thermal expansion (expansion of the liner itself), and can be a significant effect. The load acts both horizontally as a free-field stress increase, and vertically as an extensional strain as the ground surface is uplifted. Due to standoff distance from the emplacement areas, repository shafts will be largely outside the thermal gradient during their functional period, and any significant direct thermal expansion will be from ventilation effects. Induced thermal loads are unique because they build very slowly, as the heat from the decaying waste is slowly transferred to the surrounding rock, and they only reach significant values late in the functional life of the shaft liners.

Thermal analysis involves the following steps:

1. Preparing input data. The spatial layout, thermal loading, and emplacement sequence of the waste emplacement areas relative to the shaft must be determined.
2. Establishing initial and boundary conditions and model development. Depending on the situation, plane strain, axisymmetric, or complete three-dimensional analysis will be appropriate. Unless a very simple emplacement geometry is assumed, computer modeling will be required.
3. Calculating the spatial and temporal rock temperature distribution induced by the decaying waste.
4. Selecting an appropriate constitutive model for the rock, and parameters for the model.
5. Computing thermally induced free-field stresses and/or strains at the desired locations along the shaft axis.

Thermal loads will consist of a complete free-field stress or strain tensor at critical locations along the shaft. In addition, curvatures may be calculated from computed relative displacements along the shaft.

## 5.5 Seismic Loads

A seismic event, whether associated with an earthquake or an underground explosion, generates elastic waves that propagate outward from the source. The elastic waves induce transient stresses and strains in a rock mass and, hence, in any embedded structure such as a shaft. The effects on the structure will depend upon a number of parameters, including the physical properties of the rock and the structure, and the amplitude, frequency and duration of the ground motion. Seismic events may also impose direct shear displacements on the shaft lining if they cause movement along faults transecting the shaft axis.

Unlike surface structures such as buildings which tend to move and deform independently when excited by earthquake-induced ground motions, shaft liners move and distort compatibly with the ground in which they are embedded. Hence, static analysis is appropriate. Also, if the wavelength of the seismic pulse is relatively large with respect to the opening diameter (i.e. if the rise time of the seismic impulse is long

relative to the transit time of the wavefront across the opening), then there will be no severe strain gradients across the structure. Hendron and Fernandez (1983) propose that there will be little dynamic amplification if the wavelength is at least 8 opening diameters. Since the wavelength associated with the ground motion peak from an earthquake is generally at least 10 times the diameter of a typical shaft, "pseudo-static" analysis will yield sufficient accuracy for most initial liner analysis.

The general procedure for pseudo-static analysis involves:

1. Defining ground motions for a control point (usually the intersection of the shaft axis at the bedrock or ground surface). A deterministic approach can be followed in which the epicentral location and maximum credible magnitude of earthquakes on known faults are estimated, and control motions are calculated using a suitable distance-attenuation function. Alternately, a probabilistic approach may be used in which the spatial and temporal occurrence of earthquakes within each potential earthquake source zone is represented by simple probabilistic models. Using suitable attenuation functions for each travel path, the annual probability of exceedance of a given level of ground motions at the control point may be developed. Defining control ground motions is one of the most difficult parts of the design, and a level of conservatism appropriate to the level of uncertainty and consistent with liner functions should be incorporated in these values. For pseudo-static analysis the required control motion parameters are particle velocity and acceleration, and three orthogonal components (two horizontal and one vertical) will be required for each parameter.

2. Developing a suitable depth-attenuation relationship at the site so that the magnitude of ground motions at various design points along the shaft can be determined from the control motion. This is especially important for soil sites, where modeling may be appropriate.

3. Determining the types of waveforms expected to arrive at the design points, which may include dilatational (P) waves, horizontal (SH) and vertical (SV) components of shear (S) waves, and surface waves. The contribution of each waveform to the control motion must be assessed, and appropriate ranges of emergence angles of the waveforms must be determined.

4. Calculating a tensor of free-field strains at each design point for each waveform using equations for strain components in terms of particle velocities, propagation velocities, and angles of incidence. In addition to the strain tensor, curvatures can be calculated from accelerations.

5. Assessing the possibility of simultaneous arrival of different waveforms. If the epicentral distance from the shaft is great, it may be possible to assume separation of P and S waves. A probabilistic treatment of concurrent arrivals, assuming random phasing of the different waveforms, can be approximated by the 100-40 rule (Newmark and Hall, 1977), in which 100 percent of the strains due to particle motion in one particular direction are combined with 40 percent of the strains corresponding to the two orthogonal directions of motion. If it is not clear which combination will provide the maximum stresses in the liner, a number of seismic load combinations may have to be evaluated.

A fully dynamic analysis follows many of the above steps but requires complete time history input. Beyond the scope of methods for initial design, it may be part of a design confirmation for important shafts.

Loads for pseudo-static analysis consist of a complete free-field stress or strain tensor at design locations along the shaft, as well as curvatures to account for relative displacements of these points. Seismic loads differ from the other loads in that they are transient, and

they oscillate between positive and negative values

5.6 Load Combinations

Since all loads are specified as free field stresses, they can be conveniently transformed to a suitable reference axis using conventional stress transformation methods, and combined by simple addition. If there is considerable uncertainty in orientation of the stress tensor (e.g., seismic), conservative assumptions should be made when combining loads.

## 6 MECHANICAL ANALYSIS

### 6.1 General

Non-repository shaft design practice has typically involved calculating only peak tangential stresses caused by inward radial rock pressure acting on the exterior of the liner. If the liner is cast against the rock, vertical (axial) loads are assumed to be carried by the shaft walls, hence vertical stresses in the liner are assumed to be negligible. Curvature and shear are unlikely to be induced in a mine shaft liner unless there is differential subsidence caused by underground mining. For repositories, thermal loading and seismic effects require a more complete mechanical treatment. Steps for mechanical analysis of a repository shaft liner must include identifying important deformation modes, selecting appropriate mathematical models to investigate each of these modes, and properly combining deformation modes.

### 6.2 Important Deformation Modes

A three-dimensional model permits the most complete analysis if all the modes of loading on the shaft are to be considered. However, if linear elastic behavior is assumed, behavior modes can be analyzed independently and combined using superposition if required.

Figure 2 illustrates three independent deformation modes: 1) hoop deformation combined with axial deformation, 2) bending, and 3) shear. Hoop is considered with bending because the two effects will be considered together in the generalized plane-strain analysis discussed later.

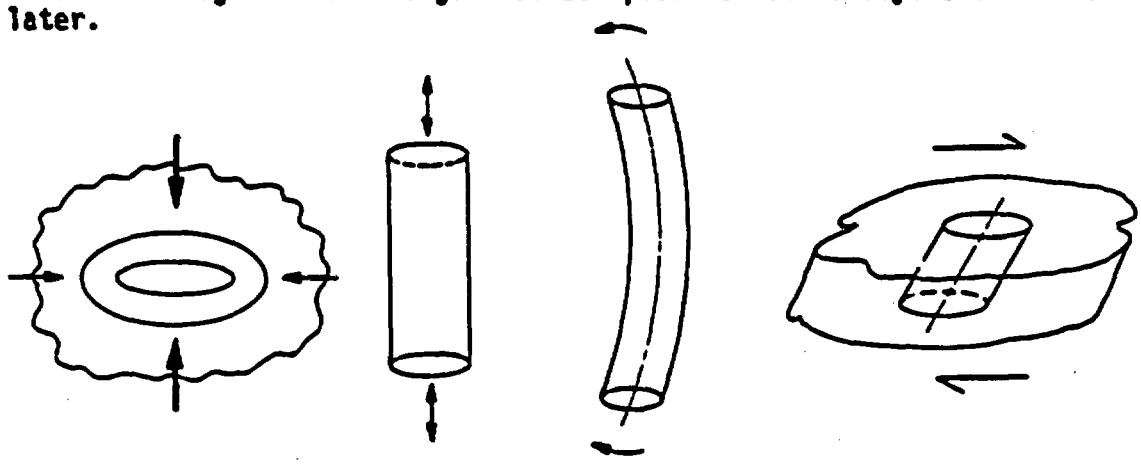

(a) Hoop deformation and axial strain (b) Bending (c) Shear

Figure 2. Modes of deformation of shaft liner.

## 6.3 Types of Models for Liner Deformation Modes

Closed-form models for liner stress analysis may be subdivided into three progressively more complex categories:

1. Models that assume the free-field strains in the rock are transferred directly to the liner. These involve the least computation. Results from this type of model will be accurate if the lining is less stiff or equal in stiffness to the ground, and conservative if the liner is substantially stiffer than the ground. Overconservatism may result in relatively soft ground conditions, which is a disadvantage of this type of analysis.
2. Models that analyze the liner as a free-standing ring-shaped compression member subjected to externally-applied loading. Moments and thrusts can then be calculated in the liner in a manner similar to beam analysis, or peak fiber stresses calculated directly using elastic equations. Interaction is not explicitly considered by these models, but may be incorporated when calculating loads.
3. Models that analyze the liner and rock together as a system and directly consider the interaction between them.

In general, any model selected should consider liner-rock interaction in some fashion.

## 6.4 Hoop Deformation and Axial Strain

Ground pressure, thermal loads, and seismic loads can result in hoop deformation, which is generally considered to be the most significant mode of deformation in vertical shaft liners.

A closed-form linear elastic interaction analysis is suggested in which loads may be applied to a model composed of a thick cylinder (liner) embedded in a matrix (rock) with independent material properties. Such a model should be capable of analyzing situations where applied loads are anisotropic. Transfer of shear stresses at the liner-rock interface (fully bonded condition) may be assumed for a cast-in-place liner. A generalized plane strain condition, in which an axial strain constraint may be specified, is necessary for the case of simultaneous axial strain and hoop deformation.

Figure 3 depicts a section through an example shaft, showing tangential stresses at the inner circumference of the liner calculated using a closed form interaction model. Nonuniform ground pressure and thermal loads result in the liner stresses shown on the upper half of the figure. A transient seismic loading caused by simultaneous arrival, at the illustrated section, of a P-wave traveling vertically along the shaft axis and a horizontally polarized, orthogonally incident S-wave results in seismic stresses, shown independently in the lower portion of the figure. Axial extensions from thermal uplift were imposed as boundary conditions on the static analysis, and axial strains from the P wave on the seismic analysis. It should be noted the specified seismic load combination is improbable and was selected for illustrative purposes only; it is unlikely that P and S waves will simultaneously arrive from orthogonal directions.

## 6.5 Bending

Axial bending may result from curvatures associated with nonuniform, thermally-induced displacements of the wall rock and with vertical or inclined S-waves incident on the shaft. Simple closed-form interaction models of axial bending of an embedded liner are not available. It may be

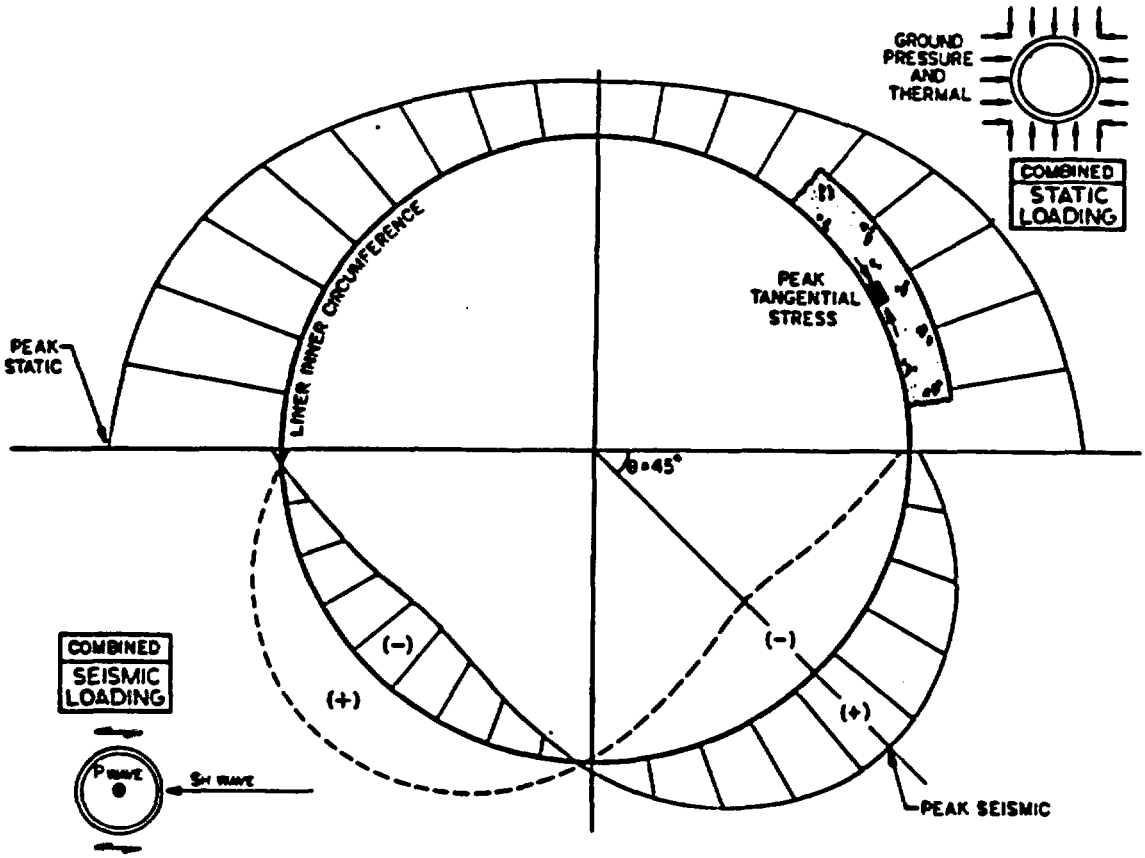


Figure 3. Tangential stresses on the inner circumference of a typical shaft liner under combined loading.

assumed that the liner will deform conformably with the rock mass. In most situations bending alone will not be the critical deformation mode. However, differential thermal loads at stratigraphic interfaces, and extreme vertical or inclined shear waves could cause significant bending strains. Bending causes axial and shear stresses, both of which should be evaluated.

### 6.6 Shear

Direct shear may be caused by inclined S-waves or by thermal loading. Closed form interaction solutions can be used to analyze shear behavior on planes normal to the axis of the shaft, in which the shear is not transferred directly from the free field, but causes the liner to flex as a vertical beam.

## 7.0 LINER PERFORMANCE

In the U.S., most concrete design is performed using the methods and criteria outlined in the American Concrete Institute codes (ACI,1983a,b).

These codes permit two alternate design methods; the "strength" or "ultimate strength" method, and the "working stress" or "elastic" method. The strength approach is currently preferred for most reinforced concrete design because it accounts for the redistribution of stresses due to the nonlinear stress/strain behavior of concrete and results in a more accurate appraisal of the ultimate strength of a member. In the working stress approach, the member is proportioned to maintain stresses below an allowable stress level. The working stress approach is sometimes called the "elastic" approach because linear elastic relationships are assumed in stress analysis. The standard ACI allowable stress level for compression is 45% of the 28-day concrete cylinder strength ($f'_c$), below which value the concrete exhibits essentially linear behavior. In unreinforced concrete, which is used in the majority of deep circular shafts in the U.S., both strength and working stress methods give essentially the same results when standard load and capacity factors and allowable stress levels are employed. Since this methodology suggests an analytical approach where stresses are calculated in the liner, the working stress method is the logical alternative.

There are important differences between liners and surface structures that may lead to overconservatism when standard structural design techniques are applied to shaft liners. A cast-in-place concrete liner is not a free-standing structure that must support an externally applied load, but reinforces the surrounding rock mass, which is often largely self supporting. A relatively thick cylindrical liner is inherently stable under external loading conditions due to its cylindrical geometry. Although it may crack, catastrophic failure cannot develop until considerable post-yield displacement occurs. Structural instability (failure in buckling modes) also is not likely. Except for water pressure and long-term creep, which have ultimate levels independent of the liner, liner loads typically lessen with liner deflection. Often detrimental in surface structures, creep and shrinkage in the concrete may be beneficial effects when loads are displacement-dependent, yet no credit is typically taken for these effects in liner designs.

To ensure the integrity of the liner and to prevent a falling object hazard in shafts where personnel are present, such as a hoisting shaft or an exploratory shaft during the site characterization period, it is recommended that an appropriate factor of safety be provided against the possibility of compressive spalling. The ACI standard of 45% $f'_c$ will be quite conservative, and will also permit elastic design methods. In shafts where personnel and equipment exposure to falling concrete is minimal, or where loads are transient, an increase to 60% $f'_c$ is justified. These criteria are to prevent the onset of crushing and spalling; it should be emphasized that exceeding these levels will not result in collapse of the structure for the reasons mentioned earlier.

Shear strength criteria should account for increases in shear strength due to the confinement of the concrete at the location of peak shear. German practice in shaft design (Link et al., 1985) permits shear stresses in plain concrete of $2.3(f'_c)$ under conditions of no confinement; to account for confinement this level is increased by the value of the smallest normal compressive stress across the plane of shear.

In general, limited tensile cracking in an unreinforced non-waterproof concrete liner may be disregarded because neither horizontal nor radial tension cracks lead to a credible collapse mechanism. Even if a waterproof liner is desired, minor tensile cracking in any outer concrete shell cast against the rock is permissible as long as the structural integrity of the waterproof membrane can be assured.

## CONCLUSIONS

Shaft liner design for a nuclear waste repository differs in several respects from liner design for other applications. The methodology proposed in this paper provides a framework for design that is especially relevant to the exploratory shaft program. It is hoped that performance data gathered in that program will benefit future design of repository shafts.

## DISCLAIMER

The views expressed in this paper are those of the authors and do not necessarily reflect those of the United State Government or any agency thereof.

## REFERENCES


ACI (American Concrete Institute) 1983a. Building code requirements for structural plain concrete. ACI-318.1-83.

ACI (American Concrete Institute) 1983b. Building code requirements for reinforced concrete. ACI-318.

Brady, B. and E. Brown 1985. Rock mechanics for underground mining. London: Allen & Unwin.

Detournay, E. & C. Fairhurst 1987. Two-dimensional elastoplastic analysis of a long cylindrical cavity under non-hydrostatic loading. Int. J. Rock. Mech. Min. Sci. 24:197-211.

DOE (Department of Energy) 1986. Generic requirements document for a mined geologic disposal system. OGR-RW-0090. OCRWM.

Hendron, A. and G. Fernandez 1983. Dynamic and static design considerations for underground chambers. Proc. symp. seismic design of embankments and caverns. (May 16-20, Philadelphia). ASCE. 157-197.

Hustrulid, W. 1984. Lining considerations for a circular vertical shaft in generic tuff. SAND 83-7068, Sandia National Laboratories. Albuquerque, N.M.

Link, H., H. Lutendorf & K. Stross 1985. Guidelines for calculating shaft linings in incompetent strata, 3rd Edition, Glukauf, Essen, (in German).

Newmark, N. and W. Hall 1977. Development of criteria for seismic review of selected nuclear power plants, NUREG/CR-0098, U.S. Nuclear Regulatory Commission, Washington, D.C.

Pariseau, W. 1977. Estimation of support load requirements for underground mine openings by computer simulation of the mining sequence. Trans. AIME. 262:100-109.

Poppen, S., A. Cooley & M. Mirza 1987. Exploratory shaft design for the salt repository project. RETC.2:1072-1090.

Ranken, P. & J. Ghaboussi 1975. Tunnel design considerations: analysis of stresses and deformations around advancing tunnels. Rept. No. FRA-OR D8DD 75-84. Dept. of Transportation.

St. John, C. and T. Zahrah 1987. Aseismic design of underground structures. Tunnlg. & Undg. Space Tech. 2:165-197.

NRC (U.S. Nuclear Regulatory Commission) 1986. Disposal of high-level radioactive wastes in geologic repositories. Code of Federal Regulations, Energy. Title 10, Part 60. Washington, D.C.

# APPENDIX

## Information from the Reference Information Base Used in this Report

This report contains no information from the Reference Information Base.

## Candidate Information for the Reference Information Base

This report contains no candidate information for the Reference Information Base.

## Candidate Information for the Site & Engineering Properties Data Base

This report contains no candidate information for the Site and Engineering Properties Data Base.

SAND 88-7120A

# SUMMARY

## A PROPOSED CONCRETE SHAFT LINER DESIGN METHOD FOR UNDERGROUND NUCLEAR WASTE REPOSITORIES

Archie M. Richardson, Birger Schmidt
Parsons Brinckerhoff Quade & Douglas, Inc., San Francisco, CA, USA
Christopher M. St. John, Principia Mechanica, London, England

OBJECTIVE With the current concern with the development of licensable underground repositories for high-level nuclear waste, it is crucial that a consistent and complete methodology for design of deep shafts at such a facility be developed. This paper outlines a proposed methodology for design of concrete shaft liners in rock.

METHODS The methodology considers static, induced thermal and seismic loads on the liner, making it appropriate for underground repositories. It is based on the following steps (Figure 1): 1) Investigation of the response of the unlined shaft; 2) Determination of loads on the liner from in situ ground pressure, thermally induced loads from waste package decay, and seismic effects from possible earthquakes; 3) Identification of the possible modes of deformation of the liner in response to these loads; 4) Stress analysis of the liner, considering it an elastic tube embedded in and bonded to an elastic medium with different material properties. Simple interaction between the lining and the rock is considered in the stress analysis, which uses a recent solution for stresses and strains in an embedded thick cylinder derived by one of the authors, that has been verified by several alternate methods for nuclear waste applications; and 5) Evaluation of predicted lining stresses vs expected concrete performance.

RESULTS The methodology is illustrated with examples appropriate to a shaft in non-creeping rocks located in a reasonably dry environment with little or no initial rock overstress.

CONCLUSIONS A collection of relatively simple analyses emphasizing closed form solutions can be used to calculate liner loads, determine critical stresses in the liner, and evaluate the performance of the liner. The overall methodology serves as a framework that remains valid for any level of analysis considered appropriate. The principal remaining uncertainty in the analysis lies in determination of loads on the structure, since they are geologic in origin.

No Comments
R.N. Pike
8-22-88

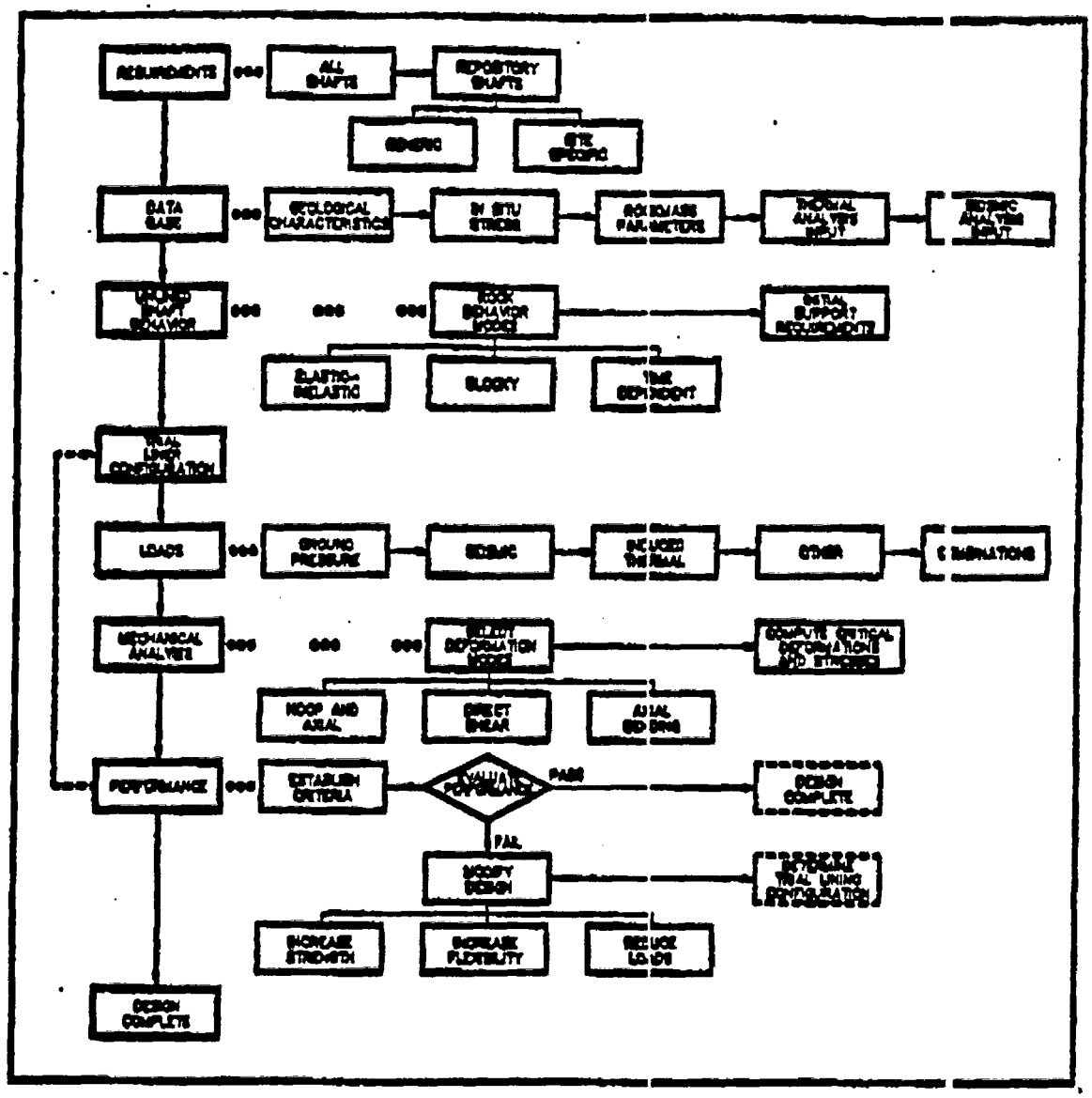


Figure 1. Flow chart of proposed liner design methodology.

SAND87-1937C

# EVALUATION OF SITE-GENERATED RADIOACTIVE WASTE TREATMENT AND DISPOSAL METHODS FOR THE YUCCA MOUNTAIN REPOSITORY

C. V. Subramanian
Sandia National Laboratories, Div. 8511
Livermore, CA

L. J. Jardine
Bechtel National, Incorporated
San Francisco, CA 94119

## OBJECTIVE

This study identifies the sources of radioactive wastes that may be generated at the proposed high level waste (HLW) repository at Yucca Mountain, Nevada, estimates the waste quantities and characteristics, compares various technologies that are available for waste treatment and disposal, and develops recommended concepts for site-generated waste treatment and disposal. The scope of this study is limited to the repository operations during the emplacement phase, in which 70,000 MTU* of high-level waste will be received and emplaced at the proposed repository. The evaluations consider all radioactive wastes generated during normal operations in surface and underground facilities. Wastes generated as a result of accidents are not addressed because accidents that could result in large quantities of radioactive waste are expected to occur very infrequently so that temporary, portable systems could be used for cleanup, if necessary. The results of this study can be used to develop more definitive plans for managing the site-generated wastes and to serve as a basis for the design of associated facilities at the proposed repository.

## WASTE CHARACTERIZATION

The conceptual design of a repository consisting of a single waste-handling building with no spent fuel consolidation facilities was used as the basis for estimating sources, quantities, and characteristics of site-generated wastes. Preliminary investigations have led to this configuration being identified as a preferred alternative to the reference NNWSI Project configuration presented in SAND84-2641, (MacDougall, 1987). This configuration is subject to further studies in future design activities.

The following assumptions were used in estimating the quantities of radioactive wastes generated at the repository facilities.

1. The repository will accept spent fuel at an annual rate of up to 3,000 MTU and will accept defense high level waste (DHLW) canisters at an annual rate equivalent to 400 MTU.

2. No spent fuel will be consolidated at the repository, and there will be only one waste-handling building to receive and package the

*An MTU of waste is that produced from one metric ton of uranium initially loaded in a reactor core.

spent fuel and DHLW. (It is noted that at-repository consolidation would result in substantially larger quantities of site-generated waste than those reported here).

3. Spent fuel transportation from reactors will be 70 percent by truck and 30 percent by rail on the basis of MTU. This study assumes that each spent fuel rail cask will contain about 4 ounces of crud (activated corrosion products) and each spent fuel truck cask will contain about 4/7 of an ounce of crud dislodged from the fuel assemblies.

4. Estimates of site-generated waste characteristics are based on the average rates of handling and processing spent fuel and DHLW during the emplacement phase. (Variations in throughput rates during the first few years of operation are not addressed.) Radioactive wastes that may be generated at the repository during caretaking, retrieval, or decommissioning are not addressed, because these quantities are not expected to affect the waste treatment system evaluations and selections.

5. Site-generated wastes are not expected to contain concentrations of transuranic or other radionuclides that would preclude near-surface disposal as specified in 10 CFR Part 61 (NRC, 1986a).

The types of activities that generate the majority of site-generated wastes in a repository include normal operations, decontamination, housekeeping, preventive and corrective maintenance, and health physics surveys. These operations generate liquid, solid and gaseous wastes.

The liquid wastes are generated primarily by decontamination operations, and include chemical wastes like decontamination solution, laboratory wastes, vehicle wash wastes, laundry drains and spent resin slurries.

The solid radioactive wastes are generated primarily by waste-handling operations, and include both compactible wastes (like items made of plastic, paper, cloth, rubber and metal, absorbant materials, filters, etc.) and noncompactible wastes (like items made of wood, metal and concrete, filters, glass, lead, dirt, etc.)

During normal operation of the repository, there will be no gaseous or airborne radioactive wastes that require treatment beyond HEPA filtration.

Table 1 summarizes the estimates of the site-generated waste volumes and concentrations of radioactivity for the repository facilities. The sources of each of the waste types are discussed in detail in SAND86-7136 (Jardine, et al., 1987).

Table 1

Estimates of Site-Generated Waste

| Waste Type | Annual Quantity | Activity | Annual Activity (Ci) |
|---|---|---|---|
| Chemical liquids | 48,000 gal | $7.5 \times 10^{-5}$ Ci/gal | 4 |
| Spent resin slurry | 4,000 gal | $1.1 \times 10^{-2}$ Ci/gal | 45 |
| Recycle liquids | 417,000 gal | $6.3 \times 10^{-4}$ Ci/gal | 261 |
| Waste-handling building cartridge filters | 182 filters | 12 Ci/filter | 2,200 |
| Recycle purification cartridge filters | 18 filters | 12 Ci/filter | 216 |
| Noncombustible/ Noncompactible dry active waste | 14,400 $ft^3$ | $3.5 \times 10^{-3}$ Ci/$ft^3$ | 51 |
| Combustible/ Compactible dry active waste | 36,800 $ft^3$ | $3.0 \times 10^{-3}$ Ci/$ft^3$ | 112 |
| Hot cell air filters | 1,200 $ft^3$ | $3.3 \times 10^{-1}$ Ci/$ft^3$ | 400 |

## WASTE TREATMENT METHODS

In accordance with 10 CFR part 60.132 (d), "radioactive waste treatment facilities shall be designed to process any radioactive wastes generated at the geologic repository operations area into a form suitable to permit safe disposal at the geologic repository operations area or to permit safe transportation and conversion to a form suitable for disposal at an alternative site in accordance with any regulations that are applicable..." (NRC, 1986b).

Waste treatment techniques must convert the waste into a form that meets the requirements associated with the particular disposal technique used. For near-surface burial, the requirements of 10 CFR Part 61 (NRC, 1986a) must be met. Major requirements of this regulation include the following:

- Liquid waste must be solidified or packaged in sufficient absorbent material to absorb twice the volume of liquid.
- Solid waste containing liquid shall contain as little freestanding and noncorrosive liquid as is reasonably achievable, but in no case shall the liquid exceed 1 percent of the volume.

- Waste must not be packaged for disposal in cardboard or fiberboard boxes.

If waste is transported off-site for disposal, the requirements of 49 CFR Part 173 (DOT, 1986) and 10 CFR Part 71 (NRC, 1986c) must be met. These regulations provide criteria for packaging and labeling the waste.

If on-site subsurface excavations are used for disposal of site-generated waste, the requirements of 10 CFR Part 60.135(d) must be met. The regulation states that criteria for such wastes "will be addressed on an individual basis if and when they are proposed for disposal in a geologic repository" (NRC, 1986b).

Site-generated wastes emplaced in the underground excavations may be required to be reduced to a noncombustible form. Regulations in 30 CFR Part 57.4104 (MSHA, 1985) require that combustible material in the subsurface excavations "shall not accumulate in quantities that could create a fire hazard." In addition, 30 CFR Part 57.4500 requires that "heat sources capable of producing combustion shall be separated from combustible materials if a fire hazard could be created."

For disposal in subsurface excavations, site-generated wastes should be located sufficiently far from the spent fuel and DHLW emplacement to prevent potential interactions due to decay heat, bacterial and radiolytic decomposition that could compromise postclosure performance issues such as radionuclide migration. This study assumes that subsurface excavations can be designed to prevent such interactions.

Waste treatment systems shall be designed so that no contaminated or potentially contaminated liquids are released to the environment. All such liquids are solidified for disposal or are treated for recycle, with no liquid discharge to the environment.

Waste treatment systems and facilities will be designed so that radiation exposures are maintained within applicable limits and as low as reasonably achievable. Also, waste treatment systems will have sufficient flexibility to accommodate unforeseen waste processing demands, such as might result from off-normal operations or equipment maintenance.

Gaseous radioactive wastes may not be released to the environment in quantities that exceed the 10 CFR Part 20 Appendix B (NRC, 1986d) limits. If it is found that those limits are exceeded, special gaseous collection and treatment systems will be installed.

Using the foregoing guidelines, treatment and disposal technologies that would be suitable for site-generated wastes were reviewed, and the technical and economic aspects of the most feasible options were evaluated. Ten treatment options and three disposal options were compared to determine the recommended methods. The comparisons involved qualitative evaluations of relative radiation doses to workers and development of relative life-cycle cost estimates that included capital costs for treatment and disposal facilities for each alternative, as well as operating costs for waste collection, treatment, packaging, transportation, and disposal.

The ten treatment options are:

1. This is the reference waste treatment case in which chemical liquids are solidified with cement. Spent resins are combined with chemical liquids for solidification. Recycle liquids are filtered and purified using ion exchangers. Spent cartridge filters are packaged in 55-gal drums with absorbent. Compactible dry active waste (DAW) is compacted using a standard box compactor, and noncompactible DAW is packaged in metal boxes without compaction. Hot cell air filters are processed by separating the frames from the media, shredding the frames, and compacting the media. Drums of highly radioactive wastes (spent cartridge filters and hot cell air filters) are packaged in canisters remotely handled.

   Radiation doses to workers are expected to be low due to remote handling features for the highly radioactive waste and the limited amount of waste volumes to be handled and disposed of.

2. In this option, the radioactivity buildup on cartridge filters is limited so that they may be contact handled. This eliminates equipment and operations associated with packaging the spent filters in canisters for remote handling.

   Much larger numbers of cartridge filters are used in this option, so that associated radiation levels will be low enough to allow contact handling. Spent cartridge filters are packaged in 55-gal drums with absorbent and are prepared for disposal without packaging in canisters. Treatment methods for other site-generated wastes are the same as those in the reference case.

   In Option 2, radiation doses to waste treatment workers are expected to be much greater than those in the reference case due to the much larger number of drums requiring handling, transporting, and disposal.

3. In this option, the highly radioactive waste is to be packaged in concrete shield boxes with wall thickness of 18 in. to allow contact handling rather than remote handling. This option eliminates equipment and operations associated with remote handling and disposal of site-generated waste.

   Shield boxes are used for packaging spent cartridge filters and hot cell air filters, so that the associated radiation levels will be low enough to allow contact handling.

   In Option 3, radiation doses to waste treatment workers are expected to be about the same as for the reference case, because approximately the same number of waste packages with similar radiation levels are being handled.

4. This Option is similar to Option 3, except that spent hot cell air filters are compacted prior to packaging in shield boxes. This reduces the number of shield boxes needed annually and also

eliminates the equipment and operations associated with remote handling (as in Option 3).

In Option 4, radiation doses to workers are expected to be about the same as in the reference case, because approximately the same number and type of waste packages are being handled.

5. Option 5 involves packaging DAW without compaction. Evaluation of this option will determine the cost-effectiveness of using the compactor in the reference case. In Option 5, the DAW compactor is eliminated; however, the number of boxes of DAW requiring disposal is increased significantly.

   In Option 5, radiation doses to waste treatment workers are expected to be slightly greater than in the reference case due to the greater number of DAW boxes requiring handling, transporting, and disposal.

6. Option 6 involves supercompaction of DAW, which further reduces the volume of waste below that of standard compaction. All DAW is initially packaged in 55-gal drums, with a standard compactor used for compactible DAW. The drums of DAW are then supercompacted, and several supercompacted drums can then be placed in an 85-gal drum.

   In Option 6, radiation doses to waste treatment workers are expected to be about the same as in the reference case, because approximately the same number of waste packages are being handled with similar radiation levels.

7. In Option 7, combustible DAW and hot cell air filter media (not frames) are loaded into wire baskets that are placed into 55-gal drums. Grout (cement, sand, and water) is then placed into each drum to surround the basket of combustible material. Drums of highly radioactive hot cell air filter media (encased in grout) are placed in casks and then returned to the waste-handling building, where they are loaded into canisters for remote handling and disposal.

   In Option 7, radiation doses to waste treatment workers are expected to be greater than in the reference case due to the additional handling requirements associated with segregating combustible and noncombustible wastes and loading combustible wastes into baskets for encasement in cement, and due to the much larger number of waste drums requiring handling, transporting, and disposal.

8. In Option 8, combustible DAW and hot cell air filter media (not frames) are shredded and transferred into an incinerator. The resulting ash is then immobilized in concrete in 55-gal drums. Drums of highly radioactive hot cell air filter ashes (solidified) are transferred (in a shielded cask) to the waste-handling building and loaded into canisters for remote handling.

In Option 8, radiation doses to waste treatment workers are expected to be about the same as those in the reference case. Slight decreases in exposures associated with the reduced number of waste packages requiring disposal are offset by additional maintenance of incineration system components contaminated with radioactivity.

9. Option 9 involves solidification of all site-generated liquid wastes with no recycle of liquids. This eliminates equipment and operations associated with the purification of recycle liquids; however, a much greater quantity of solidified waste packages is produced. Evaluation of this option will determine the cost-effectiveness of the recycle purification system.

   Radiation doses to workers are expected to be greater than those in the reference case due to the larger number of waste drums requiring handling, transporting, and disposal.

10. Option 10 involves evaporation of all site-generated liquid wastes, with recycle of the distillate. This option replaces the filtration and ion exchange system with an evaporation system. Evaporator bottoms are solidified with cement in the same manner as chemical liquids in the reference case.

    Radiation doses to workers are expected to be about the same as those in the reference case, because approximately the same number of waste packages, with similar radiation levels are being handled.

The three waste disposal options considered are:

1. On-Site Geologic Repository - This waste disposal option involves transport of site-generated waste to subsurface excavations for disposal. This approach eliminates the need for off-site transportation and reliance on a separate organization or independent site for waste disposal.

2. Off-Site Disposal at Beatty - The commercial low-level waste disposal site at Beatty, Nevada, is about 50 mi (80 km) by road from the repository site at Yucca Mountain.

   Packages of site-generated waste would be loaded onto a commercial shipping vehicle for off-site transportation to the disposal site. Shielded casks would be used as necessary to meet radiation dose limits for transportation. For highly radioactive site-generated wastes, such as spent cartridge filters and hot cell air filters, a shield cask is used for on-site transfer of drummed waste from the waste-handling building to the waste treatment building and to the commercial shipping cask.

3. Off-Site Rocky Mountain Compact - Another option for off-site disposal of site-generated waste may be use of a burial site to be developed for the Rocky Mountain Low-Level Waste Compact. The location of the site has not been selected yet; however, this study

assumes that such a site would be developed at a distance of about 1,000 miles (1600 km) from the repository location. It is assumed that the waste disposal charges at the Rocky Mountain Compact site are the same as those at Beatty. Repository site-generated waste is shipped to this site using commercial transport vehicles in a manner similar to that described in 2.

Because the life-cycle costs and technical merits of each type of treatment method depend on the disposal alternative being considered, all combinations of the above treatment and disposal methods were evaluated to determine the preferred approach.

## RESULTS

This study indicated that on-site disposal of site-generated waste in special subsurface excavations would be much more economical than off-site transport and disposal because of the difference in transportation costs.

For on-site disposal, the following waste treatment methods were recommended based on their combined technical merits and life-cycle costs:

- Filtration/ion exchange of liquids to allow recycle and solidification of chemicals and spent resins
- Standard compaction of solid wastes
- Compaction and packaging of highly radioactive solid wastes in disposable concrete shield boxes

## CONCLUSIONS

The results of this study can be used to develop more definitive plans for treating and disposing of the site-generated wastes, and to serve as a basis for the advanced conceptual design of associated facilities at the proposed repository.

Reference:

DOT (U.S. Department of Transportation), 1986, 49 CFR Part 173, Shippers - General Requirements for Shipments and Packagings, U.S. Government Printing Office, Washington, D.C.

Jardine, L. J., Lipps, D. J., and Miller, D. D., "Site-Generated Waste Treatment and Disposal Study," SAND86-7136, Sandia National Laboratories, Albuquerque, NM, October 1987.

NRC (U.S. Nuclear Regulatory Commission), 1986a, 10 CFR Part 61, Licensing Requirements for L and Disposal of Radioactive Waste, U.S. Government Printing Office, Washington, D. C.

NRC (U.S Nuclear Regulatory Commission), 1986b, 10 CFR Part 60, Disposal of High-Level Radioactive Waste in Geologic Repositories, U.S. Government Printing Office, Washington, D.C.

NRC (U.S. Nuclear Regulatory Commission), 1986c, 10 CFR Part 71, Packaging and Transportation of Radioactive Material, U.S. Government Printing Office, Washington, D.C.

NRC (U.S. Nuclear Regulatory Commission), 1986d, 10 CFR Part 20, Standards and Protection Against Radiation, U.S. Government Printing Office, Washington, D.C.

MacDougall, H. R., Scully, L. W., and Tillerson, J. R., "Site Characterization Plan Conceptual Design Report," SAND87-2641, Sandia National Laboratories, Albuquerque, NM, 1987.

MSHA (U.S. Mine Safety and Health Administration), 1985, 30 CFR Part 57, Safety and Health Standards - Metal and Nonmetal Underground Mines, U.S. Government Printing Office, Washington, D.C.

SAND 87-1915C

# SEISMIC DESIGN OF THE WASTE-HANDLING BUILDING AT THE PROSPECTIVE YUCCA MOUNTAIN NUCLEAR WASTE REPOSITORY

C. V. Subramanian
Sandia National Laboratories
Division 6311, Nuclear Waste Engineering Projects
Albuquerque, New Mexico 87185
(505) 846-0158

C. L. Wu, C. D. DeGabriele
Bechtel National, Inc.
P.O. Box 3965
San Francisco, CA 94119
(415) 768-4286

The site for the first prospective high-level nuclear waste repository is located in Yucca Mountain at the southwest corner of the Nevada Test Site in Nye County, Nevada. The preliminary site investigation and seismic hazard evaluation indicate that the design ground acceleration in the horizontal direction of 0.40 g (with a vertical acceleration equal to two-thirds the horizontal) has a recurrence interval of 2,000 years. The site evaluation also indicates a potential for some fault displacement on the geologic faults near the site. Proposed facilities at the prospective repository include a waste handling building (WHB), the primary facility used for handling radioactive waste materials. This paper summarizes the structural behavior of the WHB resulting from the seismic loads. This summary includes a preliminary seismic evaluation of the WHB, and includes estimates of the seismic design margin, building performance, and the amount of fault displacement that the WHB can accommodate without structural yield failure.

The WHB used in this study is based on a preliminary conceptual design that assumes no fuel-rod consolidation at the repository. It is irregular in plan with overall dimensions of approximately 550 ft by 210 ft. The dominant lateral load-resisting elements are reinforced concrete shear

walls which are 5ft-6in thick, sized primarily to provide radiation shielding to the hot cells. Appropriate locations of seismic joints were identified and provided in the design configuration to optimize the use of the shear walls to resist seismic loads. These locations, in effect, split the 5ft-6in thick walls into double walls, each contributing to the lateral load resistance on its respective side of the joint. Seismic joint details and materials were evaluated and selected to accommodate seismic movements and to provide radiation shielding as required.

Both elastic and inelastic seismic analyses were performed on the WHB for the design-basis earthquake of 0.40 g horizontal acceleration and 0.27 g vertical acceleration using site-specific response spectra (Blume, 1986). A lumped parameter model represented the WHB. Soil springs were included at the base of the structure, consistent with the methodology given in ASCE, 1984, to couple the structural model with the supporting soil. A damping value of 7% of critical damping for reinforced concrete structures was used from ASCE, 1984. For modes with predominant soil deformation, a maximum of 10% of critical damping based on Reference 2 was used. The response spectrum analysis method was used to perform the elastic analysis. Modal responses and spatial components were combined using the rule of the square root of the sum of the squares (SRSS), and the computed member forces were evaluated according to American Concrete Institute's ACI-349.

Results of the elastic analysis indicate that the WHB can withstand the design-earthquake loading. However, resulting shear stresses in the walls were high and the walls required substantial amounts of shear reinforcement for the response to remain completely elastic. However, adding shear walls to the existing configuration resulted in reduced shear stress in the walls and a more redundant structural system.

The inelastic analysis was performed using the modified response spectrum method (Newmark, 1975). For this, a modified acceleration response spectrum and a corresponding modified displacement response spectrum for ductility factor of 1.5 were developed. This value of ductility factor used is conservative per Kennedy, 1980. The structure's ductility factor is defined as the ratio of ultimate displacement to yield displacement for an equivalent single degree of freedom system. This analysis resulted in a 20% reduction in shear stresses from the results of the elastic analysis. The shear strains produced by the modified displacement response spectra loading are 1.3 to 1.4 times the nominal shear strain at yield deflection, or within the 1.5 ductility factor.

The seismic capacity and design margin of the WHB were determined using the Conservative Deterministic Failure Margin (CDFM) approach shown in Kennedy, 1984. This analysis resulted in wall loadings much less than those from the previous analyses and in a capacity estimate of 3 times the elastic capacity. Further, this analysis identified weaker links in the existing structural configuration as walls oriented in the north-south direction. Additional shear walls in this direction, if added, would provide redundancy to the design and a more uniform design margin.

The value for maximum fault displacement that the WHB can accommodate was based on author's engineering judgment derived from findings of a literature search and the results of simplified analyses using two-dimensional finite-element models with elastic properties. The literature search showed that structures can be designed to accommodate horizontal and vertical fault displacements ranging from 1 in. for commercial facilities (Wyllie, 1973) to about 1 m for nuclear power plant reactor structures (Reed, 1979).

The literature search also established the feasibility of using granular foundation materials beneath the WHB foundation and as backfill around the subgrade walls to accommodate the effects of fault displacement. Other isolation techniques identified for accommodating the effects of fault displacement include trenches or other forms of clearance, artificial slip surfaces, slurry trenches, strengthened conventional designs, and mechanical base isolators. However, these methods will be examined in more detail prior to use in the final WHB design.

Numerical analyses were performed on a preliminary layout of the WHB to estimate the amount of fault displacement the structure can accommodate. The method of analyses used is similar to that used by Duncan and Lefebvre, 1973. Finite-element models were constructed to represent the structure and surrounding soil for both vertical and horizontal fault displacement cases. Because of this investigation's preliminary nature, no inelastic or nonlinear effects of the soil or structure were considered. The results of the analyses provide a preliminary estimate and are intended to be an approximation of more precise calculations incorporating inelastic or nonlinear effects of the soil and structure.

The results of these analyses show that the WHB can accommodate vertical fault displacements ranging from 1.0 to 2.5 in and horizontal fault displacements ranging from 5 to 15 in. In these analyses it was assumed that the shear stress produced by the dynamic effects due to ground acceleration is accounted for by the concrete shear stress permitted by the American Concrete Institute's ACI 318 code without shear reinforcement. The stress induced by fault displacement is then accommodated by the shear

capacity of the concrete beyond the code limitations but within the range where shear cracking is known to initiate. Within this range of shear stress, localized cracking and spalling of concrete may occur, but the displacement will not cause the building structure to collapse. These estimates are conservative because these analyses did not utilize the structural capacity beyond its yield point.

The results of these preliminary evaluations of the WHB suggest that:

1. The WHB, if designed according to accepted procedures and consistent with current technology, can withstand the seismic design ground motion and any potential minor fault displacement likely to occur in the seismotectonic environment at the Yucca Mountain site.

2. Such a design will have adequate design margins to accommodate the effects of other seismic events which may be somewhat larger than the design seismic event but with a lower probability of occurring at the site.

It is noted here that more definitive analyses will be performed in the future, especially for fault displacements, and it is expected that these analyses will demonstrate that fault displacements larger than what is shown in this paper can be accommodated in the WHB design.

REFERENCES:

1. ASCE Seismic Analysis Standard Committee, "Standard for the Seismic Analysis of Safety-Related Nuclear Structures," New York, May 1984.

2. Bechtel Power Corporation, "Topical Report Seismic Analyses of Structures and Equipment for Nuclear Power Plants," BC-TOP-4-A, Rev. 3, San Francisco, CA, November 1974.

3. J. M. Duncan, and G. Lefebvre, "Earth Pressures on Structures Due to Fault Movement," Proceedings of ASCE, Vol. 99, No. SM12, December 1973.

4. R. P. Kennedy, "Various Types of Seismic Margins and Their Uses," Proceedings of EPRI/NRC Workshop on Nuclear Power Plant Reevaluation to Quantify Seismic Margin, Section 2, Palo Alto, CA, October 15-17, 1984.

5. R. P. Kennedy, et al., "Probabilistic Seismic Safety Study of an Existing Nuclear Power Plant," Nuclear Engineering and Design, Vol. 59, Amsterdam, Netherlands, 1980.

6. N. M. Newmark, "A Response Spectrum Approach for Inelastic Seismic Design of Nuclear Reactor Facilities," Transactions of the 3rd International Conference on Structural Mechanics in Reactor Technology, Volume 4 Part K, London, September 1975.

7. J. W. Reed, et al., "An Analyses of a Nuclear Test Reactor for Surface Rupture Offset," ASCE Spring Conference, Boston, Mass., 1979.

8. URS/John A. Blume & Associates, Engineers, "Ground Motion Evaluations at Yucca Mountain, Nevada, with Applications to Repository Conceptual Design and Siting," SAND85-7104, Sandia National Laboratories, Albuquerque, NM, February 1986.

9. L. A. Wyllie, Jr., "Performance of Banco Central Building," Earthquake Engineering Research Institute Conference Proceedings, San Francisco, CA, 1973.

## APPENDIX

### Information from the Reference Information Base Used in this Report

Seismic acceleration levels used (0.4 g horizontal and 0.27 g vertical) are consistent with RIB.

### Candidate Information for the Reference Information Base

This report contains no candidate information for the Reference Information Base

### Candidate Information for the Site & Engineering Properties Data Base

This report contains no candidate information for the Site and Engineering Properties Data Base.

# Gas Phase Flow Effects on Moisture Migration in the Unsaturated Zone at Yucca Mountain*

Y.W. Tsang and K. Pruess (Earth Sciences Division, Lawrence Berkeley Laboratory, University of California, Berkeley, CA 94720)

Daily and seasonal weather patterns may play a role, either directly or indirectly, in affecting overall gas and liquid movement in the unsaturated zone at Yucca Mountain, Nevada. In this study we focus on two effects at the land surface: (1) atmospheric pressure variations with time, which we denote by "barometric pumping", and (2) a lowered relative humidity condition of the soil gas. Both boundary conditions induce a net upward movement of moisture, predominantly as gas phase vapor fluxes. The objective of the present study was to use simple and idealized models to determine whether these gas phase flow effects could conceivably make a major contribution to the overall water balance (net infiltration). We performed a spectral analysis of barometric pressure data from Yucca Mountain, which yielded estimates for net moisture removal from the unsaturated zone by way of barometric pumping. Effects of the lowered relative humidity boundary condition were simulated numerically in a one-dimensional vertical tuff column. The simulations were carried out using the simulator TOUGH, which is a multidimensional numerical model for simulating the coupled transport of water, vapor, air and heat in porous and fractured rock. It takes account of fluid flow in both liquid and gaseous phases under pressure, viscous, and gravity forces as well as binary diffusion in the gas phase. We find that upward vapor fluxes for the two processes considered lie in the range of 0.1 mm/yr, which is orders of magnitude smaller than overall precipitation (approximately 150 mm/yr). It is concluded therefore, that the gas phase flow effects considered here make only a very small contribution to the overall water balance at the ground surface. However, the effects cannot be ignored because they are of the same order of magnitude as current estimates of net infiltration. Since all those estimates are indirect with large uncertainty, this study raises the question as to the possibility of an overall drying (net infiltration negative). Our preliminary investigations suggest that further measurements should be made to accurately monitor status and migration of moisture at Yucca Mountain.

* This work was supported by the US Department of Energy (US DOE) under contract DE-AC04-76DP00789.